

ISSN 0030-6096

# OSAKA CITY MEDICAL JOURNAL

---



2019

PUBLISHED BY  
OSAKA CITY MEDICAL ASSOCIATION  
OSAKA JAPAN

**Osaka City Medical Journal**  
**Vol. 65, No. 2, December 2019**

**CONTENTS**

	page
Influence of Dose-volume Prescription in Three-dimensional Conformal Radiotherapy for Patients with Stage III Non-small-cell Lung Cancer TOMOHIRO NISHIKAWA, SHINICHI TSUTSUMI, TAKUHITO TADA, NAOKI MUKUMOTO, MASARU MAKIHARA, MASAHIRO TOKUNAGA, NORIKO TANAKA, YOSHIKAZU HASEGAWA, MASAKO HOSONO, KENTARO ISHII, and YUKIO MIKI .....	77
Clinical Response to Palliative Radiotherapy for Gastric Cancer MASARU MAKIHARA, TAKUHITO TADA, MASAHIRO TOKUNAGA, NORIKO TANAKA, HIROSHI TSUKUDA, TAKAYO OTA, TOMOHIRO NISHIKAWA, KOSUKE AMANO, and KENTARO ISHII .....	85
The Neural Effects of Inadequate Pauses in Speech on the Comprehension of Logical and Illogical Speeches: A Magnetoencephalography Study YUKI KODA, and KISHIKO SUNAMI .....	93
Microcuff® Pediatric Endotracheal Tube Decreases the Tube Exchange Ratio without Increasing Postoperative Complications in Japanese Children: A Single Center Retrospective Cohort Study YOSUKE INADA, YUSUKE FUNAI, TAKASHI SHUTOU, TAKASHI MORI, and KIYONOBU NISHIKAWA .....	109
Time-lapse Observation of Stabilized Mitochondrial Membrane Potential in Chemotherapy-induced Granulosa Cell Damage Treated with L-carnitine AKI TAKASE, DAISUKE TACHIBANA, YUKIMI KIRA, AKIHIRO HAMURO, TAKUYA MISUGI, and MASAYASU KOYAMA .....	119
—Case Report—	
Bilateral Ovarian Fibromatosis Diagnosed with Magnetic Resonance Imaging: A Case Report NORIKO TAKESHITA, TAKUHITO TADA, MASAHIRO TOKUNAGA, AKIRA OKIMURA, MASARU MAKIHARA, and TOHRU TAKESHITA .....	135

# Influence of Dose-volume Prescription in Three-dimensional Conformal Radiotherapy for Patients with Stage III Non-small-cell Lung Cancer

TOMOHIRO NISHIKAWA<sup>1</sup>, SHINICHI TSUTSUMI<sup>2</sup>, TAKUHITO TADA<sup>3</sup>, NAOKI MUKUMOTO<sup>4</sup>,  
MASARU MAKIHARA<sup>3</sup>, MASAHIRO TOKUNAGA<sup>3</sup>, NORIKO TANAKA<sup>3</sup>, YOSHIKAZU HASEGAWA<sup>5</sup>,  
MASAKO HOSONO<sup>2</sup>, KENTARO ISHII<sup>6</sup>, and YUKIO MIKI<sup>1</sup>

*Departments of Diagnostic and Interventional Radiology<sup>1</sup>  
and Radiation Oncology<sup>2</sup>, Osaka City University Graduate School of Medicine;  
Departments of Radiology<sup>3</sup> and Oncology<sup>5</sup>, Izumi City General Hospital;  
Department of Radiation Oncology<sup>4</sup>, Yodogawa Christian Hospital; and  
Department of Radiation Oncology<sup>6</sup>, Tane General Hospital*

## Abstract

### **Background**

Dose-volume prescription (DVP) is usually used in intensity-modulated radiation therapy (IMRT) and point-dose prescription (PDP) is usually used in three-dimensional conformal radiotherapy (3DCRT) in Japan. This study aimed to retrospectively evaluate the impact of DVP instead of PDP on the doses and outcomes of 3DCRT for patients with lung cancer.

### **Methods**

Since 2011, the DVP has been used in place of the PDP in routine 3DCRT for patients with lung cancer in our institution. Twenty-one patients with stage III non-small-cell lung cancer who underwent definitive chemoradiotherapy using DVP were included this study. The patients received a prescribed dose of either 60 Gy or 66 Gy, both of which covered 95% of the planning target volume (PTV). The clinical target volume (CTV) was defined as the gross tumor volume plus a 5 mm or more margin, and the PTV was defined as the CTV plus a 5 mm or more margin.

### **Results**

The median ratios of the dose in the DVP to that in the PDP were 1.059 and 1.077 in the actual treatment and in the planning study using unreduced PTVs, respectively. The median follow-up was 16.2 months. The overall 2-year Kaplan-Meier survival rate was 57%. The 2-year in-field control rates for the 66 Gy group and for the 60 Gy group were 100% and 0%, respectively.

### **Conclusions**

Although the PTVs were reduced, the DVP induced a 1.059-fold overdose. Meanwhile, treatment

---

Received October 26, 2018; accepted January 15, 2019.

Correspondence to: Shinichi Tsutsumi, MD.

Department of Radiation Oncology, Osaka City University Graduate School of Medicine,  
1-4-3 Asahimachi, Abeno-ku, Osaka, 545-8585, Japan

Tel: +81-6-6645-3831; Fax: +81-6-6645-6655

E-mail: ttm@ttm.jp

outcomes using the 66 Gy dose were satisfactory.

**Key Words:** Non-small cell lung cancer; Radiotherapy; Chemotherapy; Dose-volume-prescription

## **Introduction**

Recent clinical trials using three-dimensional conformal radiotherapy (3DCRT) for non-small-cell lung cancer (NSCLC) adopted Dose-volume prescription (DVP)<sup>1-3)</sup>. However, in several countries, including Japan, intensity-modulated radiation therapy (IMRT) remains an uncommon treatment modality, and the use of 3DCRT usually involves point-dose prescription (PDP) using heterogeneity correction. In this paper, a retrospective study was performed to evaluate the influence of DVP on the doses and outcomes of 3DCRT.

## **Materials and Methods**

This study was approved by the institutional review board at Izumi Municipal Hospital and was conducted in accordance with the Declaration of Helsinki. All patients gave informed consent to participate.

Since 2011, DVP has been used instead of PDP in routine 3DCRT for patients with lung cancer in our institution. In this paper, a retrospective study was performed to evaluate the influence of DVP on the doses and outcomes of 3DCRT.

### ***Patients***

Between October 2011 and March 2015, 33 patients with stage III NSCLC underwent definitive radiotherapy in our institution. Of the 33 patients, 5 patients who underwent radiotherapy with PDP following protocols of other multicenter clinical trials and 7 patients who underwent radiotherapy alone were excluded. The remaining 21 patients who underwent concurrent chemoradiotherapy with DVP were enrolled in this retrospective study. Patients who showed relapse after surgery were excluded in this study group.

### ***Radiotherapy***

Irradiation was performed using involved radiation fields. The clinical target volume (CTV) was defined as the gross tumor volume (GTV) plus a 5 mm or greater margin, and the planning target volume (PTV) was defined as the CTV plus a 5 mm or greater margin. 3DCRT was delivered in 10-MV photons. A dose of 60 Gy was prescribed to 7 patients with the following risk factors: advanced age (80 years or more; n=3), a large PTV resulting in more than 35% of the total lung volume receiving 20 Gy or more (n=3), and severe emphysema (n=1). Meanwhile, a dose of 66 Gy was prescribed for the remaining 14 patients. The prescribed doses covered 95% of the PTV (D95 prescription). For treatment planning, a commercially available superposition-based algorithm was used.

Except for the first 2 patients, the PTV margin was reduced using heterogeneity correction to avoid inconsistency of radiation dose with historical dosing methods, that is, PDP. However, in these patients, the reduced PTVs contained at least the CTVs. The radiation field consisted of the PTV plus 5 mm or greater leaf margin. When the PTV margin was reduced, the leaf margin was expanded to 8 mm or more in most patients.

### ***Chemotherapy***

Chemotherapy was concurrently performed with radiotherapy in all 21 patients. Of these, 9, 6, 5,

and 1 received a chemotherapeutic regimen consisting of carboplatin plus paclitaxel, carboplatin alone, cisplatin plus navelbine, and TS-1 alone, respectively.

### End points

The end points were correction factors (CFs) that were defined as the ratios of the dose in the DVP to that in the PDP, in-field control, clinical response, overall survival, and acute adverse events. To obtain the CFs, PDP planning was also performed using heterogeneity correction. In the planning procedure, the same radiation field and dose weighting with those in the DVP were used. Therefore, an isodose line of A Gy in the DVP was consistent with that of A X CF Gy in the PDP. Principally, the reference points were to be in the mediastinum, where the dose gradient was minimal. Furthermore, for comparison, planning with use of the DVP using unreduced PTVs was also performed. In-field control and overall survival were evaluated using the Kaplan-Meier method. The clinical response was evaluated according to the Response Evaluation Criteria in Solid Tumor (RECIST), version 1.1<sup>4)</sup>. Meanwhile, acute adverse events were evaluated according to the National Cancer Institute's Common Terminology Criteria for Adverse Events version 4.0<sup>5)</sup>.

## Results

The patient characteristics are listed in Table 1. A total of 14 and 7 patients had squamous cell carcinoma and adenocarcinoma, respectively, and stage IIIA and stage IIIB disease were seen in 14 and 7 patients, respectively. The CFs are summarized in Table 2. For all cases, the correction factor is greater than 1. This indicates that DVP is superior to PDP in PTV dose distribution. The median CFs in the actual treatment and in the planning study using the unreduced PTVs were 1.059 and 1.077, respectively. In the present study, the PTVs ranged from 19 cm<sup>3</sup> to 472 cm<sup>3</sup> (median, 186 cm<sup>3</sup>),

**Table 1. Patient characteristics**

Characteristic	Value
Age (y)	
Range	38-85
Median	71
Sex	
Male	15
Female	6
Clinical stage	
III A	14
III B	7
Histology	
Squamous cell carcinoma	14
Adenocarcinoma	7
ECOG* Performance status	
0	1
1	14
2	6

\*ECOG; Eastern Cooperative Oncology Group.

**Table 2. Correction factors**

Correction factor	$\leq 1$	1.001-1.049	1.050-1.099	1.100-1.149	$\geq 1.150$
Actual treatment	0	9	8	4	0
Planning study	0	3	11	6	1

Correction factors were defined as the ratios of the dose in the dose-volume prescription to that in the point-dose prescription. The planning study was performed using unreduced planning target volumes.

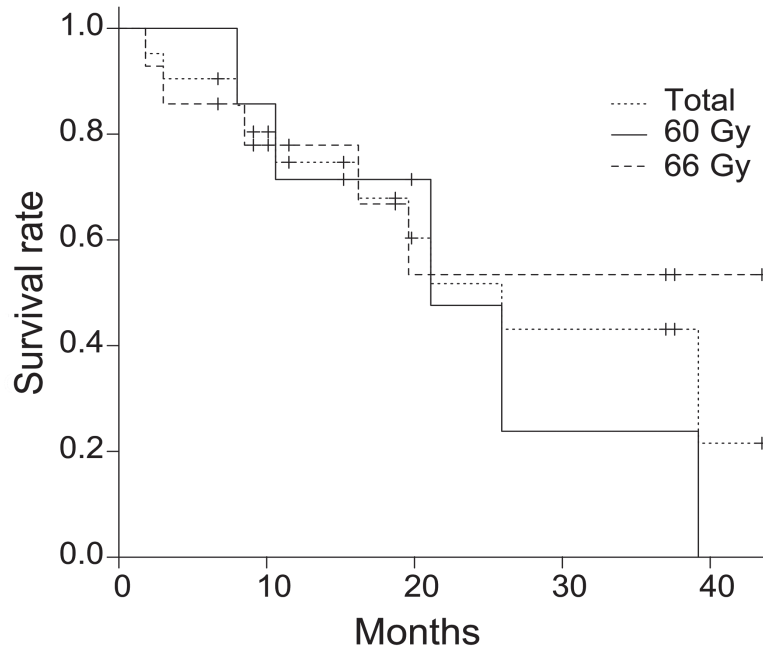


**Figure 1.** Kaplan-Meier survival curves for all patients, patients in the 66 Gy group, and those in the 60 Gy group.

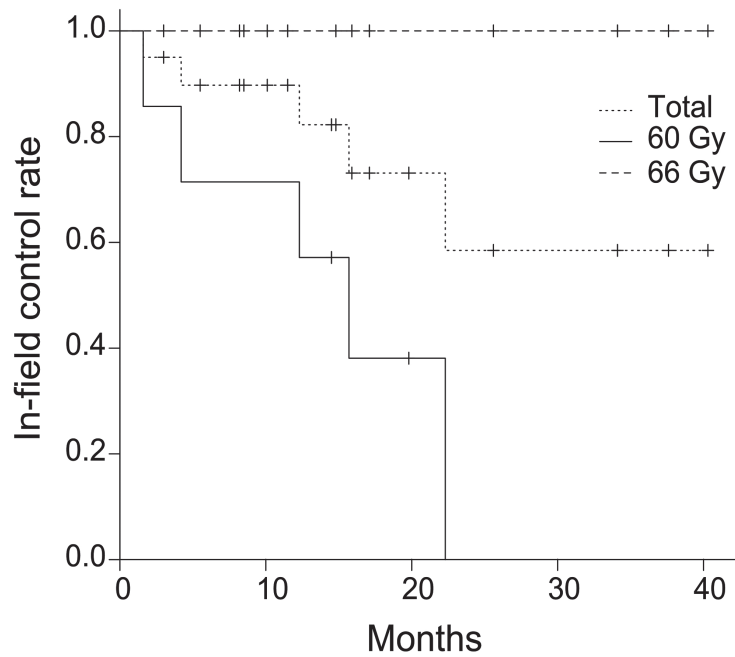


**Figure 2.** The in-field control curves for all patients, patients in the 66 Gy group, and those in the 60 Gy group.

and the unreduced PTVs ranged from 52 cm<sup>3</sup> to 557 cm<sup>3</sup> (median, 246 cm<sup>3</sup>).

The median follow-up was 16.2 months (range, 1.6-37 months). The response rate according to RECIST was 81% (complete response: 38%; partial response: 43%). The overall 2- and 3-year Kaplan-Meier survival rates were 57% and 48%, respectively (Fig. 1). The in-field control curves for all patients, for patients in the 66 Gy group, and for patients in the 60 Gy group are shown in Figure 2. The 2-year in-field control rates for all patients, for the 66 Gy group, and for the 60 Gy group were 58%, 100%, and 0%, respectively.

Grades 3 and 5 radiation pneumonitis were observed in 2 and 1 patients, respectively; all of whom were in the 66 Gy group. No other grade 3 or greater acute nonhematologic toxicity was observed.

## **Discussion**

Concurrent chemoradiotherapy is the standard of care for patients with unresectable stage III NSCLC. However, in-field control is unsatisfactory with 3DCRT<sup>6,7</sup>. Furthermore, considerable underdosing occurs in the peripheral lung in the PTV due to tissue heterogeneity and build-up effect. Therefore, several dose escalation studies have been performed. To avoid underdosing in the PTV, the D95 prescription was adopted in the RTOG0617 study<sup>2</sup>, which was started based on the hypothesis that radiotherapy with a dose of 74 Gy would yield better outcomes than that using 60 Gy. The D95 prescription was also adopted in our institution, and the prescribed dose of 66 Gy for patients without risk factors was established as follows. When DVP was adopted in our institution, the RTOG0617 study was yet to be concluded, and we presumed that the optimal dose would be between 66 Gy and 74 Gy based on former phase I and phase II studies<sup>3,8-10</sup>. The lowest dose in the range was adopted for safety.

In the first 2 patients treated with 3DCRT using the unreduced PTV, the CFs were 1.083 and 1.091. At that time, we had no experience with such a large fractional dose in concurrent chemoradiotherapy. To avoid inconsistencies with the PDP, the PTV margin was then reduced in succeeding patient treatments. As shown in the planning study using the unreduced PTV, the CFs decreased. However, the median CF remained at 1.059. When the unreduced PTVs were used, the median CF was 1.077 although the minimal size of the PTV following the protocol was used. In lung stereotactic body radiotherapy, Kawahara et al. compared the outcomes of DVP with PDP, and the produced CF was as high as 1.143<sup>11</sup>. Thus, one of the aims of the present report was to determine the difference in doses between DVP and PDP.

The risk of relapse around the margin of the radiation field increases with a decreased PTV. However, in-field control in the 66 Gy group has been satisfactory. At the least, more doses were delivered in the DVP than in the PDP even when the reduced PTVs were used. To avoid inconsistency with the PDP, the DVP was considered the optimal choice.

In 3DCRT planning using DVP, beam weighting is usually adjusted to improve the minimal dose in the PTV. Therefore, the DVP minimizes underdosing more than the simple CFs. In the present study, the 66 Gy group achieved favorable in-field control, although the follow-up time was insufficient. Meanwhile, in-field control for the 60 Gy group was unsatisfactory. However, a 60 Gy dose cannot be ruled out when considering treatment limitations, such as large GTV causing large PTV and mild chemotherapy due to advanced age.

Frank et al compared heterogeneity-corrected DVP using the D95 prescription with the classical homogeneous PDP and concluded that both produced equivalent PTV, CTV, and isocenter doses for

patients with stage I/II NSCLC<sup>12)</sup>. Therefore, adopting the DVP in place of the PDP in recent clinical trials was reasonable<sup>1-3)</sup>. However, the PTVs for stage III disease are generally larger than those for stage I/II disease. The large PTVs often resulted in overdosing in the DVP. Furthermore, institutional protocols and clinician experience can influence treatment planning<sup>13)</sup>. The overdosing can be significant in institutions with insufficient experience. These might explain the unexpected results of the RTOG0617 study, in which outcomes of radiotherapy with a dose of 74 Gy were compared with those of 60 Gy using the D95 prescription, and the results indicated that 60 Gy yielded significantly better outcomes<sup>2)</sup>. Therefore, approximately 50% of patients were treated with 3DCRT. Agreeable overdosing in the 60 Gy group prolonged survival time, whereas it negatively influenced survival time in the 74 Gy group. Notably, the favorable outcomes in the 60 Gy group were not those in the heterogeneity-corrected PDP. As such, the 60 Gy dose was not necessarily optimal in such group.

In the 66 Gy group, grade 3 or higher radiation pneumonitis was observed in 3 patients. When the lung dose is appropriately restricted, the risk of Clinically-significant symptomatic pneumonitis is about 20%<sup>14)</sup>. The incidence in this study is not high compared to past study. High-grade radiation pneumonitis is inevitable to some degree. To confirm the tolerability, further data accumulation is required.

IMRT can provide better dose distribution in the PTV and can reduce CFs. In IMRT, reducing PTV was not significantly necessary, and the optimal dose might be different from that in 3DCRT when the same PTV was used.

There were several limitations to this study. First, this was a retrospective study conducted at one institution. Any conclusion revealed here needs to be demonstrated prospectively. Additionally, it will be difficult to find significant relationships from the data because of the small number of patients. Further data accumulation is required to determine its clinical benefits and limitations.

In conclusion, the DVP yielded considerable overdosing in 3DCRT for patients with stage III NSCLC although the PTVs were reduced. In the present study, treatment outcomes from a dose of 66 Gy were satisfactory. Further data accumulation is required to determine its clinical benefits and limitations.

### Acknowledgements

All authors have no COI to declare regarding the present study.

### References

1. Senan S, Brade A, Wang LH, et al. PROCLAIM: Randomized phase III trial of pemetrexed-cisplatin or etoposide-cisplatin plus thoracic radiation therapy followed by consolidation chemotherapy in locally advanced nonsquamous non-small-cell lung cancer. *J Clin Oncol* 2016;34:953-962.
2. Bradley JD, Paulus R, Komaki R, et al. Standard-dose versus high-dose conformal radiotherapy with concurrent and consolidation carboplatin plus paclitaxel with or without cetuximab for patients with stage IIIA or IIIB non-small-cell lung cancer (RTOG 0617): a randomised, two-by-two factorial phase 3 study. *Lancet Oncol* 2015;16:187-199.
3. Socinski MA, Blackstock AW, Bogart JA, et al. Randomized phase II trial of induction chemotherapy followed by concurrent chemotherapy and dose-escalated thoracic conformal radiotherapy (74 Gy) in stage III non-small-cell lung cancer: CALGB 30105. *J Clin Oncol* 2008;26:2457-2463.
4. Eisenhauer EA, Therasse P, Bogaerts J, et al. New response evaluation criteria in solid tumours: revised RECIST guideline (version 1.1). *Eur J Cancer* 2009;45:228-247.
5. US Department of Health and Human Services. National Cancer Institute. Common terminology criteria for

- adverse events (CTCAE) version 4.0. National Institutes of Health/National Cancer Institute, 2009. pp. 1-194.
6. Tada T, Minakuchi K, Matsui K, et al. A single institutional subset analysis of the WJTOG study comparing concurrent and sequential chemoradiotherapy for stage III non-small-cell lung cancer. *Radiat Med* 2004;22:163-167.
  7. Kong FM, Ten Haken RK, Schipper MJ, et al. High-dose radiation improved local tumor control and overall survival in patients with inoperable/unresectable non-small-cell lung cancer: long-term results of a radiation dose escalation study. *Int J Radiat Oncol Biol Phys* 2005;63:324-333.
  8. Bradley JD, Bae K, Graham MV, et al. Primary analysis of the phase II component of a phase I/II dose intensification study using three-dimensional conformal radiation therapy and concurrent chemotherapy for patients with inoperable non-small-cell lung cancer: RTOG 0117. *J Clin Oncol* 2010;28:2475-2480.
  9. Schild SE, McGinnis WL, Graham D, et al. Results of a phase I trial of concurrent chemotherapy and escalating doses of radiation for unresectable non-small-cell lung cancer. *Int J Radiat Oncol Biol Phys* 2006;65:1106-1111.
  10. Stinchcombe TE, Lee CB, Moore DT, et al. Long-term follow-up of a phase I/II trial of dose escalating three-dimensional conformal thoracic radiation therapy with induction and concurrent carboplatin and paclitaxel in unresectable stage IIIA/B non-small cell lung cancer. *J Thorac Oncol* 2008;3:1279-1285.
  11. Kawahara D, Ozawa S, Kimura T, et al. Marginal prescription equivalent to the isocenter prescription in lung stereotactic body radiotherapy: preliminary study for Japan Clinical Oncology Group trial (JCOG1408). *J Radiat Res* 2017;58:149-154.
  12. Frank SJ, Forster KM, Stevens CW, et al. Treatment planning for lung cancer: traditional homogeneous point-dose prescription compared with heterogeneity-corrected dose-volume prescription. *Int J Radiat Oncol Biol Phys* 2003;56:1308-1318.
  13. Lee JS, Scott CB, Komaki R, et al. Impact of institutional experience on survival outcome of patients undergoing combined chemoradiation therapy for inoperable non-small-cell lung cancer. *Int J Radiat Oncol Biol Phys* 2002;52:362-370.
  14. Marks LB, Bentzen SM, Deasy JO, et al. Radiation dose-volume effects in the lung. *Int J Radiat Oncol Biol Phys* 2010;76:S70-S76.



# Clinical Response to Palliative Radiotherapy for Gastric Cancer

MASARU MAKIHARA<sup>1</sup>, TAKUHITO TADA<sup>1</sup>, MASAHIRO TOKUNAGA<sup>1</sup>, NORIKO TANAKA<sup>1</sup>,  
HIROSHI TSUKUDA<sup>2</sup>, TAKAYO OTA<sup>2</sup>, TOMOHIRO NISHIKAWA<sup>3</sup>, KOSUKE AMANO<sup>3</sup>, and KENTARO ISHII<sup>4</sup>

*Departments of Radiology<sup>1</sup> and Medical Oncology<sup>2</sup>, Izumi City General Hospital;  
Department of Radiation Oncology<sup>3</sup>, Osaka City University Graduate School of Medicine; and  
Department of Radiation Oncology<sup>4</sup>, Tane General Hospital*

## Abstract

### **Background**

Clinical studies on preoperative chemoradiotherapy have been performed for highly advanced gastric cancer, and gastric cancer is suggested to be radiosensitive. In order to provide data on the radiosensitivity, a retrospective study was performed.

### **Methods**

The study group comprised 14 patients, who underwent palliative radiotherapy for the primary site, the regional lymph node metastasis, or disseminated lesions between 2011 and 2016. Radiation doses were between 33 and 37.5 Gy (median, 36 Gy).

### **Results**

The response rate was 64%. The mean reduction rate was 50% (range, 0%-100%). For 7 patients who underwent concurrent chemoradiotherapy, the median reduction rate was 58% (p=0.56). Four patients achieved 100% reduction. The maximum reduction was observed between 2.0 and 6.8 months (median 4.7 months) after radiotherapy. One-year in-field control for all patients was 59%. Palliation of the symptoms was achieved in 92%, 100%, and 0% of the patients showing obstruction, abdominal pain, and bleeding, respectively.

### **Conclusions**

In conclusion, the response rate was 64% and the mean reduction rate was as high as 50% although the patients underwent palliative radiotherapy. The median time of the maximum tumor reduction was 4.7 months after radiotherapy.

Key Words: Gastric cancer; Radiotherapy; Radio sensitivity; Chemotherapy

## Introduction

Gastric cancer is the fifth most common cancer and was the second leading cause of cancer-related deaths worldwide in 2013. In developed countries, it ranks fifth for incidence and third for mortality, and in developing countries, it ranks third for both incidence and mortality<sup>1</sup>. Surgery has been a

---

Received July 10, 2018; accepted April 19, 2019.

Correspondence to: Masaru Makihara, MD.

Department of Radiology, Izumi City General Hospital,

Wake-cho 4-5-1, Izumi, 594-0073, Japan

Tel: +81-725-41-1331; Fax: +81-725-43-3350

E-mail: macky449344@yahoo.co.jp

mainstay in the treatment of gastric cancer. Several clinical studies on preoperative chemoradiotherapy showed pathological complete response in 9%-26% of patients with the disease<sup>2-4</sup>. Thus, gastric cancer is suggested to be radiosensitive.

In Japan, radiation therapy is performed mainly for palliation of symptoms from the disease, and in a limited number of the patients with unresectable, highly advanced gastric cancer. Several reports presented favorable outcome of palliative radiotherapy<sup>5-7</sup>. In this study, the clinical response to palliative radiotherapy for gastric cancer was evaluated using follow-up CT.

## Methods

The institutional review board approved this study. This study was conducted in accordance with the Declaration of Helsinki.

### **Patient population**

Between November 2011 and March 2016, a total of 17 consecutive patients with gastric cancer underwent palliative radiation therapy with a dose of 30 Gy or more for the primary site, the regional lymph node metastasis, or disseminated lesions at our institution. Three patients were excluded from the study since they had not undergone abdominal CT after radiotherapy. The remaining 14 patients who underwent CT comprised the study group. In all patients, measurable lesions with a longitudinal diameter of 10 mm or more were observed.

Patient characteristics are summarized in Table 1 and Table 2. All patients had a pathological diagnosis of adenocarcinoma and had stage IV disease. Before radiotherapy, 12 patients had received

**Table 1. Patient characteristics**

Characteristics	Value
Age (years)	
Range	47-79
Median	70
Gender	
Male	10
Female	4
Performance status (ECOG <sup>*</sup> )	
1	6
2	8
Presenting symptoms <sup>**</sup>	
Bleeding	3
Abdominal pain	5
Obstruction	12
Treatment before radiotherapy	
Curative gastrectomy	3
Chemotherapy	12
Concurrent chemotherapy	
Yes	7
No	7
Adjuvant chemotherapy	
Yes	10
No	4

<sup>\*</sup> Eastern Cooperative Oncology Group.

<sup>\*\*</sup> Symptoms partly overlap.

**Table 2. Patient characteristics and reduction rate**

Age (years)	Gender	Stage	Radiation dose (Gy)	CTV <sup>a</sup>	Concurrent chemotherapy	Surgery	Diameter <sup>b</sup> (mm)	Reduction rate	Number of CT <sup>c</sup> (range of interval)
61	M	IV	36	Primary site	CDDP, 5FU <sup>f</sup>	-	70.6	100%	5 (2.5-12.6 mo)
70	M	IV	36	Primary site	CDDP	-	44	100%	3 (1.6-6.5 mo)
47	F	IV	33	Disseminated mass	-	+	36.5	59%	4 (0.9-9.6 mo)
63	M	IV	36	Primary site	-	-	128	35%	1 (1.3 mo)
70	M	IV	36	Primary site	TS1	-	49.8	44%	5 (0.6-3.2 mo)
64	F	IV	36	Primary site	-	-	64.7	0%	1 (0.9 mo)
64	M	IV	36	Primary site	PTX <sup>g</sup>	-	95.1	100%	7 (1.4-13.3 mo)
76	M	IV	36	Primary site	-	-	79.2	65%	7 (0.7-10.3 mo)
47	M	IV	37.5 <sup>d</sup>	Disseminated mass	-	+	39.5	100%	16 (2.9-30.2 mo)
79	F	IV	36	Primary site	-	-	41.3	17%	2 (0.2-0.8 mo)
72	M	IV	36	Primary site	HER <sup>h</sup>	-	59.1	64%	2 (0.8-4.7 mo)
74	M	IV	36	Lymph Node	-	+	29.6	18%	2 (1.0-3.1 mo)
75	F	IV	36	Primary site	TS1	-	34.1	1%	1 (1.1 mo)
66	M	IV	36	Primary site	PTX	-	98.7	0%	2 (0.8-3.3 mo)

<sup>a</sup>CTV, clinical target volume; <sup>b</sup>Maximal tumor diameter; <sup>c</sup>CT, computed tomography; and <sup>d</sup>The daily dose was 2.5 Gy. For all other patients, the daily dose was 3.0 Gy. <sup>e</sup>CDDP, cis-diamminedichloridoplatinum (cisplatin); <sup>f</sup>5FU, 5-fluorouracil; <sup>g</sup>PTX, paclitaxel; and <sup>h</sup>HER, herceptin (trastuzumab).

chemotherapy. Among them, 3 patients had undergone curative gastrectomy. In these patients, relapsed tumor after the treatment was irradiated.

### **Treatment**

Radiation was administered with 10 MV photons from a linear accelerator (Mevatron Primus: Siemens, Munich, Germany). All patients underwent three-dimensional conformal radiotherapy using the involved field. Principally, the clinical target volume (CTV) contained the gross tumor volume plus a 5 mm or more margin, and the planning target volume contained the CTV plus a 5 mm or more margin. Radiation doses ranged from 33 to 37.5 Gy (median, 36 Gy). Twelve patients (86%) received 36 Gy in 12 fractions. In 7 patients, chemotherapy was performed concurrently with radiotherapy. The contents were TS-1 (n=2), paclitaxel (n=2), 5-fluorouracil plus cisplatin (n=1), cisplatin (n=1), and trastuzumab (n=1). After completion of abdominal radiotherapy, 2 patients underwent additional palliative radiotherapy for other sites.

### **Evaluation**

In the present study, the primary endpoint was response, which was evaluated using the Response Evaluation Criteria in Solid Tumors (RECIST) version 1.1<sup>8)</sup>. CT examination was performed under diet restriction in principle. In this patient group, the number of CT ranged from 1 to 16, and the interval ranged from 0.2 to 30.2 months (Table 2). Evaluation was performed when the maximum reduction was obtained. The secondary endpoint was palliation of symptoms. Palliation of obstruction and abdominal pain were evaluated based on complaint of the patients. And palliation of bleeding was evaluated using hemoglobin value. Furthermore, toxicity was evaluated according to the Common Terminology Criteria for adverse Effect (CTCAE) version 4.0<sup>9)</sup>. Follow-up was performed starting from the day 1 of irradiation.

### **Analysis**

Survival rates were calculated with the Kaplan-Meier method. Statistical analyses were performed with the Mann-Whitney U-test.

## **Results**

The follow-up time ranged from 9.6 to 30.2 months (median, 19.9 months). The response rate based on the RECIST was 64%. The mean reduction rate was 50% (range, 0%-100%). For 7 patients who underwent concurrent chemoradiotherapy, the mean reduction rate was 58% (p=0.56). Four patients achieved 100% reduction. The maximum reduction was observed between 2.0 and 6.8 months (median, 4.7 months) after radiotherapy for patients who underwent CT twice or more.

An overall survival curve is shown in Figure 1. One-year survival was 21%, and median survival time was 5.6 months. An in-field control curve was drawn in Figure 2. When relapse was classified into in-field relapse, out-field relapse, and marginal relapse according to the radiation field, one-year in-field control was 59% at this dose.

Palliation of the symptoms was achieved in 92%, 100%, and 0% of the patients showing obstruction (n=12), abdominal pain (n=5), and bleeding (n=3), respectively. Palliation of obstruction was obtained with an interval ranging from 3 to 44 days (median, 5 days) after the beginning of radiotherapy, and that of abdominal pain was obtained with an interval ranging from 4 to 87 days (median, 17 days) after the beginning of radiotherapy. Grade 3 hematologic toxicity and grade 1 gastrointestinal toxicity were observed in 2 and 3 patients, respectively. However, none of the patients showed grade 4 hematologic toxicity or greater than grade 2 non-hematologic toxicity.

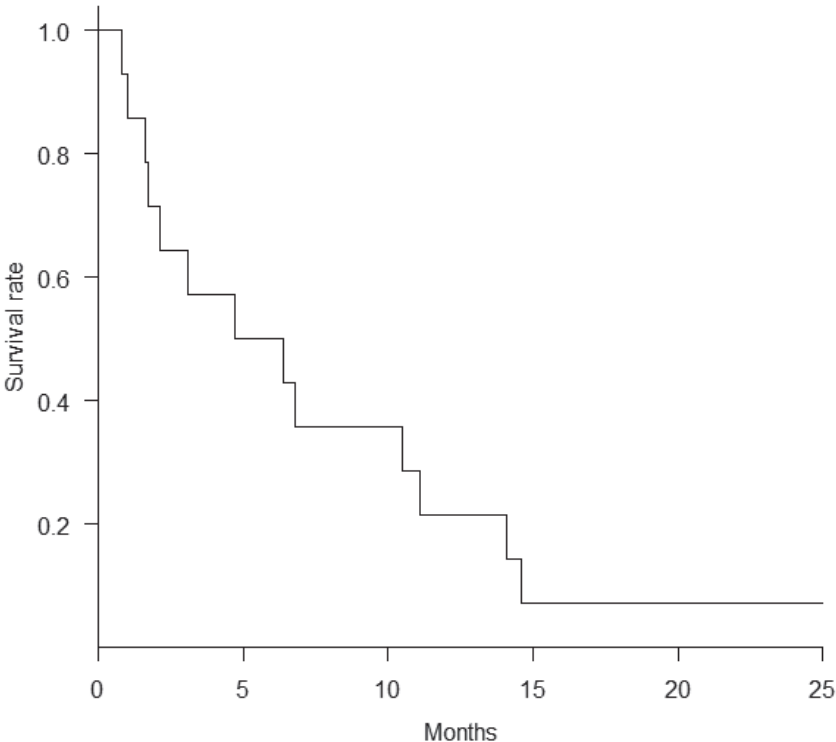


Figure 1. Kaplan-Meier survival rate curve for all patients.

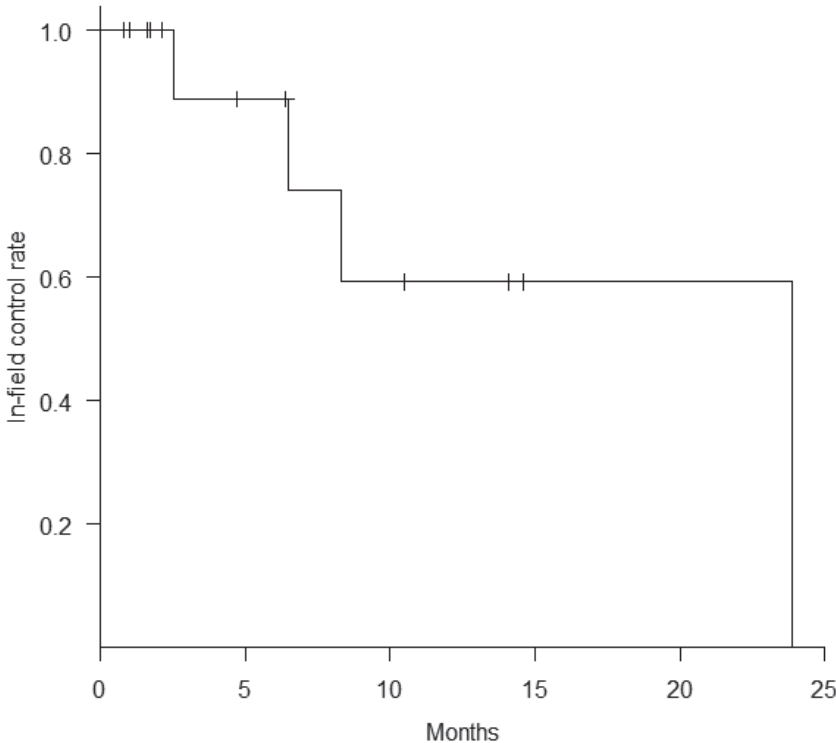


Figure 2. Kaplan-Meier in-field control rate curve for all patients.

## Discussion

Saikawa et al performed a phase II study of chemoradiation with a dose of 40 Gy in 20 fractions for patients with inoperable advanced gastric cancer and reported that clinical response rate was 66%<sup>3)</sup>. For patients with recurrent lymph node metastasis or local recurrence after curative gastrectomy, Ishido et al reported the response rate of 62% in chemoradiotherapy with a median dose of 48.6 Gy<sup>11)</sup>. The response rate of 64% in the present study was consistent with these reports in spite of palliative radiotherapy. Furthermore, 4 patients achieved 100% reduction. Thus, gastric cancer showed acceptable radiosensitivity, and it was encouraging. When this radiosensitivity is taken into account in the clinic, more aggressive treatment can be chosen for patients with lower stage disease and the dose can be modified for patients with poor performance status.

Another finding in the study was the timing of the maximum reduction. The median time of 4.7 months was longer than what we anticipated. For patients, in whom the radiation effect was insufficient just after radiotherapy, further downsizing could be expected. Berrington et al reported that annual radiation exposure was the highest in Japan<sup>10)</sup>. Unnecessary CT examination should be avoided to reduce radiation exposure for the population. However, this frequent CT examination brought these findings in this study.

Due to the acceptable radiosensitivity of gastric cancer, relief from obstruction or abdominal pain was obtained in a majority of patients. Although relief from bleeding was confirmed in none of the patients, there was a possibility that bleeding was not appropriately evaluated in this retrospective study. In addition, there were only 3 patients who suffered from bleeding in the study group. Tey et al reported that 80.6% of patients with bleeding responded to radiotherapy with a dose ranging from 8 Gy in a single fraction to 40 Gy in 16 fractions<sup>5)</sup>. When appropriate evaluation was performed, the rate of relief might increase.

Asakura et al concluded that a dose of 30 Gy in 10 fractions was adequate in patients with poor prognosis<sup>7)</sup>. Although a little higher doses were delivered in the present study, severe toxicity was not observed. These doses can be chosen when the prognosis of patients is not so poor.

Although statistical significance was not observed, the patients who underwent chemoradiotherapy showed favorable reduction rate. These results suggested existence of radiosensitizing effect of chemotherapy in gastric cancer. Past reports with use of chemoradiotherapy also presented favorable response rate.<sup>3,11)</sup>

There were several limitations in the present study since it was a retrospective one. With the eligibility criteria, 3 patients who did not undergo CT after radiotherapy were excluded. When the effect of radiotherapy was insufficient, the opportunity to perform CT decreased even in Japan. Therefore, these exclusions might cause a bias to overestimation. On the other hand, the study group contained 3 patients who underwent CT only once after radiotherapy. If additional CT could be obtained, their reduction rate might improve and that caused for a bias to underestimation. In addition, 10 patients underwent adjuvant chemotherapy was after completion of radiotherapy. This might cause for a bias to overestimation.

In conclusion, the response rate was 64% and the mean reduction rate was as high as 50% although the patients underwent palliative radiotherapy. The median time of the maximum reduction was 4.7 months after radiotherapy.

### **Acknowledgements**

All authors have no COI to declare regarding the present study.

### **References**

1. Global Burden of Disease Cancer Collaboration, Fitzmaurice C, Dicker D, et al. The global burden of cancer 2013. *JAMA Oncol* 2015;1:505-527.
2. Ajani JA, Winter K, Okawara GS, et al. Phase II trial of preoperative chemoradiation in patients with localized gastric adenocarcinoma (RTOG 9904): quality of combined modality therapy and pathologic response. *J Clin Oncol* 2006;24:3953-3958.
3. Saikawa Y, Kubota T, Kumagai K, et al. phase II study of chemoradiotherapy with S-1 and low-dose cisplatin for inoperative advanced gastric cancer. *Int J Radiat Oncol Biol Phys* 2008;71:173-179.
4. Rivera F, Galán M, Tabernero J, et al. Phase II trial of preoperative irinotecan-cisplatin followed by concurrent irinotecan-cisplatin and radiotherapy for resectable locally advanced gastric and esophagogastric junction adenocarcinoma. *Int J Radiat Oncol Biol Phys* 2009;75:1430-1436.
5. Tey J, Choo BA, Leong CN, et al. Clinical outcome of palliative radiotherapy for locally advanced symptomatic gastric cancer in the modern era. *Medicine (Baltimore)* 2014;93:e118.
6. Sun J, Sun YH, Zeng ZC, et al. Consideration of the role of radiotherapy for abdominal lymph node metastases in patients with recurrent gastric cancer. *Int J Radiat Oncol Biol Phys* 2010;77:384-391.
7. Asakura H, Hashimoto T, Harada H, et al. Palliative radiotherapy for bleeding from advanced gastric cancer: is a schedule of 30 Gy in 10 fractions adequate? *J Cancer Res Clin Oncol* 2011;137:125-130.
8. Eisenhauer EA, Therasse P, Bogaerts J, et al. New response evaluation criteria in solid tumors: revised RECIST guideline (version 1.1). *Eur J Cancer* 2009;45:228-247.
9. National Cancer Institute Common Terminology Criteria for Adverse Events (CTCAE). Washington, DC: US department of Health and Human Services, National Cancer Institute; 2010; Available from: <http://evs.nci.nih.gov/ftp1/CTCAE/About.html>.
10. Berrington de González A, Darby S. Risk of cancer from diagnostic X-rays: estimates for the UK and 14 other countries. *Lancet* 2004;363:345-351.
11. Ishido K, Higuchi K, Tanabe S, et al. Chemoradiotherapy for patients with recurrent lymph-node metastasis or local recurrence of gastric cancer after curative gastrectomy. *Jpn J Radiol* 2016;34:35-42.



# The Neural Effects of Inadequate Pauses in Speech on the Comprehension of Logical and Illogical Speeches: A Magnetoencephalography Study

YUKI KODA, and KISHIKO SUNAMI

*Department of Otolaryngology and Head & Neck Surgery, Osaka City University  
Graduate School of Medicine*

## Abstract

### **Background**

The comprehension of speech is often affected by the missing of the parts of speech due to such as background noise. The disturbance of the connections among sounds in speech which should be uttered continuously to make the speech intelligible may be a reason for the impaired comprehension of the speech. Therefore, we aimed to clarify the neural mechanisms related to the comprehension of speech in which pauses are placed at inadequate places in sentence by using magnetoencephalography (MEG).

### **Methods**

Twenty-four healthy male volunteers with normal hearing ability, whose native language is Japanese, participated in our present study. They listened to the speeches in Japanese based on logically-correct and logically-incorrect stories read with inadequate pauses and the comprehension of the speeches and the neural activity related to listening to the speeches were assessed compared with those observed when listening to the speeches read with adequate pauses.

### **Results**

The level of the comprehension of speech was lower when listening to logically-correct and logically-incorrect stories read with inadequate pauses compared with when listening to the speeches read with adequate pauses. The increase of gamma band power in the Brodmann's area (BA) 10 observed when listening to the speeches based on logically-correct stories read with inadequate pauses was negatively associated with the deterioration of the comprehension.

### **Conclusions**

Our findings may help understand the neural mechanisms related to the comprehension of speech, especially in the situation that the disturbance of the connections within the semantically related words is caused by background noise.

Key Words: Comprehension of speech; Pause; Illogical sentence;  
Magnetoencephalography (MEG)

---

Received July 22, 2019; accepted October 8, 2019.

Correspondence to: Yuki Koda, MD.

Department of Otolaryngology and Head & Neck Surgery, Osaka City University Graduate School of Medicine,  
1-4-3 Asahimachi, Abeno-ku, Osaka 545-8585, Japan  
Tel: +81-6-6645-3871; Fax: +81-6-6646-0515  
E-mail: m1162337@med.osaka-cu.ac.jp

## Introduction

The comprehension of speech is often affected by the missing of the parts of speech due to such as background noise. It has been reported that the speech discrimination in noisy environments is worse in the hearing-impaired individuals than in the normal hearing individuals<sup>18)</sup> and that the patients with cochlear implantation are susceptible to the effects of background noise on the recognition of speech<sup>9)</sup>. Thus, clarifying the neural mechanisms of the comprehension of speech in noisy environments is beneficial to develop treatment methods for those suffering from difficulty in speech comprehension in noisy environments.

It is known that the auditory system is capable of restoring missing sounds in speech replaced by extraneous sound and listeners feel as if they hear the missing sound as a result (i.e., phonemic restoration)<sup>25)</sup>. It has been proposed that the disability of phonemic restoration can impair speech comprehension in noisy environment<sup>1,23)</sup>. In the case of failure in restoring the missing sound in speech, the incomplete words and/or sentences caused by the missing of the sound would deteriorate the comprehension of the speech. In addition to the missing of the acoustic information which is necessary to identify the words used in sentences, the disturbance of the connections within the semantically related units caused by the extraneous sounds may be a reason for the deterioration of the comprehension of the speech.

There have been reports that investigated the effects caused by replacing parts of continuous speech or words with noise stimuli or temporal gaps on the comprehension of the speech and the alterations of neural activity caused by the replacements. It has been reported that the replacement of the portions of words or sentences in speech with silence caused the decrease of recognition score (i.e., intelligibility) in listeners with and without hearing impairment<sup>11,20)</sup> and that the deterioration of the intelligibility of sentence whose portions were replaced by silence was greater in older listeners with and without hearing impairment than in younger listeners with normal-hearing<sup>20)</sup>. In a study in which neural activity related to the comprehension of segmented speech created by replacing parts of speech with noise having a spectral profile and amplitude envelope identical to those of the original speech was assessed by using functional magnetic resonance imaging (fMRI), the activation in periauditory brain areas was observed in relation to the comprehension of segmented speech<sup>4)</sup>. In another fMRI study, the replacement of the parts of speech with silence affected the neural activity in the left frontal gyrus, right medial frontal gyrus, left temporal cortex, parahippocampal gyrus, posterior cingulate cortex, caudate, thalamus, and right superior temporal gyrus<sup>24)</sup>. In these studies, since parts of speech or words were replaced by noise or silence to simulate the comprehension of speech contaminated by noise in real world<sup>20)</sup>, the deterioration of the comprehension of speech may be caused by both the missing of acoustic information and the disturbance of the connections within the semantically related units. In fact, although the deterioration of the comprehension of speech caused by the insertion of silent intervals into speech (i.e., parts of speech were not replaced by silence) was reported<sup>10)</sup>, there seems to be no report that directly investigated the neural mechanisms related to the deterioration of the comprehension of speech caused by the disturbance of the connections within the semantically related units in speech. We hypothesized that there was a difference in neural activity by the disturbance of the connections among sounds in speech (between adequate pauses and unnatural intonation).

In our present study, we examined neural activity related to the comprehension of speech read aloud with inadequate pauses. Logical writings in Japanese written for general population in Japan

were read aloud by a professional announcer with and without adequate pauses: In the speeches read aloud with inadequate pauses, although pauses in speech are usually placed between the semantic units, the pauses were placed at inadequate places in the speech so as to disturb the connections within the semantically related units in the speech. We required our participants to answer whether they were able to follow the logic of each speech or not. In addition to the original writings, the logic of which were relatively easy to follow, the writings modified from original ones to be illogical were also used to assess the effects caused by the inadequate pauses on the comprehension of relatively difficult speech to follow their logic. The neural activity during listening to the speeches was assessed by using magnetoencephalography (MEG) with high temporal and spatial resolutions. It has been reported that the neural oscillations assessed by MEG are related to the processing of sentences and speeches<sup>13,15</sup>. The experiment of our study included a condition in which the writings were read aloud with unnatural intonation and a set of speeches whose conclusions were modified to be wrong; however, the data regarding these conditions and set of speeches were not analyzed in this study.

We aimed to clarify the neural activity caused by the disturbance of the connections among sounds in speech which should be uttered continuously to make the speech intelligible.

## **Methods**

### ***Participants***

Twenty-four healthy male volunteers, whose native language are Japanese, with normal hearing ability [ $23.1 \pm 2.6$  years of age (mean  $\pm$  SD)] participated in this study. The participants were all undergraduate students. All participants were right-handed according to the Edinburgh Handedness Inventory<sup>16</sup>. Current smokers, individuals with a history of mental illness, brain injury, or upper extremity disorder, and individuals taking chronic medications that affect the central nervous system were excluded. The Ethics Committee of Osaka City University approved the study protocol (approval number, 3850) and this study was conducted in accordance with the Declaration of Helsinki and the Japanese Ethical Guidelines for Medical and Health Research Involving Human Subjects. All participants provided written informed consent for participation in this study.

### ***Experimental design***

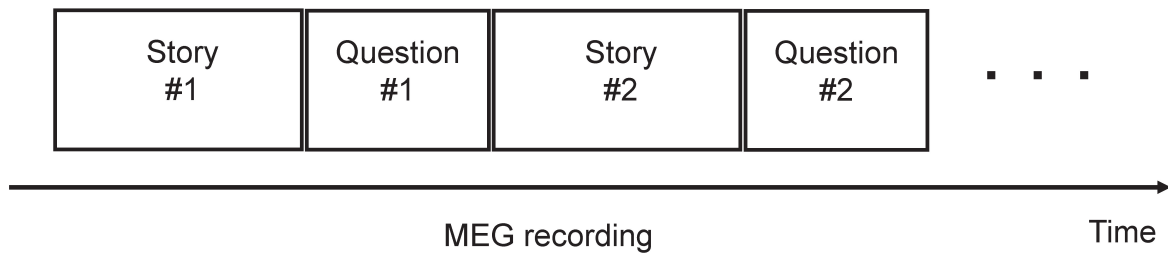
In our present study, the participants lay on a bed placed in a magnetically shielded room and listened to 45 different stories in a row with their eyes closed (Fig. 1A). The neural activity during listening to the stories was recorded by MEG. Just after listening to each story, they were asked whether they were able to follow the logic of the story and to choose their answer from three options: first option, “there was no leap in logic in the story and I was able to comprehend the points of the story”; second option, “there was a leap in logic in the story; however, I was able to comprehend each sentence in the story”; third option, “I was not able to comprehend the story even at sentence level and thus, I was not able to figure out whether there was a leap in logic or not”. They were instructed to call the number of the options (i.e, first, second, or third) they chose.

### ***Stories***

Fifteen stories in Japanese were selected from logical essays written for Japanese general population by Japanese philosophers. Another 15 stories were created by modifying original stories to be logically incorrect but the conclusions of the story were not changed (illogical stories; Fig. 1B). The other 15 stories were created by modifying the conclusions of the original stories to be contradictory to the original ones (wrong stories; Fig. 1B). Each story was read aloud by a

professional announcer with adequate pauses, with an unnatural falling intonation (i.e., a segment of a sentence which was read without pause was read with high tone at the beginning and the tone gradually decreased toward the end of the segment, irrespective of the meaning the segment conveys), and with inadequate pauses (i.e., pausing regardless of semantic unit including the pauses such that placed at the middle of a word). The voice was recorded by using Wave Pad (NCH Software). It is of note that the data regarding the speeches whose conclusions were contradictory to the original ones (i.e., wrong stories) and the speeches read aloud with unnatural intonation were not analyzed in our present study. Forty-five stories were randomly selected for each participant to include same number of stories in each of nine story-categories (i.e., original, illogical, and wrong stories read with adequate pauses, those read with inadequate pauses, and those read with unnatural intonation; Fig. 1B). The numbers of letters and the reading rates (letters/min) of the speeches each participant listened to were summarized in Table 1 (n=19, as described in the Results). The reading rates for the speeches based on the original ( $p=0.306$ ,  $t_{18}=1.0$ ) and illogical ( $p=0.105$ ,  $t_{18}=1.7$ ) stories read with inadequate pauses and the speeches based on the illogical stories read with adequate pauses ( $p=0.8689$ ,  $t_1=0.2$ ) were not different from that for the speeches based on the original stories read with adequate pauses (paired t-test). The recorded stories were played on a Windows Media player (2010) using a speaker

A



B

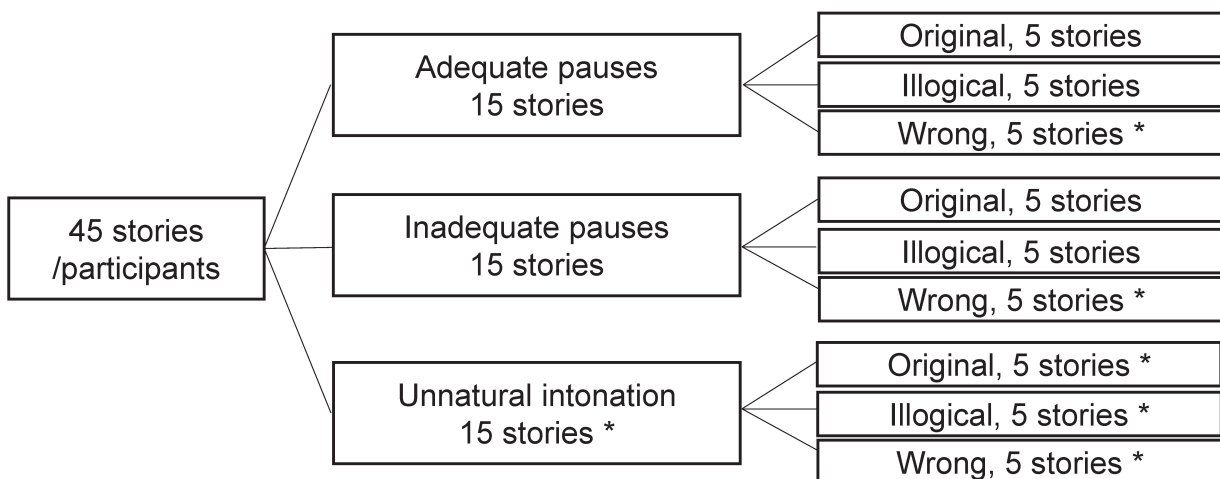


**Figure 1.** Experimental procedure.

A. It is written in the methods (*Experimental design*) in the text.

B. It is written in the method (*stories*) in the text. In our present study, the data regarding the speeches read with unnatural intonation and the speeches with modified conclusions (i.e., wrong stories) were not analyzed. The speeches whose data were not analyzed were marked with asterisk.

**Table 1. The summary of the numbers of letters and the reading rates (letters/min) of the speeches which each participant listened to during the MEG measurements**

		Adequate pauses		Inadequate pauses	
		Original stories	Illogical stories	Original stories	Illogical stories
Letters	Mean	227.2	223.2	226.3	222.1
	SD	14.7	11.9	12.1	17.2
Reading rate (letters/min)	Mean	400.6	403.2	418.0	420.3
	SD	34.7	39.6	42.9	29.5

MEG, magnetoencephalography.

system (SANWA SUPPLY INC., Okayama, Japan) placed outside the shield room during the MEG recordings. The extent to which each participant was able to follow the logic of the speeches based on the original stories was assessed by the percentage of the number of the speeches for which the participants selected the first option out of the three choices and the extent to which each participant was able to follow the logic of the speeches based on the illogical stories was assessed by the percentage of the number of the speeches for which the participants selected the second option out of the three choices. All the participants declared that they had not read or listened to the original stories presented during the experiments.

### **MEG recording**

MEG was recorded using a 160-channel whole-head-type MEG system (MEG vision; Yokogawa Electric Corporation, Tokyo, Japan) with a magnetic field resolution of  $4 \text{ fT/Hz}^{1/2}$  in the white-noise region. The sensor and reference coils were gradiometers with 15.5 mm diameter and 50 mm baseline, and the two coils were separated by 23 mm. The sampling rate was 1000 Hz and data were high-pass filtered at 0.3 Hz.

### **MEG analyses**

Before processing the MEG data, the magnetic noise that originated from outside the magnetically shielded room was eliminated by subtracting the data obtained from reference coils using specialized software (MEG160; Yokogawa Electric Corporation, Tokyo, Japan). Epochs of the raw MEG data that included artifacts were visually identified and were excluded before averaging. Spatial filtering analysis of the MEG data was performed to identify changes in oscillatory brain activity that reflected time-locked cortical activities<sup>8,17)</sup> caused by listening to the speeches based on the original and illogical stories read with adequate and inadequate pauses. The MEG data were bandpass filtered at 1-4 Hz, 4-8 Hz, 8-13 Hz, 13-25 Hz, and 25-58 Hz by a finite impulse response filtering method using Brain Rhythmic Analysis for MEG software (BRAM; Yokogawa Electric Corporation, Tokyo, Japan) to obtain delta, theta, alpha, beta, and gamma signals, respectively. After the bandpass filtering, the location and intensity of the cortical activities were estimated using BRAM, which uses a narrow-band adaptive spatial filtering algorithm<sup>2,19)</sup>. Voxel size was set at  $5.0 \times 5.0 \times 5.0 \text{ mm}$ . For each frequency band, the oscillatory power of the MEG data during listening to one type of speech was compared with that during listening to another type of speech (i.e., the beamformer images as oscillatory power ratio). To minimize any effects caused by the initiations and cessations of the

auditory stimuli, oscillatory power ratio was calculated for the MEG data from 2000 ms after the start of each speech to 2000 ms before the end of the speech.

Data were then analyzed using statistical parametric mapping (SPM8, Wellcome Department of Cognitive Neurology, London, UK), implemented in Matlab (Mathworks, Natick, MA). The individual structural MRI image was transformed into the Montreal Neurological Institute T1-weighted image template<sup>5</sup>. The beamformer images registered to the individual MRI image was normalized applying the same parameters used when the individual structural MRI was normalized. The anatomically normalized beamformer images were filtered with a Gaussian kernel of 20 mm (full-width at half-maximum) in the x-, y-, and z-axes. To enable inferences to be made at a population level, individual data were summarized and incorporated into a random-effect model<sup>7</sup>. The weighted sum of the parameters estimated in the individual analysis was used to create “contrast” images that were used for group analyses<sup>7</sup>. The resulting set of voxel values for each comparison constituted a statistical parametric map (SPM) of the t statistic [SPM(t)]. The SPM(t) was transformed to the units of normal distribution [SPM(Z)]. The significance of any difference in the oscillatory power caused by listening to the speeches based on the original and illogical stories read with inadequate pauses and those based on the illogical stories read with standard intonation, compared with those based on the original stories read with standard pauses, was assessed using t statistics (one sample t test) on a voxel-by-voxel basis<sup>7</sup>. The height threshold for the SPM(t) of the one sample t test was set at  $p < 0.0017$  (family-wise-error corrected for multiple comparisons), considering the number of contrasts (i.e., the original stories read with inadequate pauses vs the original stories read with adequate pauses, the illogical stories read with adequate pauses vs the original stories read with adequate intonation, and the illogical stories read with inadequate pauses vs the original stories read with adequate pauses) and frequency bands (i.e., delta, theta, alpha, beta, and gamma bands). In addition, the peak voxels located within the cluster larger than 1 voxel was reported. Localization of the brain regions was performed using WFU\_PickAtlas, Version 3.0.4 (<http://fmri.wfubmc.edu/software/pickatlas>) and Talairach Client, Version 2.4.3 (<http://www.talairach.org/client.html>).

### ***Magnetic resonance (MR) image overlay***

Anatomical MR imaging was performed using a Philips Achieva 3.0 TX (Royal Philips Electronics, Eindhoven, The Netherlands) to permit registration of magnetic source locations with their respective anatomical locations. Before MR scanning, five adhesive markers (Medtronic Surgical Navigation Technologies Inc., Broomfield, CO.) were attached to the skin of the head: two markers 10 mm in front of the left and right tragus, one marker 35 mm above the nasion, and two markers 40 mm to either side of the marker above the nasion. The MEG data were superimposed on MR images using information obtained from these markers and MEG localization coils.

### ***Statistical analyses***

Values are presented as mean and SD unless otherwise stated. A paired t-test with Bonferroni correction was used to compare the correction rates of the questions for speeches based on the original stories read with adequate pauses with those based on the original and illogical stories read with inadequate pauses and those based on the original stories read with adequate pauses. Relationships between the correction rates for the questions and the alterations of oscillatory band power were evaluated using Pearson’s correlation analyses. All p values were two-tailed and values less than 0.05 were considered statistically significant. These statistical analyses were performed using the IBM SPSS 21.0 software package (IBM, Armonk, NY).

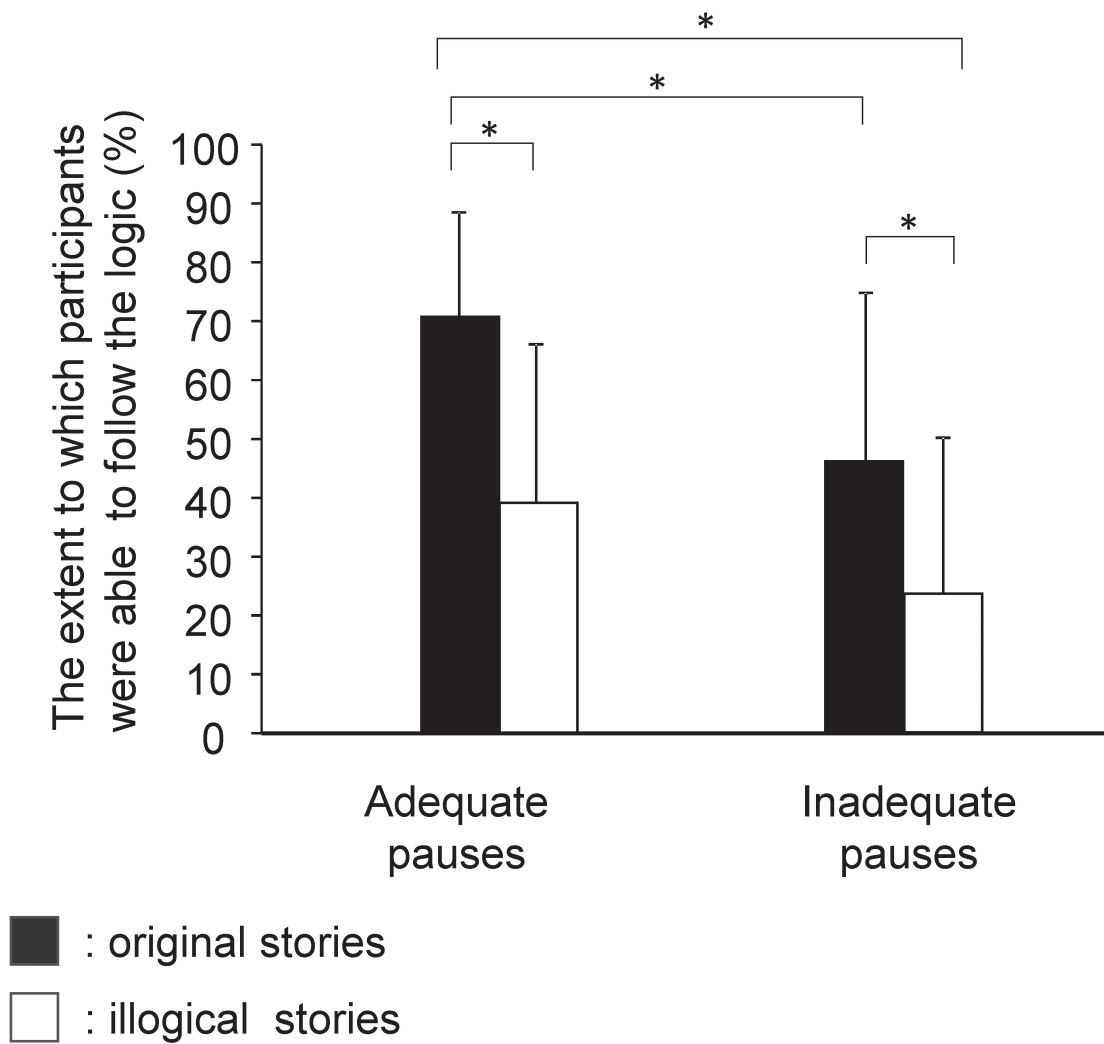


**Figure 2.** Closed column indicates the data corresponding to the speeches based on the original stories and open column indicate the data corresponding to the speeches based on the illogical stories. Data are presented as mean  $\pm$  SD. \* $p < 0.05$ , paired t-test with Bonferroni correction.

## Results

### *The extent to which participants followed the logic of the speeches*

The data from five participants were excluded from the analysis: The MEG data from three participants were contaminated with magnetic noise that originated from outside the shielded room and the MEG data from the other two participants were excluded because of their head motion during the MEG recording.

The extent to which participants were able to follow the logic of the speeches (i.e., the comprehension of logic) were calculated for the speeches based on the original stories read with standard intonation (hereinafter refer to as “original A”), those based on the original stories read with inadequate pauses (hereinafter refer to as “original I”), and those based on the illogical stories read with inadequate pauses (hereinafter refer to as “illogical I”) (Fig. 2). The comprehension of logic for the speeches based on the original I was lower than that for the speeches based on the original A ( $p < 0.011$ ,  $t_{18} = 3.6$ , paired t-test with Bonferroni’s correction). Both in the speeches read with adequate and inadequate pauses, the comprehension of logic for the speeches based on the illogical stories was lower than that

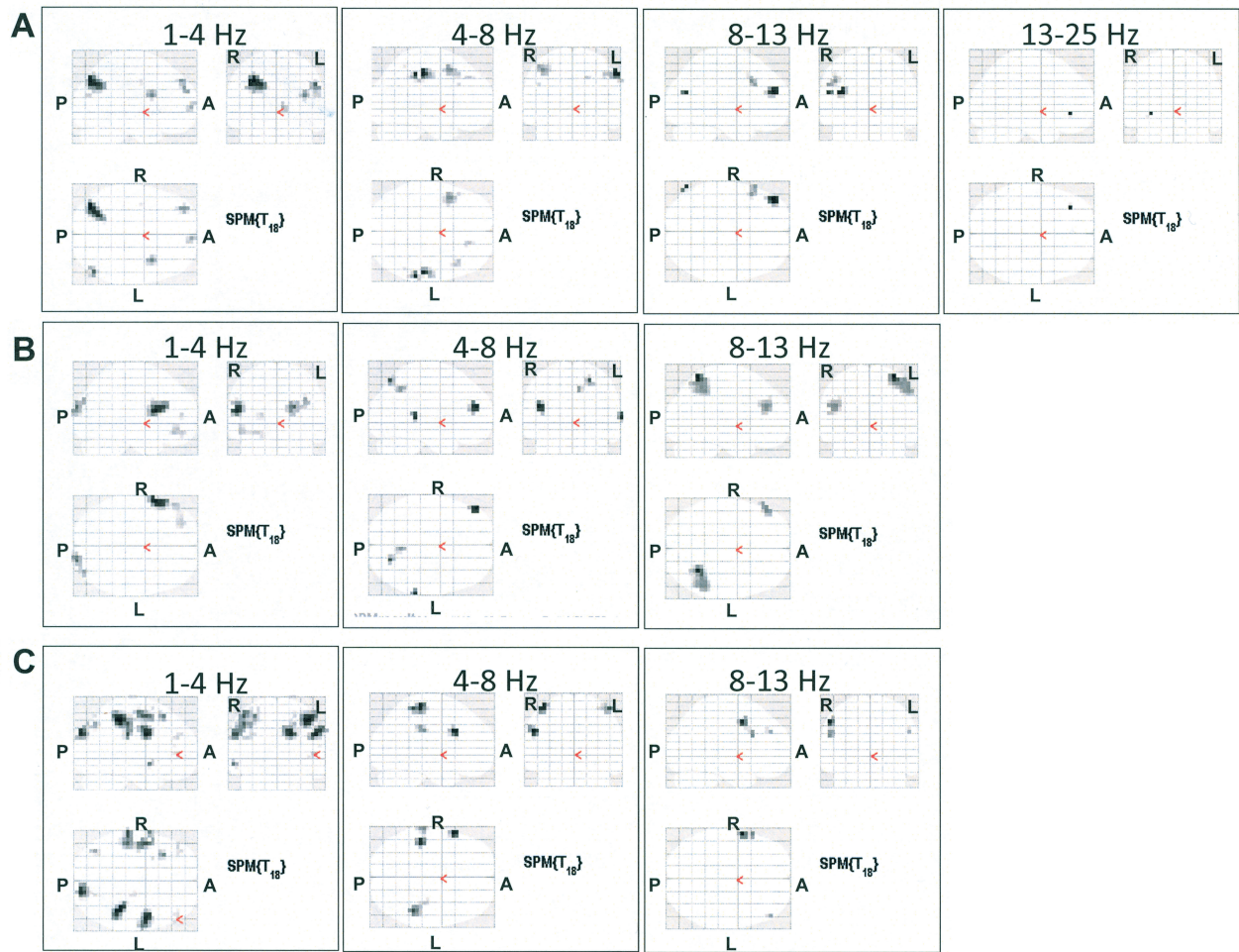


**Figure 3.** Statistical parametric maps of the brain regions where oscillatory power was lower when listening to the speeches read with inadequate pauses and those based on illogical A compared with when listening to the speeches based on the original A. The decreases of oscillatory band power caused by listening to the speeches based on the original stories read with inadequate pauses A, the decreases of oscillatory band power caused by listening to the speeches based on the illogical stories read with inadequate pauses B, and the decreases of oscillatory band power caused by listening to the speeches based on the illogical stories read with adequate pauses C were observed compared with when listening to the speeches based on the original A. Random-effect analyses of 19 participants,  $p < 0.0017$ , family-wise-error corrected for the entire search volume (A, anterior; P, posterior; L, left; and R, right).

for the speeches based on the original stories ( $p = 0.020$  and  $t_{18} = 3.4$  for the adequate pauses and  $p = 0.039$  and  $t_{18} = 3.1$  for the inadequate pauses, paired t-test with Bonferroni's correction). The comprehension of logic for the speeches based on the illogical I was lower than that for the speeches based on the original A ( $p < 0.001$ ,  $t_{18} = 6.7$ , paired t-test with Bonferroni's correction).

The number of the speeches which our participants thought to be incorrect did not differ between the speeches based on the original I and those based on the original A ( $p = 0.450$ ,  $t_{18} = 0.8$ , paired t-test without correction for multiple comparisons) and between the speeches based on the illogical I and those based on the original A ( $p = 0.450$ ,  $t_{18} = 0.8$ , paired t-test without correction for multiple comparisons).

### ***Spatial filtering analyses of MEG data***

To identify the alterations in the oscillatory power caused by the speeches based on the original I, oscillatory powers in delta, theta, alpha, beta, and gamma bands caused by listening to the speeches

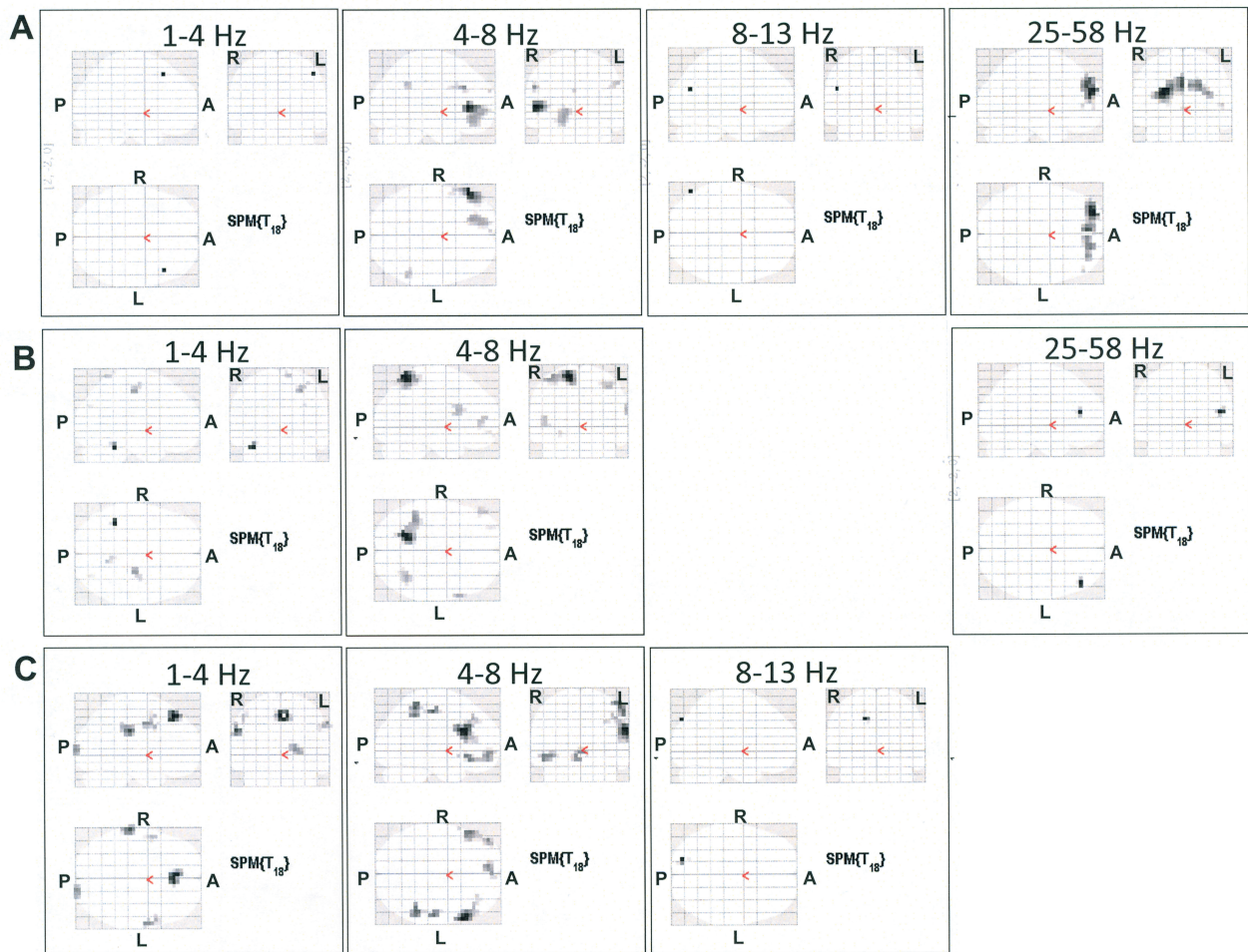


**Figure 4.** Maximum intensity projections of the statistical parametric maps of the brain regions where oscillatory power was higher when listening to the speeches read with inadequate pauses and those based on illogical A compared with when listening to the speeches based on the original A. The increases of oscillatory band power caused by listening to the speeches based on the original stories read with inadequate pauses A, the increases of oscillatory band power caused by listening to the speeches based on the illogical stories read with inadequate pauses B, and the increases of oscillatory band power caused by listening to the speeches based on the illogical stories read with adequate pauses C were observed compared with when listening to the speeches based on the original A. Random-effect analyses of 19 participants,  $p < 0.0017$ , family-wise-error corrected for the entire search volume (A, anterior; P, posterior; L, left; and R, right).

based on the original I were compared with those caused by listening to the speeches based on the original A. There were brain regions in which the oscillatory power caused by listening to the speeches based on the original I was smaller (Fig. 3A) or greater (Fig. 4A) than that caused by listening to the speeches based on the original A (Table 2).

To identify the effects caused by the speeches based on the illogical I, the oscillatory powers caused by listening to the speeches based on the illogical I were compared with those caused by listening to the speeches based on the original A. There were brain regions in which the oscillatory power caused by listening to the speeches based on the illogical I was smaller (Fig. 3B) or greater (Fig. 4B) than that caused by listening to the speeches based on the original A (Table 3).

In addition, to identify the effects caused by the speeches based on the illogical stories read with adequate pauses (hereinafter refer to as “illogical A”), the oscillatory powers caused by listening to

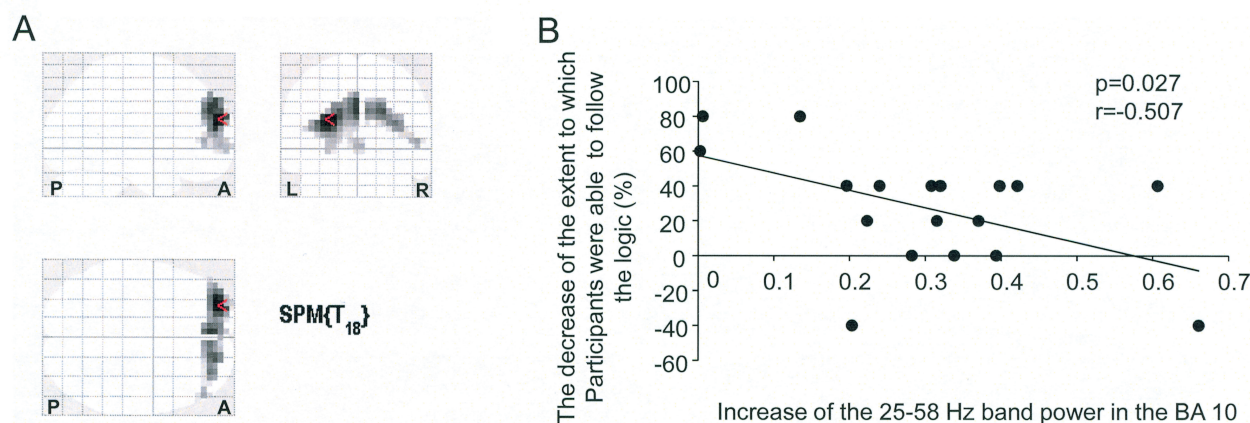


**Figure 5.** The relationship between the decrease of the extent to which participants were able to follow the logic of speech caused by the speeches based on the original I and the increase of the 25-58 Hz band power in the BA 10 when listening to the speeches. (A) The maximum intensity projections of the statistical parametric maps of the brain regions including the left BA 10 (arrow head) where the increase of the 25-58 Hz band power was associated with the decrease of the comprehension caused by the speeches based on the original I was shown. Random-effect analyses of 19 participants,  $p < 0.0017$ , family-wise-error corrected for the entire search volume (A, anterior; P, posterior; and L, left; R, right). (B) The relationship between the decrease of the extent to which participants were able to follow the logic of speech caused by the speeches based on the original I and the increase of the 25-58 Hz band power in the BA 10 when listening to the speeches was shown. The linear regression line, Pearson's correlation coefficient, and the p value are shown.

the speeches based on the illogical A were compared with those caused by listening to the speeches based on the original A. There were brain regions in which the oscillatory power caused by listening to the speeches based on the illogical A was smaller (Fig. 3C) or greater (Fig. 4C) than that caused by listening to the speeches based on the original A (Table 2). Whether each brain regions listed in Table 3 was included in the brain areas in which alterations in oscillatory brain activity were observed when the speeches based on the original I and when the speeches based on the illogical A were indicated in Table 3.

To examine the neural activity related to the comprehension of logic affected by listening to the speeches based on the original I, the correlations between the alterations of oscillatory brain activity caused by listening to the speeches based on the original I (Figs. 3A and 4A) and the decrease of the extent to which participants were able to follow the logic of the speeches were examined. The increase of the 25-58 Hz band power in the Brodmann's area (BA) 10 (Fig. 5A) caused by listening to the speeches based on the original I was negatively associated with the decrease of the extent to which participants were able to follow the logic in the speeches based on the original I ( $p = 0.027$ ,  $r = -0.507$ ; Fig. 5B). To examine the neural activity related to the comprehension of logic affected by listening to the speeches based on the illogical I, the correlations between the alterations of oscillatory brain activity caused by listening to the speeches based on the illogical I (Figs. 3B and 4B) and the decrease of the extent to which participants were able to follow the logic of the speeches were examined. However, there were no brain regions in which the alterations of oscillatory brain activity were associated with the decrease of the extent to which participants were able to follow the logic of the speeches.

**Table 2. Brain regions that showed a decrease or increase in oscillatory power caused either by the original stories read with inadequate pauses or by the illogical stories read with adequate pauses compared with those caused by the original stories read with adequate pauses**

Contrast	Frequency (Hz)	Location	BA	MNI (mm)			Z-value	
				x	y	z		
Original/inadequate>Original/adequate	4-8 Hz	Inferior Frontal Gyrus	45	-58	33	5	5.6	
		Middle Frontal Gyrus	46	-58	28	30	5.1	
		Middle Frontal Gyrus	11	-18	38	-10	5.0	
	25-58 Hz	Supramarginal Gyrus	40	57	-52	35	4.9	
		Middle Frontal Gyrus	10	-28	58	25	5.1	
		Superior Frontal Gyrus	9	22	53	30	4.9	
		Inferior Frontal Gyrus	46	52	43	5	4.7	
		Medial Frontal Gyrus	10	2	58	0	4.7	
		1-4 Hz	Precuneus	19	-38	-77	40	5.4
	Angular Gyrus		39	52	-72	35	5.2	
	Insula		13	37	8	20	5.1	
	Superior Frontal Gyrus		10	-33	53	30	5.1	
	Medial Frontal Gyrus		10	7	63	5	5.0	
	Precentral Gyrus		6	-38	-7	40	4.8	
	Original/inadequate<Original/adequate	4-8 Hz	Postcentral Gyrus	2	57	-27	45	5.6
Middle Frontal Gyrus			6	-43	13	50	5.2	
Middle Frontal Gyrus			8	42	23	45	4.9	
Superior Frontal Gyrus			9	17	38	40	4.9	
8-13 Hz		Middle Frontal Gyrus	46	-38	48	20	5.0	
		Middle Temporal Gyrus	39	-58	-72	20	5.0	
		Middle Frontal Gyrus	9	-48	18	35	4.8	
13-25 Hz		Middle Frontal Gyrus	47	-33	38	-5	4.7	
Illogical/adequate>Original/adequate		1-4 Hz	Superior Frontal Gyrus	8	-3	33	50	5.4
	Inferior Parietal Lobule		40	-63	-27	30	5.2	
	Cuneus		18	17	-102	5	5.1	
	Precentral Gyrus		6	62	-7	40	5.1	
	Middle Frontal Gyrus		6	-53	3	45	4.9	
	4-8 Hz	Inferior Frontal Gyrus	9	62	18	25	5.3	
		Inferior Parietal Lobule	40	52	-47	55	5.1	
		Inferior Frontal Gyrus	47	-53	28	-15	5.1	
		Medial Frontal Gyrus	11	-8	53	-10	5.0	
	8-13 Hz	Precuneus	19	-18	-87	40	4.8	
	Illogical/adequate<Original/adequate	1-4 Hz	Inferior Parietal Lobule	40	42	-37	50	5.5
			Precentral Gyrus	6	52	-2	30	5.4
			Cuneus	19	17	-92	30	5.4
			Inferior Parietal Lobule	40	-58	-27	30	5.3
			Middle Temporal Gyrus	21	-63	3	-10	5.2
Superior Frontal Gyrus			8	-33	23	55	5.2	
Superior Parietal Lobule			7	-38	-72	45	5.0	
Middle Frontal Gyrus			10	-43	43	25	4.9	
Inferior Frontal Gyrus			46	52	43	5	4.9	
Superior Parietal Lobule			7	22	-72	55	4.9	
4-8 Hz		Inferior Frontal Gyrus	9	-58	13	30	5.4	
		Postcentral Gyrus	1	-43	-32	65	5.3	
		Inferior Parietal Lobule	40	47	-42	60	5.2	
		Inferior Parietal Lobule	40	-63	-27	30	5.0	
		8-13 Hz	Middle Frontal Gyrus	6	-58	3	45	5.4
			Middle Frontal Gyrus	46	52	43	30	4.9

Data were obtained from random-effect analyses. Only significant changes are shown (one-sample t test,  $p < 0.0017$ , family-wise error rate). x, y, z: Stereotaxic coordinate. BA, Brodmann area; and MNI, Montreal Neurological Institute.

**Table 3. Brain regions that showed a decrease or increase in oscillatory power caused by the illogical stories read with inadequate pauses compared with those caused by the original stories read with adequate pauses**

Contrast	Frequency (Hz)	Location	BA	MNI (mm)			Z-value	Included in	
				x	y	z		Original/ inadequate	Illogical/ adequate
Illogical/inadequate >Original/adequate									
	1-4 Hz	Precentral Gyrus	4	27	-22	50	5.0		
		Postcentral Gyrus	7	12	-57	70	4.9		
		Cuneus	19	32	-82	30	4.8		
	4-8 Hz	Cingulate Gyrus	31	-18	-57	65	5.8		
		Inferior Frontal Gyrus	45	62	13	20	5.1		○
		Superior Parietal Lobule	7	37	-57	50	5.1		
		Inferior Frontal Gyrus	46	-48	43	5	5.0	○	
		Superior Frontal Gyrus	11	-28	58	-10	4.9		
	25-58 Hz	Inferior Frontal Gyrus	46	47	38	15	4.8		
Illogical/inadequate <Original/adequate									
	1-4 Hz	Inferior Frontal Gyrus	44	-58	13	15	5.8		
		Cuneus	19	22	-97	20	5.4		
		Inferior Frontal Gyrus	47	-53	38	-15	5.0		
		Middle Frontal Gyrus	10	-23	48	10	4.9		
	4-8 Hz	Middle Frontal Gyrus	46	-48	48	20	5.1		
		Superior Temporal Gyrus	22	67	-37	5	5.0		
		Superior Parietal Lobule	7	22	-72	55	5.0		
		Precuneus	7	7	-57	45	4.9		
	8-13 Hz	Superior Parietal Lobule	7	32	-57	65	5.5		
		Middle Frontal Gyrus	46	-48	38	25	5.1		

Data were obtained from random-effect analyses. Only significant changes are shown (one-sample t test,  $p < 0.0017$ , family-wise error rate). x, y, z: Stereotaxic coordinate. ○ : brain activities observed. BA, Brodmann area; and MNI, Montreal Neurological Institute.

## Discussion

In our present study, the extent to which participants were able to follow the logic in the speeches based on original I were lower than that in speeches based on original A, confirming that the comprehension of speech is impaired by the disturbance of the connections within the semantically related units in the speech. The extent to which participants were able to follow the logic in the speeches read with inadequate pauses was further deteriorated when the speeches were modified to be illogical (i.e., the extent to which participants were able to follow the logic in the speeches based on the illogical I was lower than that in the speeches based on the original I).

In relation to listening to the speeches based on the original I, alteration of oscillatory brain activity in several brain regions, such as the inferior, middle, medial, and superior frontal gyrus, the supramarginal gyrus, the angular gyrus, and so on, were observed (Figs. 3A, 3B, 4A, and 4B). The alterations of the level of activations caused by listening to the speeches in which parts of continuous speech sound were replaced by silence have been reported in an fMRI study: The increase of neural activity was observed in the left postcentral gyrus and the right medial frontal gyrus, and the decrease of neural activity was observed in the left temporal cortex, the parahippocampal gyrus, the posterior cingulate gyrus, the caudate and thalamus, and the right superior temporal gyrus<sup>24</sup>. There seems to be considerable overlap between the brain regions in which alterations of oscillatory brain

activity caused by listening to the speeches based on the original I were observed in our present study and those in which the alterations of the level of activations observed in the previous fMRI study. However, since the alterations of oscillatory brain activity assessed by MEG is not necessarily parallel to the alterations of hemodynamic responses measured by fMRI, it is difficult to draw a conclusion on whether the neural mechanism of listening to the speeches read with inadequate pauses is different from that of listening to the speeches in which parts of continuous speech sound were replaced by silence.

Since the comprehension of speech is thought to be impaired by the disturbance of the connections within the semantically related units in the speech and the increase of the 25-58 Hz (i.e., gamma) band power in the BA 10 caused by listening to the speeches based on the original I was associated with the decrease of the level of the comprehension of speech, the BA 10 may be a brain region that plays an important role in the comprehension of speech affected by the disturbance of the connections within the semantically related units in the speech. It has been reported that the alteration of oscillatory brain activity in each frequency band (i.e., delta, theta, alpha, beta, and gamma bands) was related to various aspects of information processing such as sensory, motor, and cognitive processes (Klimesch 1996; Pfurtscheller and Lopes da Silva 1999). As for the neural activity related to language processing, it has been reported that the increase of gamma (36-76 Hz) and beta (14-30 Hz) oscillations are related to the prediction of the upcoming word<sup>13,15</sup>. It has been thought that the anticipation of the upcoming words of a sentence by using lexical-semantic knowledge is an essential process for language comprehension and the gamma oscillation (>35 Hz) is involved in the process to check the incoming lexical-semantic representations with the predicted upcoming words<sup>15</sup>. Therefore, it is plausible that the increase of gamma band oscillation in the BA 10 observed in our present study is related to the prediction of the upcoming words, which seems to be more crucial in the speeches read with inadequate pauses than in the speeches read with adequate pauses. In fact, the individuals with higher beta band power in the BA 10 showed lesser decrement of the extent to which participants were able to follow the logic of the speeches caused by the speeches read with inadequate pauses in our present study.

The alterations of oscillatory brain activity observed when listening to the speeches based on illogical I did not include the increase of gamma band power in the BA 10. This may reflect the fact that the comprehension of the speeches based on the illogical I was significantly worse compared with that of the speeches based on the original A: The prediction of the upcoming words was impaired when listening to the speeches based on the illogical I, resulting in the deteriorated comprehension of the speeches. In addition, among the brain regions in which the alterations of oscillatory brain activity were observed when listening to speeches based on illogical I, the increases of theta band power in the BA 45 and BA 46 were the only brain activities observed when listening to the stories based on the illogical A and the stories based on the original I, respectively. These findings show that the neural processing of the speeches based on the illogical I was different from that of the speeches based on the original I and that of the speeches based on the illogical A rather than the extreme version of these neural processing (i.e., the neural processing of the speeches based on the original I and that of the speeches based on the illogical A).

There are limitations to our study. First, the participants of our present study were healthy male individuals. To generalize our results, studies with female and the individuals with hearing loss are necessary. Second, all the speeches based on the original stories were logically correct and all the

speeches based on the illogical stories were logically incorrect. For example, it has been reported that the processing of false sentences is related to the activation of the BA 46 and the BA10 in an fMRI study<sup>14)</sup>. However, in our present study, because the number of the speeches which our participants thought to be incorrect did not differ between the speeches based on the original I and those based on the original A, the increase of gamma band power observed in the BA 10 when listening to the speeches based on the original I seems not to be due to the fact that all the speeches based on the illogical stories were logically incorrect while those based on the original stories were logically incorrect. Third, cognitive capacity of our participants was not assessed. However, since the participants were all undergraduate students and elderly individuals were not included, it is assumed that their cognitive capacities were similar among the participants.

In conclusion, we demonstrated that the comprehension of speech is impaired by the disturbance of the connections within the semantically related units in speech caused by placing pauses at inadequate places in the speech and that the BA 10 is involved in the comprehension of the speeches with inadequate pauses. Our findings may help understand the neural mechanisms related to the comprehension of speech, especially in the situation that the disturbance of the connections within the semantically related units may be caused by such as extraneous sounds.

We believe to clarify the neural activity caused by the disturbance of the connections among sounds in speech is beneficial to develop treatment methods for those suffering from difficulty in speech comprehension depending on how to speak and intonation. We want to use our present study for the development of auditory rehabilitation. We hope to clarify the neural activity caused by the disturbance of the connections among sounds in speech may be connected to rehabilitation for the hearing impaired and the patients with cochlear implantation.

### **Acknowledgements**

The All authors have no COI to declare regarding the present study.

We thank Forte Science Communications for editorial help with the manuscript and Manryoukai Imaging Clinic for MRI scans.

### **References**

1. Baskent D, Eiler CL, Edwards B. Phonemic restoration by hearing-impaired listeners with mild to moderate sensorineural hearing loss. *Hear Res* 2010;260:54-62.
2. Dalal SS, Guggisberg AG, Edwards E, et al. Five-dimensional neuroimaging: localization of the time-frequency dynamics of cortical activity. *Neuroimage* 2008;40:1686-1700.
3. David O, Kilner JM, Friston KJ. Mechanisms of evoked and induced responses in MEG/EEG. *Neuroimage* 2006; 31:1580-1591.
4. Davis MH, Johnsrude IS. Hierarchical processing in spoken language comprehension. *J Neurosci* 2003;23: 3423-3431.
5. Evans AC, Kamber M, Collins DL, et al. Magnetic resonance scanning and epilepsy. In: Shorvon SD, Fish DR, Andermann F, Bydder GM, Stefan H, editors. *An MRI-Based Probabilistic Atlas of Neuroanatomy*. 1st ed. New York: Plenum Press, 1994. pp.263-274.
6. Fetterman BL, Domico EH. Speech recognition in background noise of cochlear implant patients. *Otolaryngol Head Neck Surg* 2002;126:257-263.
7. Friston KJ, Holmes AP, Worsley KJ. How many subjects constitute a study? *Neuroimage* 1999;10:1-5.
8. Hillebrand A, Singh KD, Holliday IE, et al. A new approach to neuroimaging with magnetoencephalography. *Hum Brain Mapp* 2005;25:199-211.
9. Hochberg I, Boothroyd A, Weiss M, et al. Effects of noise and noise suppression on speech perception by cochlear implant users. *Ear Hear* 1992;13:263-271.
10. Huggins AWF. Temporally segmented speech. *Perception & Psychophysics* 1975;18:149-157.

11. Kidd GR, Humes LE. Effects of age and hearing loss on the recognition of interrupted words in isolation and in sentences. *J Acoust Soc Am* 2012;131:1434-1448.
12. Klimesch W. Memory processes, brain oscillations and EEG synchronization. *Int J Psychophysiol* 1996;24:61-100.
13. Lam NHL, Schoffelen JM, Udden J, et al. Neural activity during sentence processing as reflected in theta, alpha, beta, and gamma oscillations. *Neuroimage* 2016;142:43-54.
14. Marques JF, Canessa N, Cappa S. Neural differences in the processing of true and false sentences: insights into the nature of 'truth' in language comprehension. *Cortex* 2009;45:759-768.
15. Meyer L. The neural oscillations of speech processing and language comprehension: state of the art and emerging mechanisms. *Eur J Neurosci* 2018;48:2609-2621.
16. Oldfield RC. The assessment and analysis of handedness: the Edinburgh inventory. *Neuropsychologia* 1971;9:97-113.
17. Pfurtscheller G, Lopes da Silva FH. Event-related EEG/MEG synchronization and desynchronization: basic principles. *Clin Neurophysiol* 1999;110:1842-1857.
18. Prosser S, Turrini M, Arslan E. Effects of different noises on speech discrimination by the elderly. *Acta Otolaryngol Suppl* 1990;476:136-142.
19. Sekihara K, Nagarajan SS. Adaptive spatial filters. In: Nagel, Joachim H, editors. *Adaptive Spatial Filters for Electromagnetic Brain Imaging*. 1st ed. Berlin:Springer Verlag, 2008. pp.37-63.
20. Shafiro V, Sheft S, Risley R. The intelligibility of interrupted and temporally altered speech: effects of context, age, and hearing loss. *J Acoust Soc Am* 2016;139:455-465.
21. Shafiro V, Sheft S, Risley R, et al. Effects of age and hearing loss on the intelligibility of interrupted speech. *J Acoust Soc Am* 2015;137:745-756.
22. Sivonen P, Maess B, Lattner S, et al. Phonemic restoration in a sentence context: evidence from early and late ERP effects. *Brain Res* 2006;1121:177-189.
23. Sunami K, Ishii A, Takano S, et al. Neural mechanisms of phonemic restoration for speech comprehension revealed by magnetoencephalography. *Brain Res* 2013;1537:164-173.
24. Takeichi H, Koyama S, Terao A, et al. Comprehension of degraded speech sounds with m-sequence modulation: an fMRI study. *Neuroimage* 2010;49:2697-2706.
25. Warren RM. Perceptual restoration of missing speech sounds. *Science* 1970;167:392-393.



# Microcuff® Pediatric Endotracheal Tube Decreases the Tube Exchange Ratio without Increasing Postoperative Complications in Japanese Children: A Single Center Retrospective Cohort Study

YOSUKE INADA, YUSUKE FUNAI, TAKASHI SHUTOU, TAKASHI MORI, and KIYONOBU NISHIKAWA

*Department of Anesthesiology, Osaka City University Graduate School of Medicine*

## Abstract

### **Background**

The usefulness of the Microcuff® pediatric endotracheal tube (Microcuff® PET) has been reported from other countries, but few reports include Japanese children because Microcuff® PET was recently introduced in Japan in 2015. Therefore, we compared the tube exchange ratio and postoperative complications between Microcuff® PET and uncuffed tubes in Japanese children.

### **Methods**

We conducted a single center retrospective cohort study with approval from our ethics committee. Patients aged 2 to 8 years, who underwent general anesthesia with endotracheal intubation between October 2015 and September 2017, were included. Patients who were intubated with either uncuffed tube (UC group) or Microcuff® PET (MC group) were retrospectively analyzed. The primary outcome was the tube exchange ratio, and the secondary outcome was the incidence of perioperative complications. Data are presented as numbers or medians.

### **Results**

We analyzed 250 patients (UC vs MC, 127 vs 83). There were no differences between groups in baseline characteristics. The tube inner diameter was narrower (5 vs 4.5 mm,  $p < 0.01$ ), the tube depth was shallower (15 vs 14.5 cm,  $p = 0.011$ ), and the tube exchange ratio was smaller (23.6% vs 1.2%,  $p < 0.01$ ) in the MC group. There were no severe air leakage cases in the MC group. In a multiple logistic regression analysis, usage of Microcuff® PET was the only independent negative risk factor for tube exchange ( $p < 0.01$ ). There were no significant differences in postoperative complications between the groups.

### **Conclusions**

Compared to uncuffed tube, Microcuff® PET significantly reduced the tube exchange ratio without increasing postoperative complications in Japanese children.

Key Words: Cuffed endotracheal tube; Microcuff®; Pediatrics

---

Received August 16, 2019; accepted October 8, 2019.

Correspondence to: Yusuke Funai, MD, PhD.

Department of Anesthesiology, Osaka City University Graduate School of Medicine,  
1-4-3 Asahimachi, Abeno-ku, Osaka 545-8586, Japan  
Tel: +81-6-6645-2186; Fax: +81-6-6645-2489  
E-mail: yusuke.funai@gmail.com

## Introduction

Traditionally, uncuffed endotracheal tubes have been commonly used for children under 8 to 10 years old to reduce the risks of: (1) airway mucosal injury by the cuff, especially at the cricoid ring that surrounds the narrowest portion of the pediatric trachea, and (2) increasing airway resistance because of the narrower inner diameter of cuffed tubes<sup>1</sup>. Conversely, an uncuffed endotracheal tube is sometimes necessary to be exchanged for a different size because of ventilation failure owing to air leakage or overtightened seal. Multiple trials of laryngoscopy and reintubation may cause airway injury and increase postoperative airway complications such as laryngeal edema, vocal cord injury, hoarseness, or sore throat. In recent years, many studies have reported the usefulness of cuffed endotracheal tubes for pediatric patients that appear to have the same benefits as that in adults<sup>2-8</sup>. Specifically, several studies have demonstrated the superior efficacy and safety of the Microcuff<sup>®</sup> pediatric endotracheal tube (Microcuff<sup>®</sup> PET; Avanos Medical, Inc. Alpharetta, GA, USA), which has a high-volume low-pressure cuff designed especially for children<sup>9-18</sup>. Microcuff<sup>®</sup> PET has a polyurethane thin-wall cuff that improves sealing characteristics with lower cuff pressure, resulting in a reduction in the number of endotracheal tube exchanges<sup>8,14,18</sup>. Additionally, its short cuff helps to avoid subglottic compression by the cuff thus preventing perioperative airway complications<sup>19</sup>. However, Microcuff<sup>®</sup> PET has only been commercially available in Japan since June 2015, and thus, previous reports about its usefulness in Japanese children are very limited. We conducted a single center retrospective cohort study to elucidate the usefulness and safety of Microcuff<sup>®</sup> PET for Japanese children aged 2 to 8 years by comparing it to the uncuffed tracheal tube (Portex<sup>®</sup> Tracheal Tube; Smiths Medical ASD, Inc. Minneapolis, MN, USA) that has been mainly used in our hospital. The aim of this study was to compare the tube exchange ratio and perioperative complications between the Microcuff<sup>®</sup> PET and Portex<sup>®</sup> Tracheal Tube in Japanese children.

## Methods

A single center (Osaka City University Hospital) retrospective cohort study was conducted. This study was approved by the Ethics Committee of Osaka City University (approval number: 3978) and registered in the UMIN Clinical Trials Registry (No: 000035767). All patients were informed about this study on our website (<http://www.med.osaka-cu.ac.jp/medinf/rinri/public/koukai-jisshi.html>) and given the opportunity to opt-out at any time.

Patients (American Society of Anesthesiologists Physical Status; ASA-PS 1-2) aged 2 to 8 years, who underwent general anesthesia with tracheal intubation surgery in a supine or lateral position between October 2014 and September 2017 at Osaka City University Hospital were included. Patients' exclusion criteria were as follows: known or suspected difficult airway, known hoarseness or airway infection, and the usage of endotracheal tubes other than Portex<sup>®</sup> or Microcuff<sup>®</sup> PET. Although the selection of each tube size was specified in the product documents (Portex<sup>®</sup>: ID 4.0 mm for 3 to 6 months, ID 4.5 mm for 6 to 12 months, ID 5.0 mm for 2 or 3 years, ID 5.5 mm for 4 or 5 years, ID 6.0 mm for 6 or 7 years; Microcuff<sup>®</sup> PET: ID 4.0 mm for 2 to 4 years, ID 4.5 mm for 4 to 6 years, and ID 5.0 mm for 6 to 8 years), the final decision of the tube size was made by each anesthesiologist. The tube insertion depth was also decided by each anesthesiologist; the tube was withdrawn from bronchial intubation depth under auscultation or the ring mark was adjusted according to the vocal cord in certain cases of Microcuff<sup>®</sup> PET. There were no limitations with respect to performing general anesthesia, but all patients were intubated by the oral route under direct

laryngoscopy after administration of rocuronium. Anesthesia was maintained by inhaled anesthetics (sevoflurane or desflurane) in all patients. Each anesthesiologist was responsible for determining the necessity for exchanging tubes. All patients were extubated at the end of the operation. All data were retrospectively extracted from our electronic anesthesia record system (ORSYS; Philips Electronics Japan, Tokyo, Japan) and electronic medical records (EGMAIN-EX; Fujitsu Co., Ltd., Tokyo, Japan). We extracted information about each patient (age, sex, height, weight, and ASA-PS), the operation (surgical procedure, operative time, anesthesia time, blood loss volume, urinary volume, and infusion volume), intubation (tube type, tube size, insertion depth, cuff pressure, number of intubation trial times, and Cormack-Lehane grade), and perioperative complications. The primary outcome was the number of patients who needed tube exchange, and the secondary outcome was the incidence of perioperative complications, including respiratory complications (stridor, increased sputum, bronchospasm, atelectasis, and hoarseness), sore throat, postoperative nausea and vomiting (PONV), and others.

### **Statistical Analysis**

Data are presented as median and interquartile ranges [IQR, 25%-75%] or numbers (percentages). Baseline patient characteristics were analyzed using the Mann-Whitney U test for continuous variables and the Fisher's exact test or  $\chi^2$  analysis for nominal data. A multivariate logistic regression analysis was performed to identify the significant covariates associated with the requirement of an endotracheal tube exchange after the first intubation. As explanatory variables, we chose factors with  $p < 0.3$  in the univariate analysis and excluded factors that were too closely related to tube exchange and tube type. Results are presented as odds ratios (OR) with 95% confidence intervals (CI). Statistical significance was determined at  $p < 0.05$  in all cases. Based on previous studies of other facilities, the tube exchange ratio was assumed to be 10% for the MC group and 30% for the UC group. When performing a power analysis with  $\alpha$  error=0.05 and detection power=0.8, 72 cases were required in each group for a total of 144 cases. Statistical analysis was performed using EZR software (version 1.30; Saitama Medical Center, Jichi Medical University, Saitama, Japan)<sup>20</sup>.

## **Results**

A total of 250 children (ASA-PS 1-2, aged 2 to 8 years) who underwent general anesthesia at Osaka City University Hospital between October 2014 and September 2017 were eligible for our analysis (Fig. 1). Seven patients were excluded owing to incomplete data (no record of the selected tube type). Thirty-three patients were excluded because a cuffed endotracheal tube other than the Microcuff® PET was used. There were no cases of known or suspected difficult airway, hoarseness, or airway infection. Among the remaining 210 patients, 127 (UC group) intubated with uncuffed endotracheal tubes (Portex®) and 83 (MC group) intubated with the Microcuff® PET were finally analyzed (Fig. 1).

Baseline patient characteristics and information about general anesthesia for both groups are summarized in Table 1. In brief, the median age of our participants was 4 years [IQR, 3-5 years], and the sex distribution among the groups was comparable (males,  $n=111$ , 52.9%). Most patients had ASA-PS 1 ( $n=175$ , 83.3%). The median operative and anesthesia times were 39 [IQR, 25-63.8] minutes and 82 [IQR, 64-118] minutes, respectively. The median infusion volume during anesthesia was 110 [80-200] mL. There was little blood loss and urinary volume during anesthesia in most

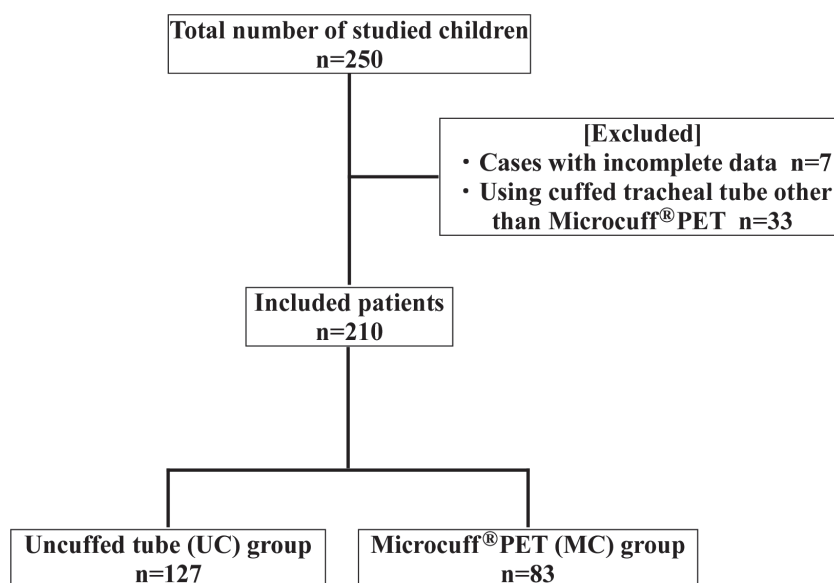


**Figure 1.** Study synopsis. Abbreviations: UC, uncuffed tube (means Portex®); and MC, Microcuff® PET.

cases. A total of 31 patients (14.8%) underwent endotracheal tube exchange after the first intubation. The inner diameter of the intubated tubes was 4.0 to 6.0 mm. The median cuff pressure in the MC group was 20 [11.25-20] mm Hg (n=71, 12 cases were excluded due to absence of records). Most patients were intubated once (n=172, 81.9%); easy success was achieved in most cases (Cormack-Lehane grade 1, n=185, 92.0%; 9 cases were excluded due to absence of records). In the univariate analysis, the insertion depth was significantly shallower (UC vs MC, 15 [14-16] vs 14.5 [13-15] cm,  $p=0.011$ ), and the inner diameter of the selected tube was significantly narrower (5 [5-5.5] vs 4.5 [4-5] mm,  $p<0.001$ ) in the MC group. The number of patients needing tracheal tube exchange after the first intubation was 30 (23.6%) in the UC group, although there was only 1 (1.2%) such case in the MC group ( $p<0.01$ ). Table 2 shows the details of cases in which endotracheal tubes were exchanged after the first intubation. Most of the cases required a tube size larger because of ventilation failure due to air leakage in the UC group (n=23, 18.1%), although no patients experienced severe air leakage in the MC group. Conversely, 7 cases in the UC group and 1 in the MC group required a tube size smaller because of resistance to intubation or overly tight sealing pressure.

Surgical sites of the patients are summarized in Table 3. The most frequent surgical site was the abdominal region (n=95, 45.2%), followed by head and neck (n=51, 24.3%) and skin (n=48, 22.9%). Most cases of abdominal surgery were laparoscopic inguinal hernia repair, and 45% of the head and neck surgeries involved laryngopharyngeal surgery. All cases categorized under laryngopharyngeal surgery were tonsillectomies, adenoid resections, or both. Operations included under the skin category comprised laser therapy for nevus, skin tumor resection, and repair of cicatricial contracture. There was no statistical difference between the groups in the distribution of any surgical sites.

Next, we performed a multivariate logistic regression analysis to identify the risk factors for the requirement of endotracheal tube exchange after the first intubation. Tube type, sex, and ASA-PS were chosen as explanatory variables because their  $p$  values were  $<0.3$  in the univariate analysis (Table 4). Tube insertion depth and inner diameter were voided as explanatory variables unless their  $p$  values were  $<0.3$  because their statistical relationship with the selection of Microcuff® PET was too

**Table 1. Baseline characteristics of study population, overall and by tube type**

	Overall (n=210)	UC group (n=127)	MC group (n=83)	p value
Age (yr)	4 [3-5]	4 [3-5]	4 [3-5]	0.7
Male sex	111 (52.9%)	63 (49.6%)	48 (57.8%)	0.26
Height (cm)	101.9 [92.3-110.7]	101.9 [93.4-110.0]	101.8 [91.6-111.8]	0.94
Weight (kg)	15.8 [13.2-18.5]	15.9 [13.5-18.2]	15.5 [13.2-19.2]	0.92
ASA-PS				0.13
1	175(83.3%)	110 (86.6%)	65 (78.3%)	
2	35 (16.7%)	17 (13.4%)	18 (21.7%)	
Operative time (min)	39 [25-63.8]	39 [25-61]	40 [24.5-69.5]	0.87
Anesthetic time (min)	82 [64-118]	83 [66-118.5]	81 [62-116.0]	0.99
Blood loss (g)	0 [0-1]	0 [0-75]	0 [0-70]	0.67
Urinary volume (mL)	0 [0-0]	0 [0-0]	0 [0-0]	0.39
Infusion volume (mL)	110 [80-200]	100 [80-192.5]	122 [85-200]	0.43
Cases of exchanging tube	31 (14.8%)	30 (23.6%)	1 (1.2%)	<0.001 *
Insertion depth (cm)	15.0 [14-15.5]	15.0 [14-16]	14.5 [13-15]	0.01 *
Tube inner diameter (mm)				<0.001 *
4	30 (14.3%)	2 (1.6%)	28 (33.7%)	
4.5	47 (22.4%)	24 (18.9%)	23 (27.7%)	
5	77 (36.7%)	45 (35.4%)	32 (38.6%)	
5.5	42 (20.0%)	42 (33.1%)	0 (0%)	
6	14 (6.7%)	14 (11.0%)	0 (0%)	
Cuff pressure (mm Hg) (n=71)	20 [11.25-20]	-	20 [11.25-20]	
Number of intubation trials				<0.01 *
1	172 (81.9%)	91 (71.7%)	81 (97.6%)	
2	34 (16.2%)	32 (25.2%)	2 (2.4%)	
3	4 (1.9%)	4 (3.1%)	0 (0%)	
Cormack-Lehane grade (n=201)				0.42
1	185 (92.0%)	114 (92.7%)	71 (91.0%)	
2	14 (7.0%)	7 (5.7%)	7 (9.0%)	
3	2 (1.0%)	2 (1.6%)	0 (0%)	

Data are presented as median [interquartile range, IQR] or number (percentage). Mann-Whitney U test was performed for continuous variables and Fisher's exact test or  $\chi^2$  analysis was used for categorical data. Asterisk (\*) indicates statistical significance ( $p < 0.05$ ).

Abbreviations: ASA-PS, American Society of Anesthesiologists physical status; UC, uncuffed tube (means Portex®); and MC, Microcuff® PET.

strong. Additionally, the number of intubation trials was also not chosen as an explanatory variable because its relationship with tube exchange was too strong. As a result, we identified using Microcuff® PET as an independent negative risk factor for tube exchange. The odds ratio for the requirement of endotracheal tube exchange after the first intubation with Microcuff® PET compared to Portex® was 0.0408 (95% CI: 0.007-0.466;  $p = 0.002$ ). Sex and ASA-PS were not significantly associated with the requirement of tube exchange.

Postoperative complications were also compared between both groups (Table 5). There were no

statistically significant differences in the incidence of any perioperative complications (UC vs MC): respiratory complications (3.1% vs 4.8%,  $p=0.72$ ), postoperative sore throat (3.9% vs 10.8%,  $p=0.09$ ), postoperative nausea and vomiting (13.4% vs 16.1%,  $p=0.49$ ), and others (1.6% vs 2.4%,  $p=0.65$ ). Respiratory complications included hoarseness (UC vs MC, 1 vs 1 case), atelectasis (1 vs 0), laryngospasm after extubation (2 vs 1), and increased sputum (0 vs 2). Other complications included

**Table 2. Details of tube exchange after the first intubation**

	UC group (n=127)	MC group (n=83)
Size up	23 (18.1%)	0 (0%)
Size down	7 (5.5%)	1 (1.1%)
Total	30 (23.6%)	1 (1.1%)

“Size up” presents the number and percentage of patients who were reintubated using a tube with a larger inner diameter. “Size down” presents the number and percentage of patients who were reintubated using a tube with a smaller inner diameter.

Abbreviations: UC, uncuffed tube (means Portex®); and MC, Microcuff® PET.

**Table 3. Surgical site in the study population, overall and by tube type**

Surgical site	Overall (n=210)	UC group (n=127)	MC group (n=83)	p value
Head and Neck	51 (24.3%)	30 (23.6%)	21 (25.3%)	0.78
-Brain	2 (1.0%)	1 (0.8%)	1 (1.2%)	1
-Eye	6 (2.9%)	3 (2.4%)	3 (3.6%)	0.68
-Laryngopharyngeal	23 (11.0%)	13 (10.2%)	10 (12.0%)	0.68
-Ear	16 (7.6%)	10 (7.9%)	6 (7.2%)	0.86
-Nose	2 (1.0%)	1 (0.8%)	1 (1.2%)	1
-Neck	2 (1.0%)	2 (1.6%)	0 (0%)	0.52
Thorax	7 (3.3%)	4 (3.1%)	3 (3.6%)	1
Abdomen	95 (45.2%)	55 (43.3%)	40 (48.2%)	0.49
Extremities	9 (4.3%)	5 (3.9%)	4 (4.8%)	0.74
Skin	48 (22.9%)	33 (26.0%)	15 (18.1%)	0.18

Data are presented as number (percentage). P values were generated by Fisher’s exact test or  $\chi^2$  analysis. Statistical significance was set at  $p<0.05$ .

Abbreviations: UC, uncuffed tube (means Portex®); and MC, Microcuff® PET.

**Table 4. Multivariate logistic regression analysis for detecting the risk factors for endotracheal tube exchange**

	Odds ratio	95% CI	p value
Tube type (UC=0, MC=1)	0.0408	0.007-0.466	* 0.002
Gender (Male=1, Female=2)	1.06	0.473-2.37	0.89
ASA-PS	0.619	0.167-2.29	0.47

Statistical significance was set at  $p<0.05$ . Asterisk (\*) indicates statistical significance.

Abbreviations: ASA-PS, American Society of Anesthesiologists physical status; UC, uncuffed tube (Portex®); MC, Microcuff® PET; and CI, Confidence interval.

**Table 5. Postoperative complications by tube type**

	UC group (n=127)	MC group (n=83)	p value
Respiratory complication	4 (3.1%)	4 (4.8%)	0.72
Sore throat	5 (3.9%)	9 (10.8%)	0.09
PONV	17 (13.4%)	14 (16.1%)	0.49
Others	2 (1.6%)	2 (2.4%)	0.65
Total	27 (21.3%)	26 (31.3%)	0.10

Data are presented as number (percentage). P values were generated by Fisher's exact test or  $\chi^2$  analysis. Statistical significance was set at  $p < 0.05$ .

Abbreviations: UC, uncuffed tube (means Portex®); MC, Microcuff® PET; and PONV, Postoperative nausea and vomiting.

agitation (1 vs 0), delayed awakening (1 vs 0), headache (0 vs 1), and nasal bleeding (0 vs 1). Because some patients experienced multiple complications, the total number of patients who experienced any postoperative complications was 27 (21.3%) in the UC group and 26 (31.3%) in the MC group. Although the total incidence of perioperative complications, especially sore throat, was higher in the MC group, this result was not statistically significant ( $p=0.10$ ).

## Discussion

In this study, we revealed that the use of Microcuff® PET for Japanese children aged 2 to 8 years old significantly decreased the risk of requiring endotracheal tube exchange after the first intubation (UC vs MC, 23.6% vs 1.2%). No patients suffered from severe air leakage in the MC group, whereas 18.1% of UC group cases needed an endotracheal tube exchange due to ventilation failure. Moreover, there were no significant differences in the frequency of perioperative complications between the UC and MC groups.

There are several known benefits of cuffed endotracheal tubes over uncuffed endotracheal tubes. The tight airway seal provided by the cuff may reduce the risk of aspiration<sup>15,21</sup>, may improve the accuracy of capnogram and gas monitoring, and may reduce air contamination with volatile anesthetics in the operation room<sup>5</sup>. Specifically, many studies demonstrated the superiority of the Microcuff® PET, which is a cuffed tube specially designed for children<sup>9-18</sup>. Previous studies demonstrated that the tube exchange ratio was 1.6%-3.3% when using Microcuff® PET<sup>13,14,18</sup>. Our study showed an even lower tube exchange ratio of 1.2% in the MC group compared to 23.6% in the UC group, and there were no cases of air leakage in the MC group. As described in previous studies, our results also reflect the excellent air sealing properties of Microcuff® PET with high-volume low-pressure cuffs that work effectively, regardless of any individual differences in tracheal shape. Considering the air sealing property, Microcuff® PET seems to be especially useful for surgeries that require high peak inspiratory pressure, such as laparoscopic surgeries or surgeries for obese patients. Furthermore, Microcuff® PET may be useful for nasopharyngeal surgeries including those with a high risk of aspiration, such as tonsillectomy. The tube sizes for each age described in the package leaflet of Microcuff® PET appeared to be well-adapted for Japanese children. The low incidence of reintubation of Microcuff® PET prevents multiple laryngoscopy and intubation procedures, which may result in reduced postoperative laryngeal edema.

In our study, the median intubation depth was slightly but significantly shallower in the MC

group than in the UC group (UC vs MC, 15 vs 14.5 cm), but there were no complications associated with the tube depth, such as endotracheal intubation or accidental extubation during surgery. This result is attributable to each anesthesiologist's different definition of the tube depth between cuffed and uncuffed tubes. In most cases wherein Portex<sup>®</sup>, which has no depth mark, was used, the anesthesiologists adjusted the tube position by pulling the tube back from unilateral intubation depth with an auscultation technique. Conversely, anesthesiologists may have decided the tube depth by adjusting the ring mark according to the vocal cord in most cases of Microcuff<sup>®</sup> PET use. As Weiss et al demonstrated, the ring mark of Microcuff<sup>®</sup> PET allowed adequate placement of the tube with a cuff-free subglottic zone without the risk of unilateral intubation in children from birth to 14 years of age<sup>19</sup>. The cuff length and ring mark of Microcuff<sup>®</sup> PET is well-considered and specially designed for the pediatric airway. Thus, we think the differences in the intubation depth between the UC and MC groups is not so important in most clinical situations. However, we should take care to avoid accidental extubation in surgeries requiring strong neck retroflexion or handling the transesophageal echo probe, especially when using Microcuff<sup>®</sup> PET.

Several studies demonstrated that cuffed tubes did not increase morbidity among children under 8 years of age<sup>2,13,18</sup>. We also found no significant differences in postoperative complications between the UC and MC groups; however, postoperative sore throat seemed to be more frequent in the MC group (10.8%) than in the UC group (3.9%). This may be attributed to the intraoperative management of cuff pressure. In our patients, 56.6% (47 patients) of the MC group underwent adjustment of the intraoperative cuff pressure to 20 cm H<sub>2</sub>O, and 6 of 9 patients who experienced postoperative sore throat in the MC group were managed with a cuff pressure of 20 cm H<sub>2</sub>O. There is no clear standard regarding cuff pressure in children for now, but Seegobin et al reported that a cuff pressure over 30 cm H<sub>2</sub>O impaired endotracheal mucosal blood flow in adults<sup>22</sup>. Because the acceptable cuff pressure seems to be lower in children, previous studies using Microcuff<sup>®</sup> PET reported an even lower mean sealing pressure of 9.6-11.7 cm H<sub>2</sub>O<sup>10,16,18</sup>. Al-Melwalli et al reported that the incidence and severity of sore throat were significantly lower when the cuff pressure was properly maintained under 20 mm Hg compared to that with 57.55 mm Hg as determined by the finger estimation technique<sup>23</sup>. However, we did not find any significant statistical association between cuff pressure and postoperative sore throat ( $p=1$ , Fisher's exact test). It is possible that we could reduce the incidence of postoperative sore throat by managing with minimum cuff pressure to prevent air leakage. Further prospective studies with a strict protocol are needed to assess the association between cuff pressure and postoperative complications.

This study had several limitations. First, neonates and infants under 2 years of age were not included in this study. We did not use Microcuff<sup>®</sup> PET under the size of ID 3.5 mm in our hospital because the usage of cuffed endotracheal tubes for neonates and infants is still controversial<sup>24</sup>. Previous studies reported that cuffed tubes could be used without increasing complications for neonates and older children<sup>5,8,18</sup>, while other studies showed that cuffed tubes for premature and low-birth-weight neonates increased the incidence of post-extubation strider<sup>25</sup>. Cuffed endotracheal tubes might be too large in some cases, and it is possible that the tube exchange ratio and the incidence of postoperative complications may increase in neonates and infants. Second, we retrospectively obtained the information about postoperative complications from the electronic medical record system; thus, the diagnostic criteria of each complication were not strictly defined. Moreover, there may have been some omissions in the data in medical records; thus, it is possible that the data

regarding the incidence of postoperative complications were less accurate in both groups. Third, this was a single center retrospective cohort study with a small number of patients, and thus, the evidence level may be low to allow generalization. To address these issues, a well-structured, prospective randomized study is needed in the future.

In conclusion, Microcuff® PET showed a lower tube exchange ratio and exhibited superior airway sealing properties compared to Portex® endotracheal tubes in Japanese children aged 2 to 8 years. The incidence of postoperative complications, especially sore throat, was slightly higher in the MC group; however, no statistically significant difference was noted between the groups. Further prospective randomized study is needed to validate our results.

### **Acknowledgements**

All authors have no COI to declare regarding the present study.

### **References**

1. Motoyama EK. Induction of Anesthesia and Maintenance of the Airway in Infants and Children. In: Motoyama EK, Peter JD editor. *Smith's Anesthesia for Infants and Children 7 th ed.* St Louis: Mosby; 2006. pp. 319-358.
2. Deakers TW, Reynolds G, Stretton M, et al. Cuffed endotracheal tubes in pediatric intensive care. *J Pediatr* 1994; 125:57-62.
3. Eschertzhuber S, Salgo B, Schmitz A, et al. Cuffed endotracheal tubes in children reduce sevoflurane and medical gas consumption and related costs. *Acta Anaesthesiol Scand* 2010;54:855-858.
4. Fine GF, Borland LM. The future of the cuffed endotracheal tube. *Paediatr Anaesth* 2004;14:38-42.
5. Khine HH, Corddry DH, Kettrick RG, et al. Comparison of cuffed and uncuffed endotracheal tubes in young children during general anesthesia. *Anesthesiology* 1997;86:627-631; discussion 27A.
6. Newth CJ, Rachman B, Patel N, et al. The use of cuffed versus uncuffed endotracheal tubes in pediatric intensive care. *J Pediatr* 2004;144:333-337.
7. Pearson TE, Frizzola MA, Khine HH. Uncuffed endotracheal tubes: not appropriate for pediatric critical care transport. *Air Med J* 2019;38:51-54.
8. Shi F, Xiao Y, Xiong W, et al. Cuffed versus uncuffed endotracheal tubes in children: a meta-analysis. *J Anesth* 2016;30:3-11.
9. Dullenkopf A, Gerber A, Weiss M. Fluid leakage past tracheal tube cuffs: evaluation of the new Microcuff endotracheal tube. *Intensive Care Med* 2003;29:1849-1853.
10. Dullenkopf A, Schmitz A, Gerber AC, et al. Tracheal sealing characteristics of pediatric cuffed tracheal tubes. *Paediatr Anaesth* 2004;14:825-830.
11. Dullenkopf A, Gerber A, Weiss M. The Microcuff tube allows a longer time interval until unsafe cuff pressures are reached in children. *Can J Anaesth* 2004;51:997-1001.
12. Dullenkopf A, Schmitz A, Frei M, et al. Air leakage around endotracheal tube cuffs. *Eur J Anaesthesiol* 2004; 21:448-453.
13. Dullenkopf A, Gerber AC, Weiss M. Fit and seal characteristics of a new paediatric tracheal tube with high volume-low pressure polyurethane cuff. *Acta Anaesthesiol Scand* 2005;49:232-237.
14. Funai Y, Miura Y, Mori Y, et al. The clinical assessment of Microcuff® periatric endotracheal tubes in Japanese children. *Nihon Syounimasui Gakkaishi* 2016;22:215-220. (In Japanese)
15. Lau AC, Lam SM, Yan WW. Benchtop study of leakages across the Portex, TaperGuard, and Microcuff endotracheal tubes under simulated clinical conditions. *Hong Kong Med J* 2014;20:7-15.
16. Mhamane R, Dave N, Garasia M. Use of Microcuff® endotracheal tubes in paediatric laparoscopic surgeries. *Indian J Anaesth* 2015;59:85-88.
17. Weiss M, Dullenkopf A, Gysin C, et al. Shortcomings of cuffed paediatric tracheal tubes. *Br J Anaesth* 2004;92: 78-88.
18. Weiss M, Dullenkopf A, Fischer JE, et al. Prospective randomized controlled multi-centre trial of cuffed or uncuffed endotracheal tubes in small children. *Br J Anaesth* 2009;103:867-873.
19. Weiss M, Gerber AC, Dullenkopf A. Appropriate placement of intubation depth marks in a new cuffed paediatric tracheal tube. *Br J Anaesth* 2005;94:80-87.
20. Kanda Y. Investigation of the freely available easy-to-use software 'EZR' for medical statistics. *Bone Marrow*

Transplant 2013;48:452-458.

21. Browning DH, Graves SA. Incidence of aspiration with endotracheal tubes in children. *J Pediatr* 1983;102:582-584.
22. Seegobin RD, van Hasselt GL. Endotracheal cuff pressure and tracheal mucosal blood flow: endoscopic study of effects of four large volume cuffs. *Br Med J (Clin Res Ed)* 1984;288:965-968.
23. Al-Metwalli RR, Sadek S. Safety and reliability of the sealing cuff pressure of the Microcuff pediatric tracheal tube for prevention of post-extubation morbidity in children: a comparative study. *Saudi J Anaesth* 2014;8:484-488.
24. De Orange FA, Andrade RG, Lemos A, et al. Cuffed versus uncuffed endotracheal tubes for general anaesthesia in children aged eight years and under. *Cochrane Database Syst Rev* 2017;11:CD011954.
25. Sathyamoorthy M, Lerman J, Asariparampil R, et al. Stridor in neonates after using the Microcuff® and uncuffed tracheal tubes: a retrospective review. *Anesth Analg* 2015;121:1321-1324.

# Time-lapse Observation of Stabilized Mitochondrial Membrane Potential in Chemotherapy-induced Granulosa Cell Damage Treated with L-carnitine

AKI TAKASE<sup>1)</sup>, DAISUKE TACHIBANA<sup>1)</sup>, YUKIMI KIRA<sup>2)</sup>,  
AKIHIRO HAMURO<sup>1)</sup>, TAKUYA MISUGI<sup>1)</sup>, and MASAYASU KOYAMA<sup>1)</sup>

*Departments of Obstetrics and Gynecology<sup>1)</sup> and Research Support Platform<sup>2)</sup>, Osaka City University Graduate School of Medicine*

## Abstract

### **Background**

Chemotherapy-induced infertility has become problems faced by reproductive-age women receiving chemotherapy and many anticancer drugs mainly affect proliferating cells such as granulosa cells, which support the oocyte. The aims of this study were to investigate mitochondrial membrane potential and to test the protective effect of L-carnitine (LC) in the granulosa cells treated with anticancer drugs.

### **Methods**

Female ICR mice were divided into 5 groups (control, cisplatin, cisplatin+LC, paclitaxel, paclitaxel+LC) and the number of follicles in three sections of ovaries was counted every 100  $\mu\text{m}$  at each development stage. Immunohistochemical analysis of cleaved caspase-3 was performed. The changes due to administration of anticancer drugs with/without LC treatment were analyzed by cell viability and western blotting for active caspase-3, using COV434 cells. The mitochondrial membrane potential was analyzed with the time-lapse function.

### **Results**

Low-dose chemotherapy, which affected the number of primordial cells, caused morphological changes in murine granulosa cells and significant prolongation of mitochondrial membrane potential was observed in pretreatment with LC in chemotherapy-induced cell damage in the COV434 cell line. In addition, cleaved caspase-3 levels were strikingly decreased in LC-treated groups.

### **Conclusions**

Our study is the first to investigate the mitochondrial membrane potential in granulosa cell line COV434 using time-lapse methods, and we found that LC pretreatment had a protective effect to stabilize the mitochondrial membrane potential and postpone apoptosis. Our findings may provide new insight into protection against chemotherapy-induced ovarian failure for women who wish to

---

Received August 20, 2019; accepted October 8, 2019.

Correspondence to: Daisuke Tachibana MD. PhD.

Department of Obstetrics and Gynecology, Osaka City University Graduate School of Medicine,  
1-4-3 Asahimachi, Abeno-ku, Osaka 545-8585, Japan  
Tel: +81-6-6645-3862; Fax: +81-6-6646-5800  
E-mail: dtachibana@med.osaka-cu.ac.jp

preserve fertility.

Key Words: L-carnitine; Granulosa cell; Mitochondrial membrane potential; Time-lapse; Chemotherapy

## Introduction

The survival period and quality of life for patients with various cancers have improved due to development of chemotherapy. However, as the number of reproductive-age women receiving chemotherapy is increasing, chemotherapy-induced infertility and premature ovarian failure have become problems faced by an increasing number of patients<sup>1</sup>. At birth, the ovary contains a finite number of oocytes that are surrounded by a single layer of pregranulosa cells to form primordial follicles, and the female ovary establishes a fixed number of primordial follicles by 5 months of gestational age. Therefore the number of primordial follicles is a direct indicator of fertility reserve, and the prevention of chemotherapy-induced follicle loss is a critical problem.

Anticancer drugs act on the ovary by different mechanisms, and both oocytes and granulosa cells are vulnerable to the chemotherapeutic agents. Direct toxicity to the ovary results in diminished primordial follicle pool, ovarian atrophy, and irreversible change of blood vasculature<sup>2</sup>. A recent study has proposed a new hypothesis, called the burn-out theory. The burn-out theory is a mechanism in which the anticancer drugs induce that development from the primordial follicles to the antral follicles continues to be accelerated wastefully, and these follicles become follicle atresia, and to cause the depletion of ovarian reserve and consequently ovarian failure. On the other hand, granulosa cells are active to proliferate and highly sensitive to the anticancer drugs, so chemotherapy causes the granulosa cell apoptosis<sup>3,4</sup>.

Mitochondrial membranes are important sites for steroidogenesis in granulosa cells. Cholesterol, a substrate of steroid hormones, is transferred from the outer to the inner mitochondrial membrane by steroidogenic acute regulatory (StAR) protein, which is in turn metabolized to pregnenolone by cytochrome P450 cholesterol side-chain cleavage enzyme (P450scc). Damage to mitochondrial membranes by oxidative stress impairs steroidogenesis in granulosa cells. In fact, oxidative stress has been reported to inhibit steroidogenic enzymes and a mitochondrial carrier protein (StAR protein) involved in cholesterol transport into mitochondria of luteal cells<sup>5</sup>. Therefore, stabilized the mitochondrial membrane potential of granulosa cells may have protective effect against chemotherapy-induced follicle apoptosis. However, the exact mechanism of granulosa cell apoptosis induced by chemotherapy remains unclear.

L-carnitine (LC) is a natural nutrient and essential for  $\beta$ -oxidation of fatty acids in mitochondria to generate ATP. Because hydrophobic anions exhibit detergent-like action and perturb membrane/lipid bilayers, abnormally elevated long-chain fatty acids might impair mitochondrial membranes and induce permeability transition, a prerequisite reaction to cytochrome *c* release. In addition, LC effectively inhibits mitochondrial dysfunction induced by oxidative stress and mitochondria-dependent apoptosis of various cell types<sup>6</sup>, and to prove these phenomena, several reports have used techniques that can capture changes in mitochondrial membrane potential at the very early stage of apoptosis temporally and quantitatively<sup>7,8</sup>. Therefore, we hypothesized that chemotherapy induces mitochondrial membrane impairment of granulosa cells and treatment with LC can inhibit chemotherapy-induced follicle apoptosis.

## Methods

### ***Animal experiments***

Experimental protocols used in this study conformed to the Institutional Committee for Animal Care and Experiments in Osaka City University, Graduate School of Medicine, and were approved by the Fundamental Guidelines for Proper Conduct of Animal Experiment and Related Activities in Academic Research Institutions under the jurisdiction of the Ministry of Education, Culture, Sports, Science, and Technology. Seven-week-old female ICR mice weighing 30g were purchased from SLC (Japan SLC). The animals were kept in a cage under controlled light (12-h light/12-h dark cycle), temperature, and humidity conditions.

Fifty mice were divided evenly into 5 groups. Group 1 was a control group in which the ovaries were removed at 10 weeks of age. Group 2 was the cisplatin group in which cisplatin (10 mg/kg)<sup>9)</sup> was intraperitoneally injected. Group 3 was the paclitaxel group in which paclitaxel (5 mg/kg)<sup>10)</sup> was intraperitoneally injected. Groups 4 and 5 were LC pretreatment groups, and mice consumed LC in their drinking water (LC concentration 1 mg/mL)<sup>11)</sup> for 2 weeks (LC intake: 200 mg/kg/day). Group 4 received the same amount of cisplatin as group 2, and Group 5 received the same amount of paclitaxel as in group 3. Mice in Groups 2-5 were euthanized 1 week after administration of anticancer drugs, and ovaries were removed at 10 weeks of age. For histology, one ovary from each mouse was fixed with formalin and embedded in paraffin.

### ***Change in follicle number by follicular development stage***

Ovaries were fixed with formalin, embedded in paraffin, and sectioned at 4  $\mu\text{m}$ . Sections were stained with hematoxylin and eosin, and the number of follicles in three sections was counted every 100  $\mu\text{m}$ . Follicles were categorized as primordial follicles (oocyte surrounded by a single layer of flat follicular epithelium cells), primary follicles (oocyte surrounded by a single layer of cubic granulosa cells), secondary follicles (oocyte surrounded by at least two cell layers of cubic granulosa cells), and antral follicles (consisting of oocytes, many layers of granulosa cells, and a cavity filled with follicular fluid)<sup>12)</sup>.

### ***Immunohistochemistry***

Paraffin-embedded sections were deparaffinized by rinsing with 100% xylene three times, 100% ethanol twice, 70% ethanol once, and 50% ethanol once. Citrate buffer (pH 6.0) was used for antigen activation. Endogenous peroxidases were quenched with 3% H<sub>2</sub>O<sub>2</sub>, and blocking was performed with 5% goat serum. Then, sections were incubated with primary antibody (active caspase-3, #9661, 1:200, Cell Signaling Technology) overnight at 4°C. After two washes in Tris Buffered Saline (TBS), sections were incubated with secondary antibody (Histofine Simple Stain Mouse MAX-PO®, Nichirei Biosciences). A diaminobenzidine solution was dropped onto sections and incubated until the desired staining was achieved. Finally, sections were stained with hematoxylin and eosin (HE).

### ***Cell lines***

COV434 cells<sup>13)</sup>, which are a human granulosa cell tumor cell line, were used. COV434 cells are derived from a 27-year-old female with a metastatic granulosa cell tumor but possess many characteristics of normal granulosa cells. COV434 cells were cultured in Dulbecco's Modified Eagle Medium F12 (Wako Pure Chemical Industries) supplemented with 5% fetal bovine serum in a 5% CO<sub>2</sub> incubator at 37°C.

### ***Cell viability***

Cell viability was analyzed using a Cell Counting Kit-8 (CCK-8) kit (Dojindo Laboratories).

COV434 cells were plated at  $2.5 \times 10^4$ /well in a 96-well microplate and allowed to attach overnight. COV434 cells were cultured at different concentrations of cisplatin and paclitaxel for 24 h, and anticancer drug concentrations at which 50%-60% cell viability was observed were applied in this study. After cells were treated with or without 0.5 mM LC<sup>14)</sup> for 12 h, culture medium was changed to medium containing anticancer drugs at the indicated concentration (without LC), and then 12 h later a CCK-8 solution was added at 10  $\mu$ L/well. Plates were incubated at 37°C for 2 h and the absorbance was measured at 450 nm using a microplate reader (Varioskan™ LUX, Thermo Fisher Scientific). Cell viability was calculated based on the absorbance of control cells and changes due to administration of anticancer drugs with/without LC treatment were analyzed.

#### ***Detection of mitochondrial membrane potential***

COV434 cells were cultured with/without LC treatment for 6 h in 3-cm glass-bottom dishes and mitochondrial membrane potential was assessed by fluorescence microscopy after applying the JC-1 Mitochondrial Membrane Potential Assay Kit (BD™ MitoScreen Kit, Biosciences)<sup>15)</sup>. The fluorescent carbocyanine dye, JC-1, labels mitochondria with high membrane potential as red and mitochondria with low membrane potential as green. After incubating COV434 cells with/without LC treatment, cells were incubated in 5  $\mu$ M JC-1 fluorescence dye in a 5% CO<sub>2</sub> incubator for 30 min at 37°C. Cells were slowly washed with JC-1 working solution three times. The mitochondrial membrane potential was analyzed by imaging every 1 min after administration of anticancer drugs with the time-lapse function of the LSM 700 confocal laser scanning microscope system. The green signal of JC-1 was measured at 485/555 nm, whereas that of the red signal was measured at 590/610 nm<sup>16)</sup>.

#### ***Western blotting***

Cells were pretreated with LC for 12 h, incubated with anticancer drugs for 24 h, and then collected. The supernatant was also collected. After centrifugation for 5 min, the supernatant was discarded, washed with Phosphate Buffered Saline (PBS), centrifuged again for 5 min, and the pellet was recovered. Proteins were extracted with radioimmunoprecipitation assay buffer. Total protein was quantified using the Bicinchoninic acid (BCA) protein assay. Protein samples with loading buffer were separated by 15% sodium dodecyl sulfate-polyacrylamide gel electrophoresis and transferred to polyvinylidene difluoride membranes. Membranes were blocked with blocking buffer (5% skim milk in TBST) for 1 h and then incubated with the following primary antibodies diluted in blocking buffer at 4°C overnight: anti-caspase-3, anti-active caspase-3, and anti- $\beta$ -actin (1:1000, 1:1000, 1/10000; Cell Signaling Technology). Bound antibodies were detected after incubation with horseradish peroxidase-conjugated rabbit anti-mouse immunoglobulin G using ImmunoStar LD (Wako Pure Chemical Industries, Ltd.) and Fusion SOLO.7S (Vilber Lourmat). Chemiluminescent bands were quantified with Image Quant TL (GE Healthcare Life Sciences).

#### ***Statistical analysis***

Results are expressed as the mean  $\pm$  standard deviation. All statistical analyses were performed using the Mann-Whitney U-test. A value of  $p < 0.05$  was considered significant.

## **Results**

### ***L-carnitine affects the number of follicles at each development stage***

In the primordial follicle stage, the number of follicles in the chemotherapy-only group was significantly lower than that in the control group (cisplatin,  $p = 0.003$ ; paclitaxel,  $p = 0.030$ ) and the number of follicles in the paclitaxel+LC group was significantly higher than that in the non-

treatment group ( $p=0.0001$ ). In the primary follicle stage, the number of follicles in the chemotherapy-only group was significantly lower than that in the control group (cisplatin,  $p=0.015$ ; paclitaxel,  $p=0.028$ ). In the secondary follicle stage, the number of follicles in the LC pretreatment group was significantly higher than in the non-treatment group (cisplatin,  $p=0.033$ ; paclitaxel,  $p=0.044$ ). In the antral follicle stage, there was no significant difference between groups. (Fig. 1).

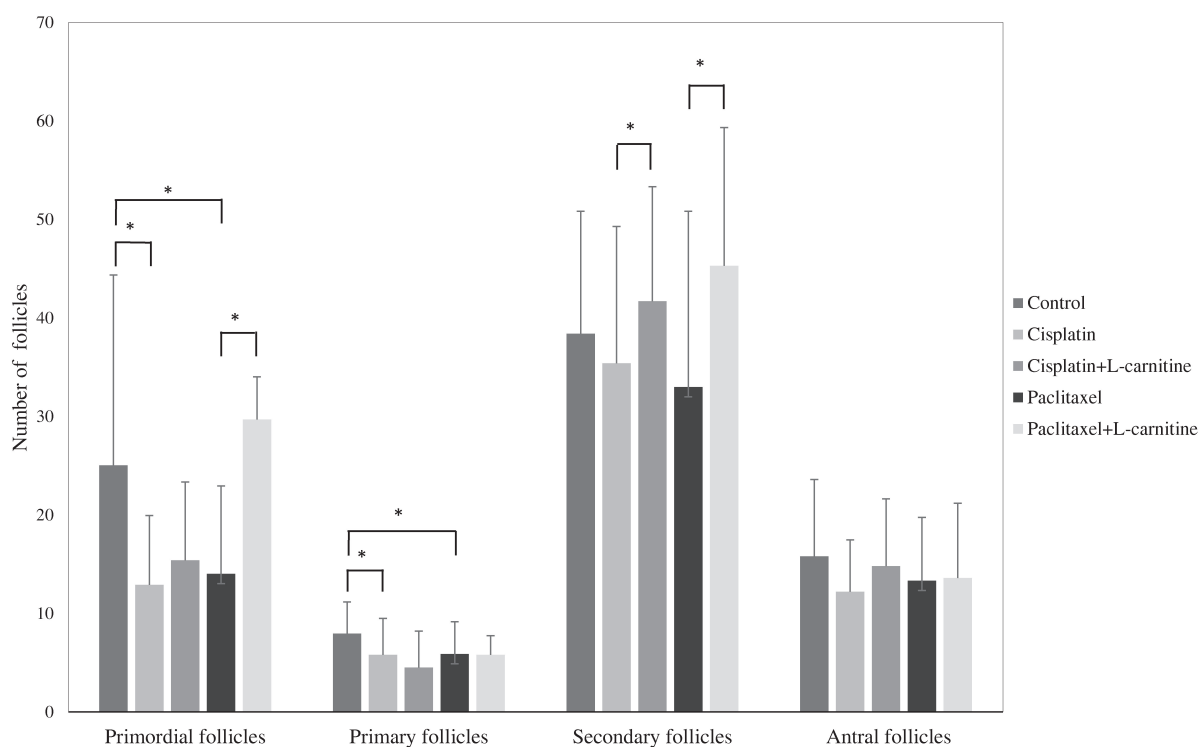


**Figure 1.** The number of follicles at each development stage (primordial, primary, secondary, and antral follicles). Fifty mice were divided evenly into 5 groups. Sections of ovary were stained with hematoxylin and eosin, and the number of follicles in three sections was counted every 100  $\mu\text{m}$ . In the primordial follicle stage, the number of follicles in the chemotherapy-only group was significantly lower than that in the control group (cisplatin,  $p=0.003$ ; paclitaxel,  $p=0.030$ ) and the number of follicles in the paclitaxel+LC was significantly higher than that in the non-treatment group ( $p=0.0001$ ). In the primary follicle stage, the number of follicles in the chemotherapy-only group was significantly lower than that in the control group (cisplatin,  $p=0.015$ ; paclitaxel,  $p=0.028$ ). In the secondary follicle stage, the number of follicles in the LC pretreatment group was significantly higher than in the non-treatment group (cisplatin,  $p=0.033$ ; paclitaxel,  $p=0.044$ ). In the antral follicle stage, there was no significant difference between groups. Data represent the mean  $\pm$  SD. Asterisks denote significant differences ( $* p < 0.05$ ). LC, L-carnitine.

### ***Immunohistochemical analysis of cleaved caspase-3 in mouse ovaries***

In antral follicles, the structure of granulosa cell layers around the oocyte was disordered in the anticancer drugs treatment group (Figs. 2C and 2G), whereas cell layers were maintained in the LC pretreatment group (Figs. 2E and 2I). As a result of immunohistochemical analysis of active caspase-3, which is a mitochondrial-dependent apoptosis marker, granulosa cells were stained only in the anticancer drugs treatment groups (Figs. 2D and 2H). However, in the LC pretreatment group, almost no staining was seen (Figs. 2F and 2J). In primordial follicles, the structure was relatively maintained even in the anticancer drugs treatment group (Figs. 3C and 3G). Active caspase-3 was detected in granulosa cells of the anticancer drugs treatment groups (Figs. 3D and 3H). However, active caspase-3 was not detected in granulosa cells of the LC pretreatment groups (Figs. 3F and 3J).

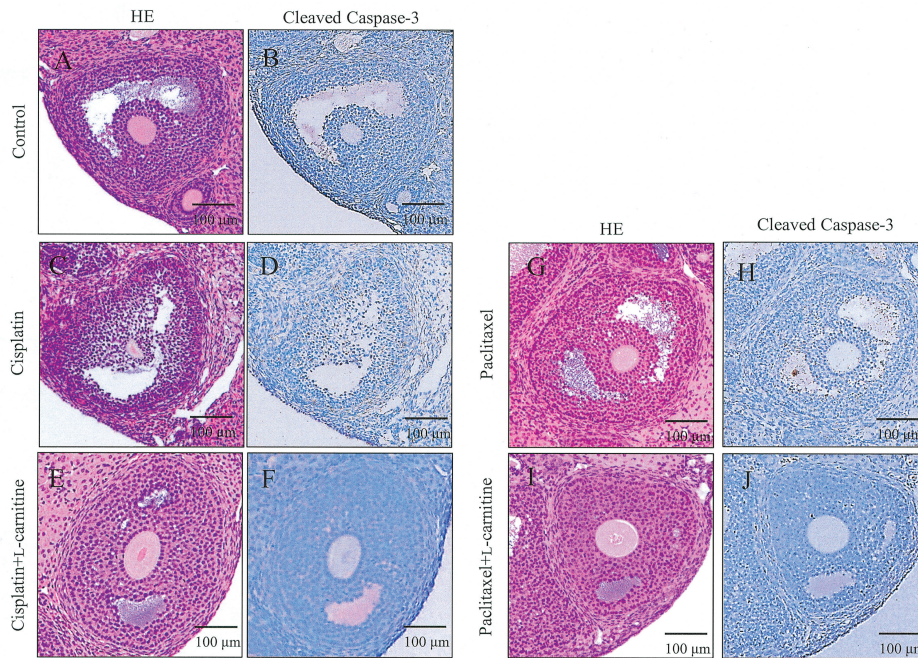


**Figure 2.** Representative histological sections of mouse ovaries stained with hematoxylin and eosin (A, C, E, G, and I), and immunohistochemical analysis of cleaved caspase-3 (B, D, F, H, and J). Antral follicles from (A and B) control, (C and D) cisplatin-only, (E and F) cisplatin+LC, (G and H) paclitaxel-only, and (I and J) paclitaxel+LC groups are shown. Active caspase-3 was detected in granulosa cells of cisplatin-only (D) and paclitaxel-only (H) groups. However, active caspase-3 was not detected in granulosa cells of cisplatin+LC (F) and paclitaxel+LC (J) groups. Scale bars= 100 μm. LC, L-carnitine.

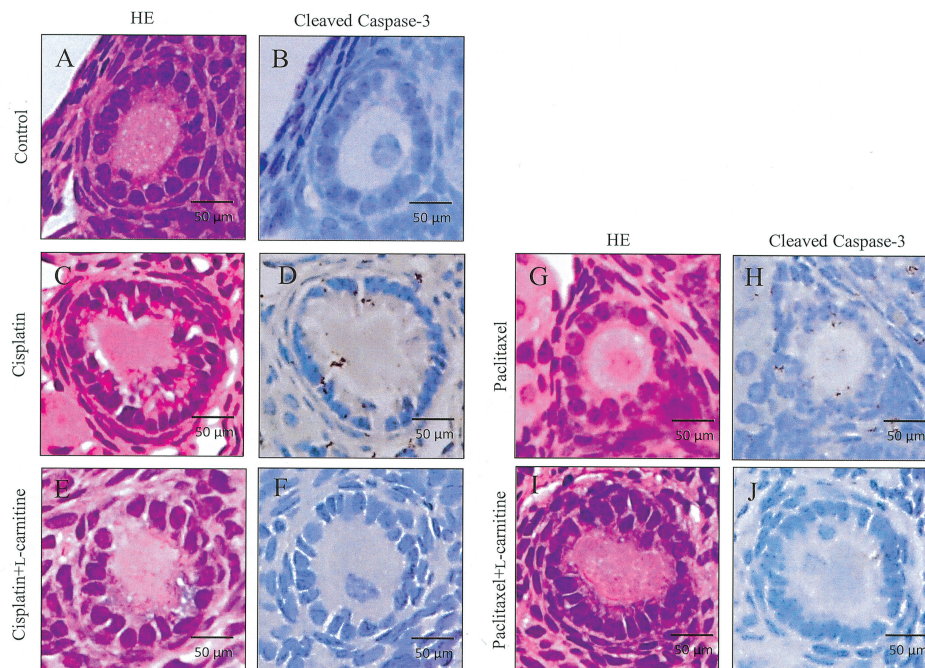


**Figure 3.** Representative histological sections of mouse ovaries stained with hematoxylin and eosin (A, C, E, G, and I), and immunohistochemical analysis of cleaved caspase-3 (B, D, F, H, and J). Primordial follicles from (A and B) control, (C and D) cisplatin-only, (E and F) cisplatin+LC, (G and H) paclitaxel-only, and (I and J) paclitaxel+LC groups are shown. Active caspase-3 was detected in granulosa cells of cisplatin-only (D) and paclitaxel-only (H) groups. However, active caspase-3 was not detected in granulosa cells of cisplatin+LC (F) and paclitaxel+LC group (J) groups. Scale bars=50 μm. LC, L-carnitine.

This result demonstrates that mitochondria-dependent apoptosis caused by anticancer drugs was suppressed by LC pretreatment.

### **Effect of LC in cell viability**

The effect of different concentrations of cisplatin (1-100  $\mu\text{M}$ ) or paclitaxel (10-500 nM) for 24 h on the viability of COV434 cells was measured by CCK-8. Anticancer drug concentrations at which 50%-60% cell viability was observed were determined as 25  $\mu\text{M}$  for cisplatin (Fig. 4A) and 250 nM for paclitaxel (Fig. 4B). These concentrations were applied in the following experiment.

COV434 cells were treated with each anticancer drug for 12 h after LC pretreatment, and then the CCK-8 assay was performed. Cell viability of the cisplatin+LC group was approximately 15% higher than that of the cisplatin-only group. Furthermore, the viability of the paclitaxel+LC group was approximately 20% higher than that of the paclitaxel-only group (Fig. 5). These results suggest that LC has a protective effect against anticancer drug-induced cell death.

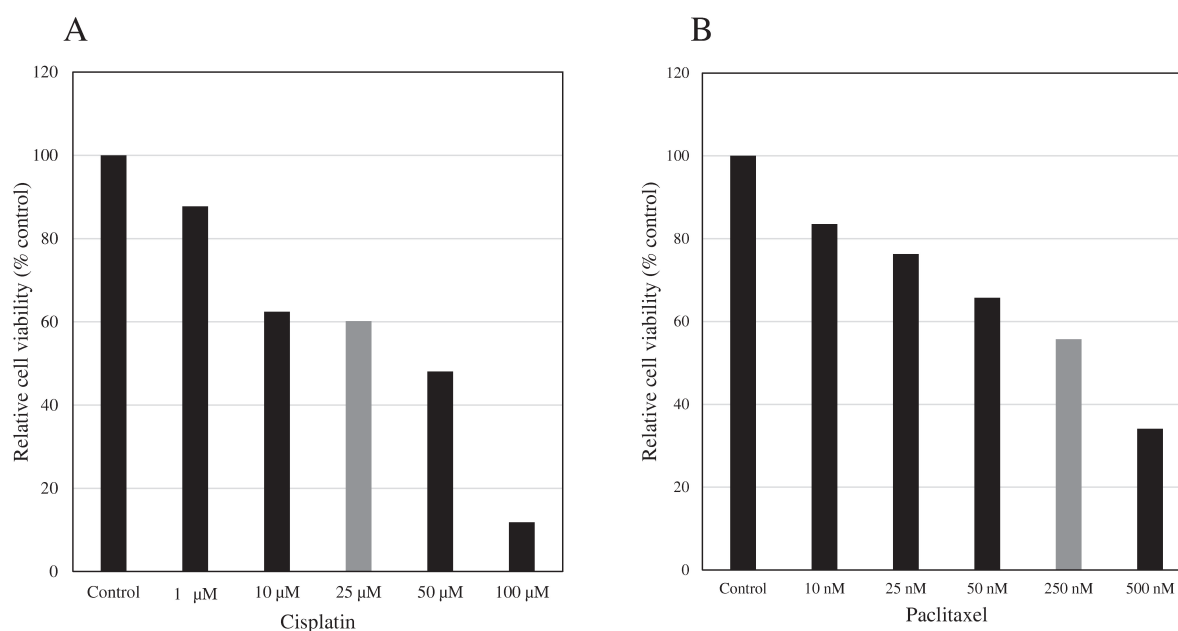


**Figure 4.** Cell viability of each group using Cell Counting Kit-8 (CCK-8). The effect of treatment with different concentrations of cisplatin (1-100  $\mu\text{M}$ ) or paclitaxel (10-500 nM) for 24 h on the viability of COV434 cells was measured by CCK-8. Anticancer drug concentrations at which 50%-60% cell viability was observed were applied in this study.

### **Effect of LC pretreatment in mitochondrial membrane potential**

COV434 cells had high mitochondrial membrane potential before chemotherapy (Fig. 6A), which disappeared following chemotherapy (Fig. 6B). COV434 cells were incubated with or without LC (0.5 mM) for 6 h before the addition of cisplatin or paclitaxel. Time-lapse images of mitochondrial membrane potential were detected by JC-1 and captured every 1 min (Figs. 7A, 7C, 9A, and 9C). The shift in mitochondrial membrane potential (crossing point between red and green signals) occurred 3 min after administration of cisplatin (Fig. 7B). When LC pretreatment was performed, the crossing point was prolonged to 7 min (Fig. 7D). The fluorescence ratio (red/green) indicates the mitochondrial membrane potential. The mitochondrial membrane potential of the LC pretreatment group was significantly increased as compared with the cisplatin-only group (0 min,  $p=0.046$ ) (Fig. 8).

The crossing point occurred 3-4 min after administration of paclitaxel (Fig. 9B). When LC pretreatment was performed, the crossing point was prolonged to 10-11 min (Fig. 9D). The mitochondrial membrane potential of the LC pretreatment group was significantly increased as compared with the paclitaxel-only group (0 min,  $p=0.009$ ; 5 min,  $p=0.016$ ; 10 min,  $p=0.016$ ) (Fig. 10).

**LC pretreatment decreased active caspase-3**

In cisplatin- and paclitaxel-treated COV434 cells, active caspase-3 was significantly increased

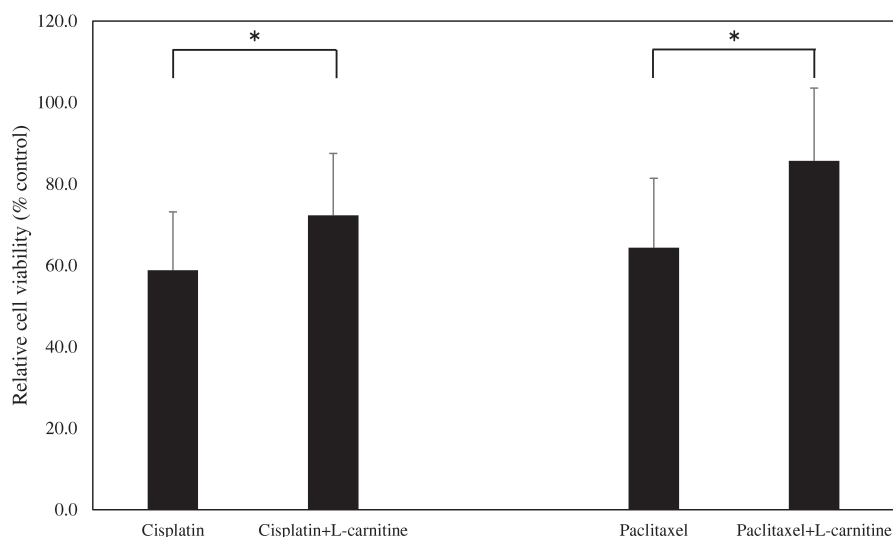


**Figure 5.** COV434 cells were incubated in the presence or absence of LC (0.5 mM) for 12 h before the addition of cisplatin or paclitaxel. Cell viability of the cisplatin+LC group was significantly higher than that of the cisplatin-only group ( $p=0.024$ ). Cell viability of the paclitaxel+LC group was significantly higher than that of the paclitaxel-only group ( $p=0.035$ ). Asterisks denote significant differences ( $* p<0.05$ ). LC, L-carnitine.

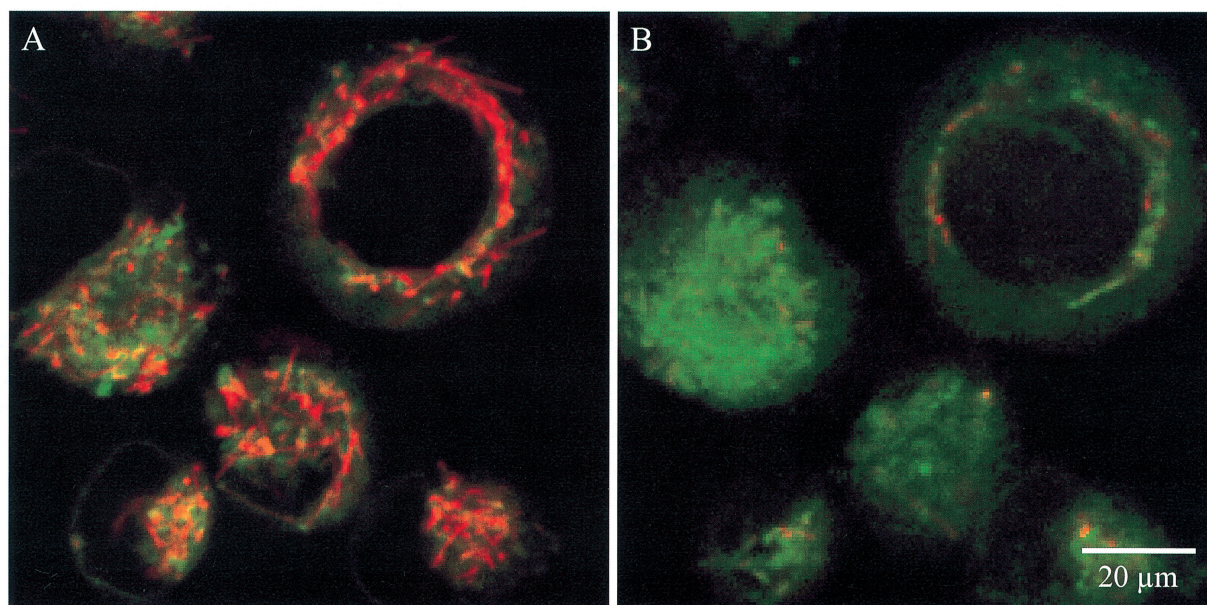


**Figure 6.** Representative images of mitochondrial membrane potential using JC-1 are shown. (A) COV434 cells before chemotherapy and (B) COV434 cells after chemotherapy. JC-1 labels mitochondria with high membrane potential as red and mitochondria with low membrane potential as green.

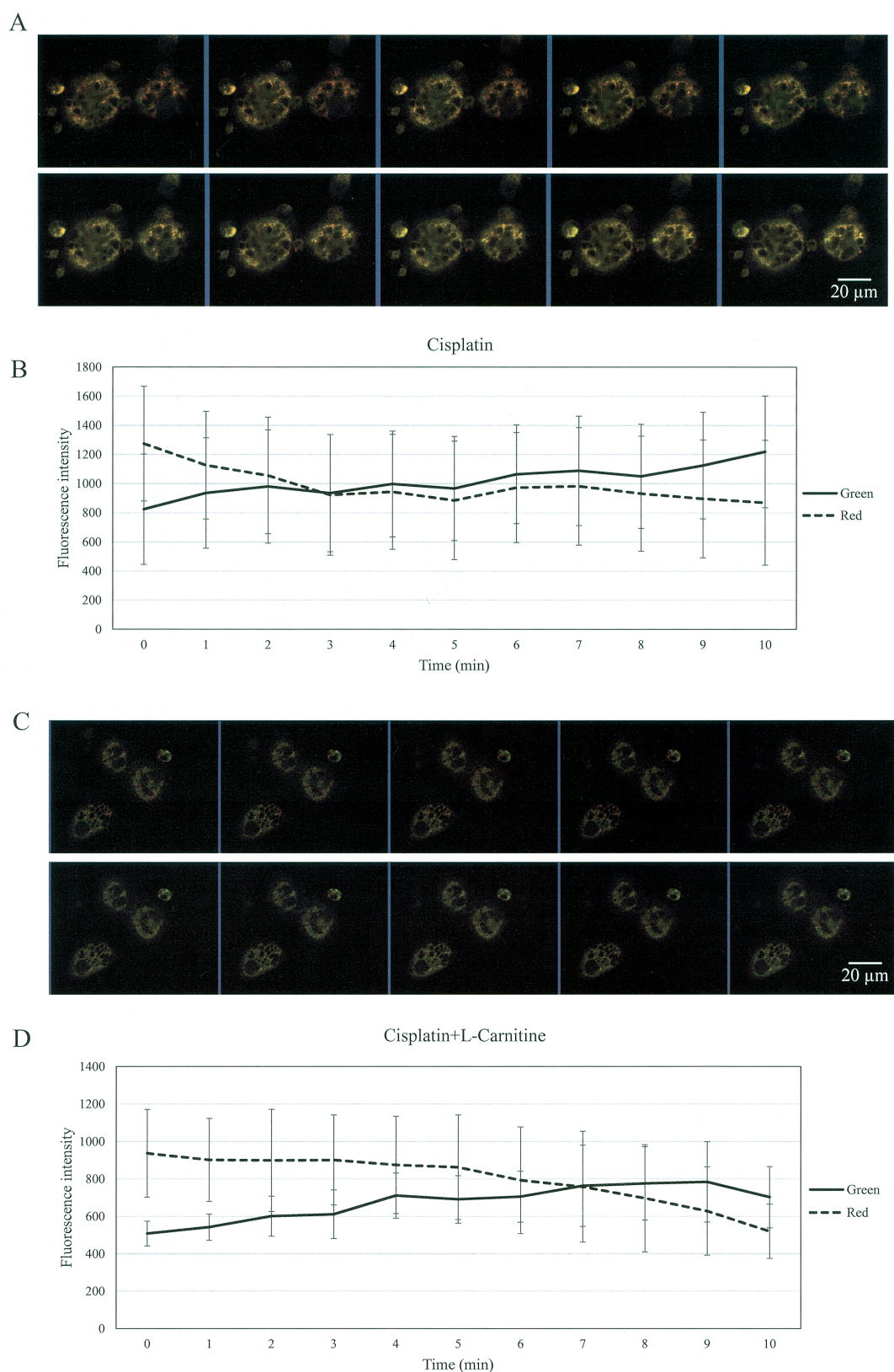


**Figure 7.** COV434 cells were incubated with (A and B) or without (C and D) LC (0.5 mM) for 6 h before the addition of cisplatin. Parts A and C shows time-lapse images of mitochondrial membrane potential every 1 min, and parts B and D shows the time-lapse of mitochondrial membrane potential intensity. Note the crossing point between red and green signals. The crossing point in the without LC group was <4 min after cisplatin administration, whereas the crossing point in the LC treatment group was postponed by >10 min. LC, L-carnitine.

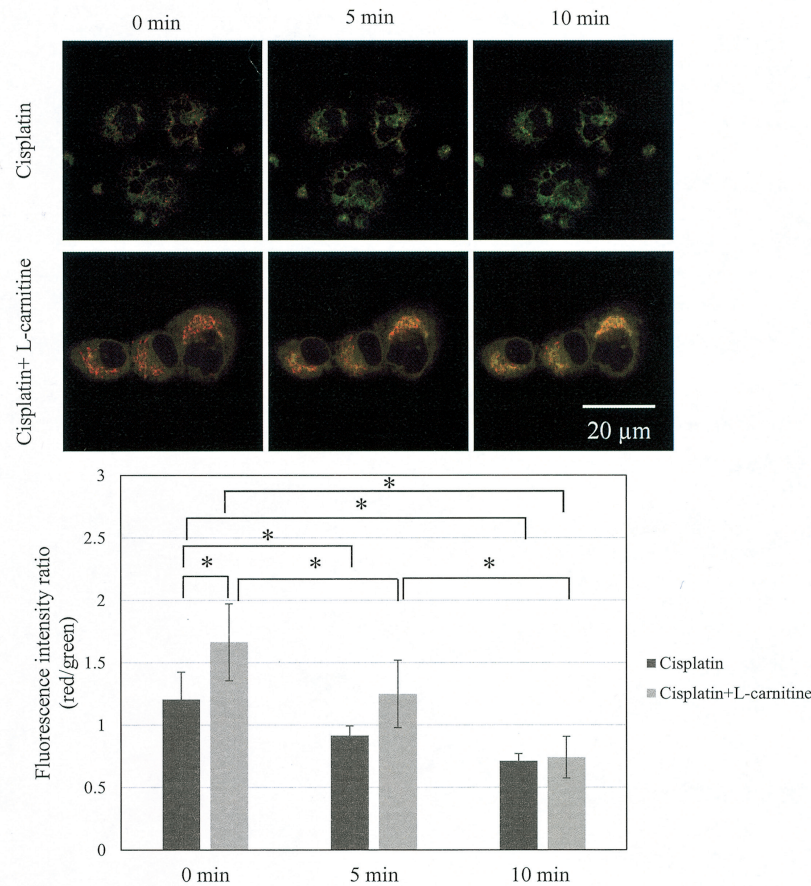


**Figure 8.** Representative images taken at 0, 5, and 10 min after cisplatin administration were selected from a set of time-lapse dual images for comparison. The fluorescence ratio (red/green) indicates the mitochondrial membrane potential. The mitochondrial membrane potential of the LC pretreatment group was significantly increased as compared with that of the cisplatin-only group. Asterisks denote significant differences ( $* p < 0.05$ ). LC, L-carnitine.

compared with that of the control. Conversely, in the LC pretreatment group, active caspase-3 was significantly decreased compared with treatment with anticancer drugs only (cisplatin,  $p = 0.025$ ; paclitaxel,  $p = 0.025$ ) (Fig. 11A). Pro-caspase-3 was not significantly changed in the groups (Fig. 11B). These results suggest that cell death of COV434 cells occurred due to mitochondria-dependent apoptosis by anticancer drug treatment, and LC can rescue this cell death through mitochondrial protective effects.

## Discussion

The present results showed that low-dose chemotherapy, which affected the number of primordial cells, caused morphological changes in murine granulosa cells. Furthermore, we first observed that pretreatment with LC showed significant prolongation of mitochondrial membrane potential in chemotherapy-induced cell damage in the COV434 cell line. In addition, active caspase-3 levels were strikingly decreased in LC-treated groups. These phenomena might be due to stabilization of the mitochondrial membrane potential, which is thought to play pivotal roles in cell apoptosis<sup>17</sup>.

Cancer treatment can have devastating consequences for young females, resulting in ovarian damage accompanied by diminished fertility potential. The extent of damage is related to chemotherapeutic regimen and dosage. Mitochondrial damage caused by cisplatin has been reported

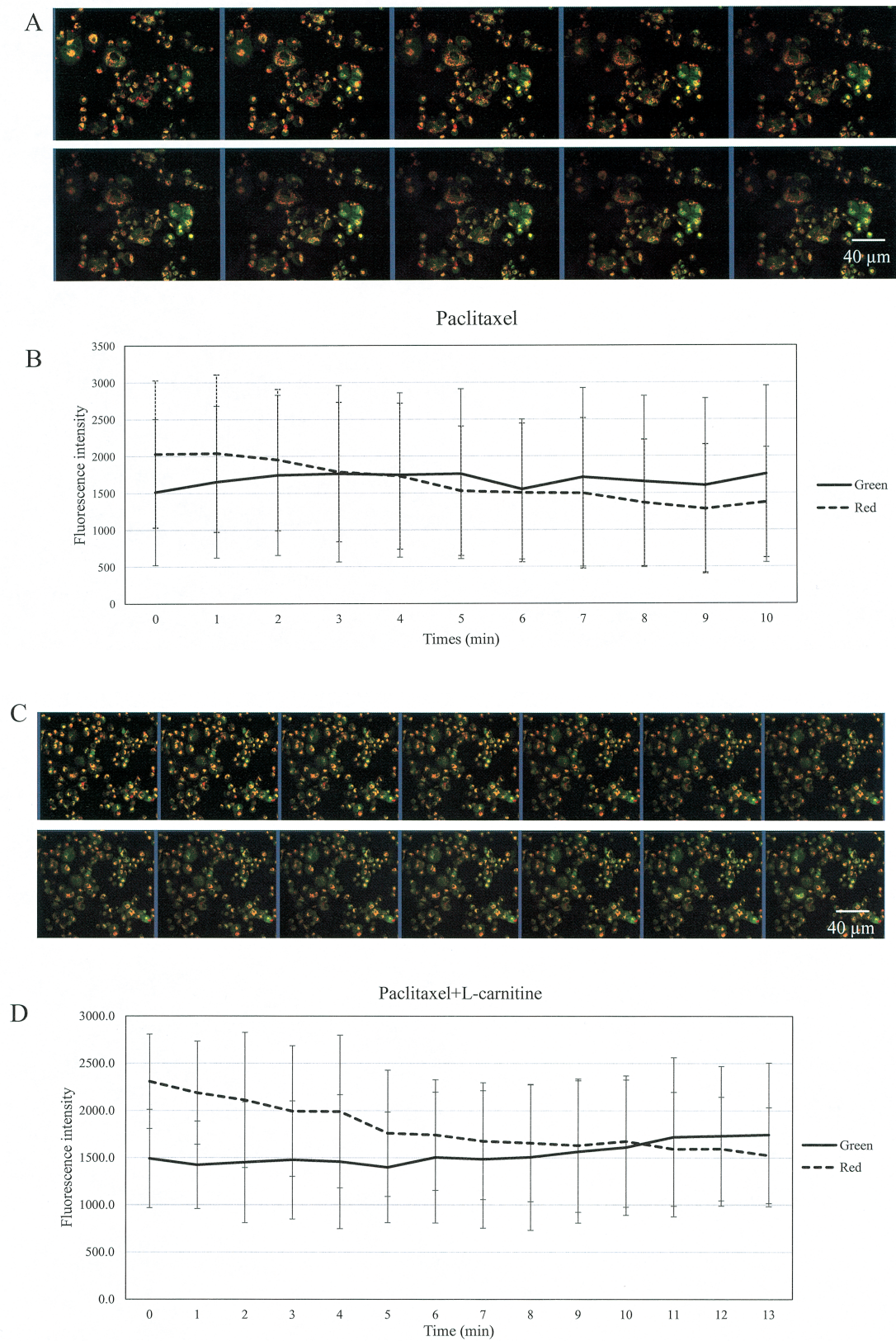


**Figure 9.** COV434 cells were incubated with (A and B) or without (C and D) LC (0.5 mM) for 6 h before the addition of paclitaxel. Parts A and C shows time-lapse images of mitochondrial membrane potential every 1 min, and parts B and D shows time-lapse of mitochondrial membrane potential intensity. Note the crossing point between red and green signals. The crossing point in the without LC group was <3 min after paclitaxel administration, whereas the crossing point in the LC treatment group was postponed by >7 min. LC, L-carnitine.

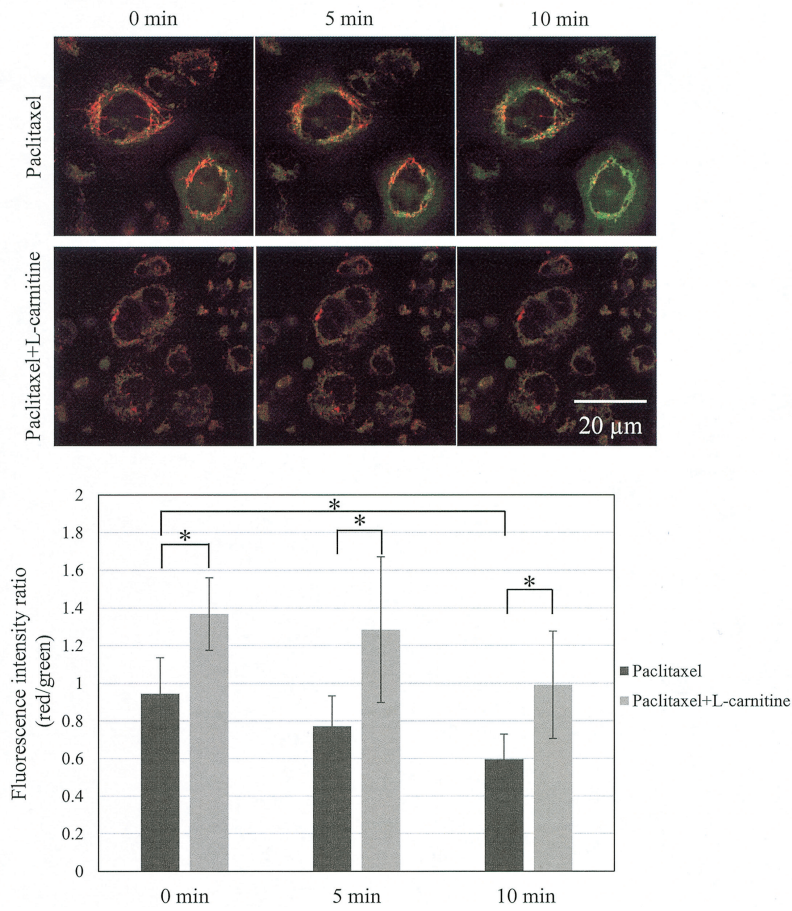


**Figure 10.** Representative images taken at 0, 5, and 10 min after paclitaxel administration were selected from a set of time-lapse dual images for comparison. The fluorescence ratio (red/green) indicates the mitochondrial membrane potential. The mitochondrial membrane potential of the LC pretreatment group was significantly increased as compared with that of the paclitaxel-only group. Asterisks denote significant differences (\*  $p < 0.05$ ). LC, L-carnitine.

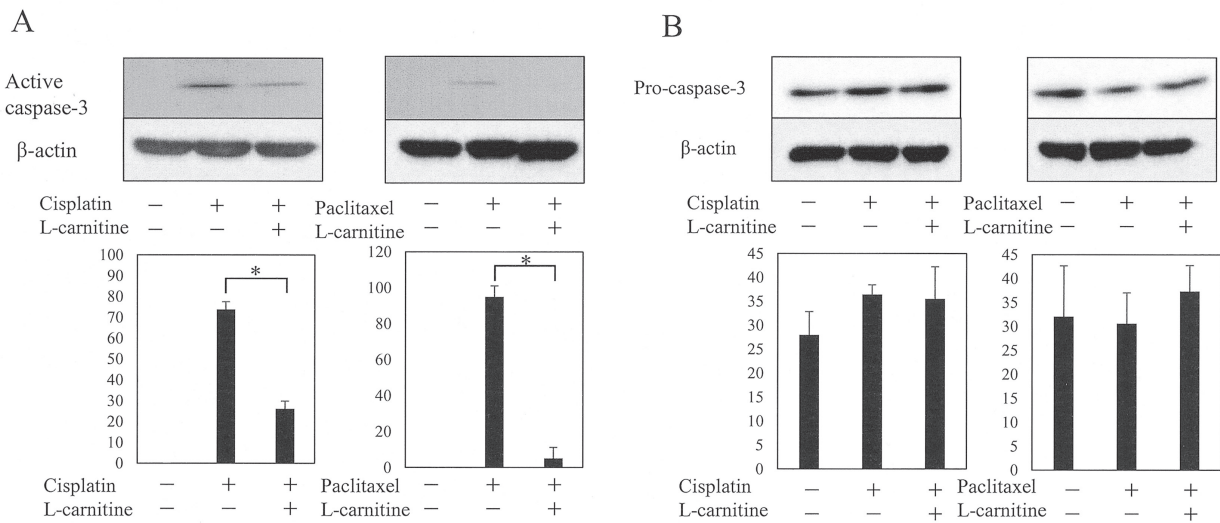


**Figure 11.** Western blot analysis was performed with COV434 cells for (A) cleaved caspase-3 and (B) pro-caspase-3. Data represent the mean  $\pm$  SD. Asterisks denote significant differences (\*  $p < 0.05$ ). In the anticancer drug-only treatment group, active caspase-3 was significantly increased compared with that of the control group ( $p = 0.025$ ). In the LC pretreatment group, active caspase-3 was significantly decreased compared with that of the anticancer drug-only treatment group. Pro-caspase-3 was not significantly changed in any group. LC, L-carnitine.

in several models of cisplatin-induced nephrotoxicity, neurotoxicity, and auditory toxicity<sup>18-20</sup>. Cellular exposure to cisplatin causes direct damage to mitochondrial DNA (mtDNA) resulting in a reduction of mitochondrial protein synthesis, impairment of electron transport chain function, and subsequently, increases in intracellular reactive oxygen species (ROS) levels. ROS promote mitochondria-dependent apoptosis and enhance cytotoxic effects of cisplatin through nuclear DNA damage<sup>21</sup>. Paclitaxel activates Raf-1 and causes phosphorylation of Bcl-2, which leads to an increase in the level of free intracellular Bax. Free intracellular Bax activates caspase proteins through Bax-induced release of cytochrome *c*, which finally promotes mitochondrial apoptosis<sup>22</sup>. Cisplatin causes direct damage to mitochondrial DNA and induces apoptosis by promoting ROS production. On the other hand, paclitaxel increases the permeability of the mitochondrial membrane by increasing BAX (apoptosis inducing factor) and induces apoptosis. Regarding the different effects of LC for two anticancer drugs, one possible mechanism might be explained that paclitaxel gradually damages the mitochondria, and it may take time to reach the mitochondrial membrane through some steps mentioned above, and the protective effect of pretreated LC on the mitochondrial membrane was promptly and profoundly observed.

The apoptosis pathway, which starts with mitochondrial damage, has been recently studied by measuring the magnitude and time courses of mitochondrial membrane potential in pancreatic beta-cells and astrocytes<sup>7,8</sup>. Furthermore, using isolated mitochondria purified by Percoll gradient centrifugation to exclude any indirect mechanism of the effect of paclitaxel on permeability transition, Varbiro et al<sup>22</sup> showed that paclitaxel induces mitochondrial permeability transition, including large amplitude swelling of mitochondria, dissipation of mitochondrial membrane potential, opening of the permeability transition pore by an enzymatic mechanism, and cytochrome *c* release. Jou et al<sup>7</sup> reported that cell stress caused by ROS showed unstabilized mitochondrial permeability transition and mitochondrial oxidation. They also reported that melatonin provided multiple levels of mitochondria-targeted protection. Antioxidant agents such as melatonin are suggested to have substantial roles for protective stabilization of mitochondrial function.

The present results showed that the number of the antral follicles tended to decrease with the administration of anticancer drugs, and to protect with LC pretreatment, but there was no significant difference. However, in the secondary follicles, the number of follicles was significantly increased by LC pretreatment. The primordial follicle develops step by step into the primordial follicle, the primary follicle, the secondary follicle, and finally the antral follicle. By the damage of multilayered granulosa cells, the number of secondary follicles decreases and the developmental damage from the secondary follicles to the antral follicles occurs. The protective effect of LC against the damage to granulosa cells in the antral follicles shown in Figure 3 was not effective to increase the number of the antral follicles, but at least in the level of secondary follicles, LC was contributed to stabilize the mitochondrial membrane potential of granulosa cells.

LC is a water-soluble nutrient with a choline-like structure and is distributed mainly in the liver, kidney, heart, brain, and skeletal muscles in humans. LC is biosynthesized from lysine and methionine in the liver and kidney and plays an essential role for  $\beta$ -oxidation of free fatty acids on the inner mitochondrial membrane for ATP production<sup>6</sup>. Accumulated data of LC in female infertility have been recently documented and a beneficial effect of antioxidant properties and amelioration of energy supply to reproductive organs have been shown in vitro as well as in vivo<sup>23</sup>. One potential mechanism of LC action within the oocyte is that LC is converted to acetyl L-carnitine and balances

the acetyl CoA/CoA ratio to maintain glucose metabolism through the TCA cycle, yielding higher energy production<sup>24</sup>. This further reduces oxidative stress and lipotoxicity by scavenging free radicals and removing excess palmitate<sup>25</sup>. As such, while the roles of LC in oocytes have been studied extensively, apoptosis in granulosa cells, especially that induced by chemotherapy, lacks experimental observation.

To the best of our knowledge, our study is the first to investigate the mitochondrial membrane potential in granulosa cell line COV434 using time-lapse methods. In addition, we found that LC pretreatment had a protective effect to stabilize the mitochondrial membrane potential and postpone apoptosis. Our findings may provide new insight into protection against chemotherapy-induced ovarian failure for women who wish to preserve fertility. Further studies are needed to elucidate mechanisms underlying the interaction between inhibition of granulosa cell apoptosis and preservation of oocyte quality.

### Acknowledgements

All authors have no COI to declare regarding the present study.

The authors would like to acknowledge Keisuke Inoue, Emi Donoue and Yoriko Yabunaka (Research support platform of Osaka City University Graduate School of Medicine) for special technical assistance.

### References

1. Kasum M, Beketić-Orešković L, Peddi PF, et al. Fertility after breast cancer treatment. *Eur J Obstet Gynecol Reprod Biol* 2014;173:13-18.
2. Nelson SM, Telfer EE, Anderson RA. The ageing ovary and uterus: new biological insights. *Hum Reprod Update* 2013;19:67-83.
3. Bedoschi G, Navarro PA, Oktay K. Chemotherapy-induced damage to ovary: mechanisms and clinical impact. *Future Oncol* 2016;12:2333-2344.
4. Meiorow D, Biederman H, Anderson RA, et al. Toxicity of chemotherapy and radiation on female reproduction. *Clin Obstet Gynecol* 2010;53:727-739.
5. Tanabe M, Tamura H, Taketani T, et al. Melatonin protects the integrity of granulosa cells by reducing oxidative stress in nuclei, mitochondria, and plasma membranes in mice. *J Reprod Dev* 2015;61:35-41.
6. Vaz FM, Wanders RJ. Carnitine biosynthesis in mammals. *Biochem J* 2002;361:417-429.
7. Jou MJ, Peng TI, Reiter RJ. Protective stabilization of mitochondrial permeability transition and mitochondrial oxidation during mitochondrial Ca<sup>2+</sup> stress by melatonin's cascade metabolites C3-OHM and AFMK in RBA1 astrocytes. *J Pineal Res* 2019;66:e12538.
8. Gerencser AA, Mookerjee SA, Jastroch M, et al. Measurement of the absolute magnitude and time courses of mitochondrial membrane potential in primary and clonal pancreatic beta-cells. *PLoS One* 2016;11:e0159199.
9. Chang EM, Lim E, Yoon S, et al. Cisplatin induces overactivation of the dormant primordial follicle through PTEN/AKT/FOXO3a pathway which leads to loss of ovarian reserve in mice. *PLoS One* 2015;10:e0144245.
10. Gücer F, Balkanlı-Kaplan P, Doganay L, et al. Effect of paclitaxel on primordial follicular reserve in mice. *Fertil Steril* 2001;76:628-629.
11. Makowski L, Noland RC, Koves TR, et al. Metabolic profiling of PPARalpha<sup>-/-</sup> mice reveals defects in carnitine and amino acid homeostasis that are partially reversed by oral carnitine supplementation. *FASEB J* 2009;23:586-604.
12. Ozcelik B, Turkyilmaz C, Ozgun MT, et al. Prevention of paclitaxel and cisplatin induced ovarian damage in rats by a gonadotropin-releasing hormone agonist. *Fertil Steril* 2010;93:1609-1614.
13. Havelock JC, Rainey WE, Carr BR. Ovarian granulosa cell lines. *Mol Cell Endocrinol* 2004;228:67-78.
14. Wang Q, Ju X, Chen Y, et al. Effects of L-carnitine against H<sub>2</sub>O<sub>2</sub>-induced oxidative stress in grass carp ovary cells (*Ctenopharyngodon idellus*). *Fish Physiol Biochem* 2016;42:845-857.
15. Chang S, Ren G, Steiner RD, et al. Elevated autophagy and mitochondrial dysfunction in the Smith-Lemli-Opitz syndrome. *Mol Genet Metab Rep* 2014;1:431-442.
16. Chen W, Xu X, Wang L, et al. Low expression of Mfn2 is associated with mitochondrial damage and apoptosis

- of ovarian tissues in the premature ovarian failure model. *PLoS One* 2015;10:e0136421.
17. Kumar S, Yedjou CG, Tchounwou PB. Arsenic trioxide induces oxidative stress, DNA damage, and mitochondrial pathway of apoptosis in human leukemia (HL-60) cells. *J Exp Clin Cancer Res* 2014;33:42.
  18. De Koning P, Neijt JP, Jennekens FG, et al. Evaluation of cis-diamminedichloroplatinum (II) (cisplatin) neurotoxicity in rats. *Toxicol Appl Pharmacol* 1987;89:81-87.
  19. Stadnicki SW, Fleischman RW, Schaeppi U, et al. Cis-dichlorodiammineplatinum (II) (NSC-119875): hearing loss and other toxic effects in rhesus monkeys. *Cancer Chemother Rep* 1975;59:467-480.
  20. Ward JM, Fauvie KA. The nephrotoxic effects of cis-diammine-dichloroplatinum (II) (NSC-119875) in male F344 rats. *Toxicol Appl Pharmacol* 1976;38:535-547.
  21. Marullo R, Werner E, Degtyareva N, et al. Cisplatin induces a mitochondrial-ROS response that contributes to cytotoxicity depending on mitochondrial redox status and bioenergetic functions. *PLoS One* 2013;8:e81162.
  22. Varbiro G, Veres B, Gallyas F Jr, et al. Direct effect of Taxol on free radical formation and mitochondrial permeability transition. *Free Radic Biol Med* 2001;31:548-558.
  23. Agarwal A, Sengupta P, Durairajanayagam D. Role of L-carnitine in female infertility. *Reprod Biol Endocrinol* 2018;16:5.
  24. Infante JP, Tschanz CL, Shaw N, et al. Straight-chain acyl-CoA oxidase knockout mouse accumulates extremely long chain fatty acids from alpha-linolenic acid: evidence for runaway carousel-type enzyme kinetics in peroxisomal beta-oxidation diseases. *Mol Genet Metab* 2002;75:108-119.
  25. Dunning KR, Robker RL. Promoting lipid utilization with l-carnitine to improve oocyte quality. *Anim Reprod Sci* 2012;134:69-75.



# Bilateral Ovarian Fibromatosis Diagnosed with Magnetic Resonance Imaging: A Case Report

NORIKO TAKESHITA<sup>1</sup>, TAKUHITO TADA<sup>1</sup>, MASAHIRO TOKUNAGA<sup>1</sup>, AKIRA OKIMURA<sup>2</sup>,  
MASARU MAKIHARA<sup>1</sup>, and TOHRU TAKESHITA<sup>3</sup>

*Departments of Radiology<sup>1</sup> and Pathology<sup>2</sup>, Izumi City General Hospital; and  
Department of Radiology<sup>3</sup>, PL Hospital*

## Abstract

This report describes a case of ovarian fibromatosis, which is a rare non-neoplastic disease. In ovarian fibromatosis, one or both ovaries are enlarged owing to fibroblastic proliferation associated with collagen deposition within the ovarian stroma. Ovarian fibromatosis is not a well-recognized entity. It is often misdiagnosed as a neoplastic disease, and treated with excessive surgery.

In our case of ovarian fibromatosis, preoperative magnetic resonance imaging revealed normal ovarian tissue surrounded by thick fibrous tissue not infiltrated, but preserved with a “black garland-like” appearance. This reflects the pathognomonic finding of the disease. Under the clinical diagnosis of ovarian fibromatosis, the outer portions of both ovarian masses were resected and ovarian function was preserved.

The pathogenesis of ovarian fibromatosis appears to be related to massive ovarian edema. The patient in the present case had a history of ovarian hyperstimulation syndrome, which may have caused the massive ovarian edema and may be suggestive of the hypothesis that massive ovarian edema and ovarian fibromatosis are a series of pathological conditions.

Key Words: Ovarian fibromatosis; Non-neoplastic lesion; Black garland-like appearance; Magnetic resonance imaging

## Introduction

Ovarian fibromatosis is a miscellaneous non-neoplastic lesion that was defined by Young and Scully in 1984<sup>1</sup>. It presents with a tumor-like enlargement of one or both ovaries. When surgery is performed on the basis of a clinical diagnosis of ovarian neoplasm, ovarian function is lost. This report describes a case of ovarian fibromatosis that was correctly diagnosed using magnetic resonance imaging (MRI) before surgery.

---

Received November 19, 2018; accepted April 19, 2019.

Correspondence to: Noriko Takeshita, MD.

Department of Radiology, Izumi City General Hospital,  
Wake-cho 4-5-1, Izumi, Osaka, 594-0073, Japan  
Tel: +81-725-41-1331; Fax: +81-725-43-3660  
E-mail: mqfwk775@ybb.ne.jp

### Case Report

A 39-year-old woman was referred to our institution for menstrual abnormalities. She had neither abdominal pain nor masculinization and hirsutism. She was nulliparous and had a history of ovarian hyperstimulation syndrome at the age of 34 years. She had no malignant medical history.

Her physical examination was normal. Routine laboratory test results were within the normal limits, with the exception of increased levels of CA 19-9 (68 U/mL) and CA 125 (77.7 U/mL). Transvaginal ultrasonography revealed bilateral solid ovarian masses and neoplasm was suspected. To obtain further information, non-enhanced MRI was performed. It revealed bilateral enlarged ovaries, with lobulated surfaces. T1-weighted images showed a homogeneous, low signal intensity (Fig. 1). In both ovarian masses, T2-weighted images demonstrated a high signal intensity at the inner portion, which indicated a normal stroma, and a low signal intensity similar to that of skeletal muscles at the outer portion (Fig. 2). Several small high-intensity areas were also observed at the outer portion, which indicated spared normal stroma (Fig. 2). Diffusion-weighted images showed a high signal intensity at the inner portion, which indicated a normal ovarian stroma, and a low signal intensity at the outer portion (Fig. 3). In addition to the bilateral ovarian masses, several uterine myomas and ascites were observed. When the MRI findings were summarized, normal ovarian tissue was surrounded by thick fibrous tissue. Therefore, a clinical diagnosis of ovarian fibromatosis was made in spite of elevated tumor markers.

In accordance with the diagnosis, the outer portion of both ovarian masses was resected and myomectomy was also performed. On gross examination of the specimen, the surface of both ovarian masses was coarsely lobulated; the sectioned specimen was mostly light gray and partly yellowish

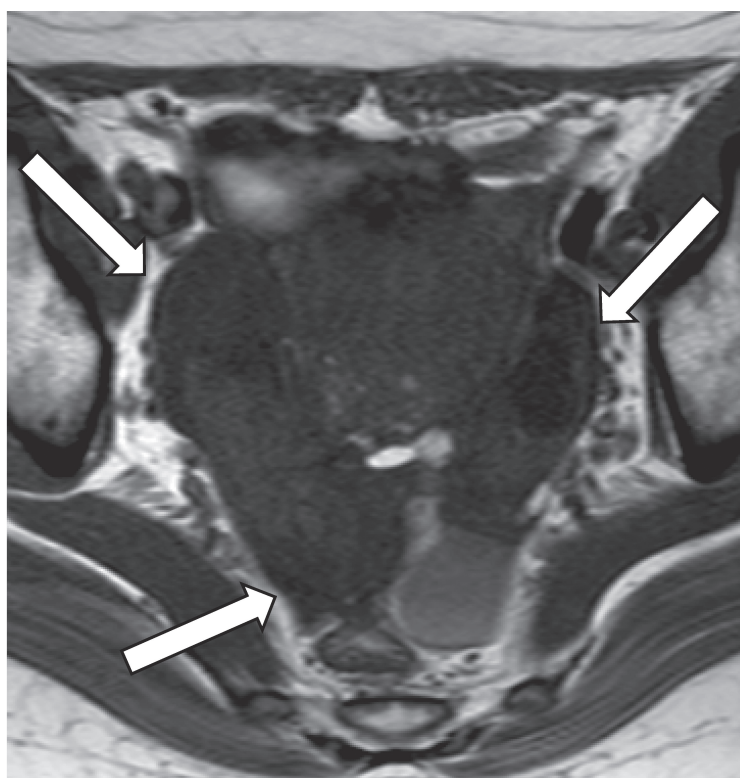


**Figure 1.** T1-weighted magnetic resonance image, of both ovarian masses, showing homogeneous low signal intensity (white arrows).

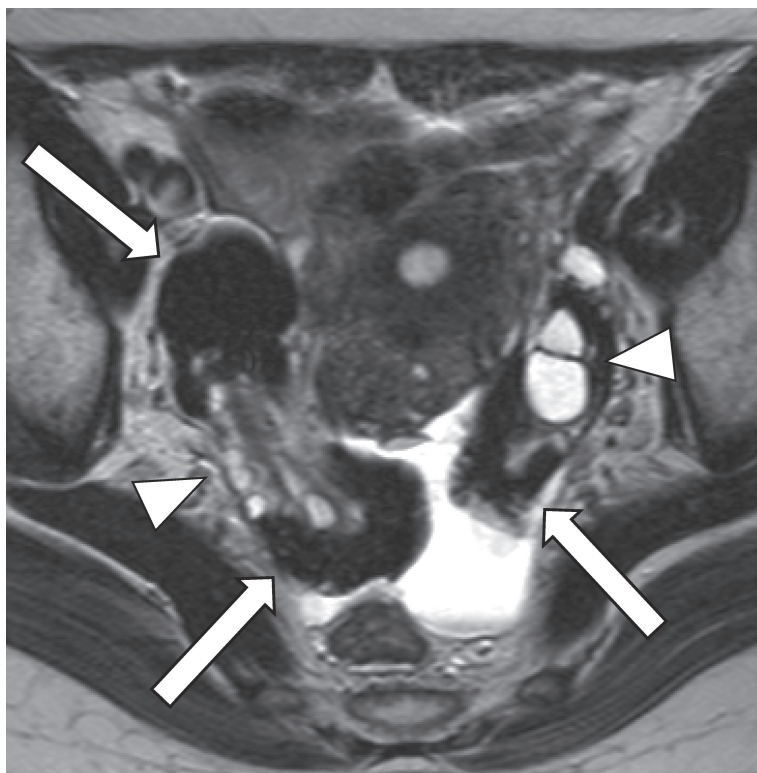


**Figure 2.** T2-weighted magnetic resonance image showing high signal intensity (white arrow-heads) in the inner portion of each ovarian masses, which is surrounded by a low signal intensity (white arrows) similar to that of skeletal muscles.

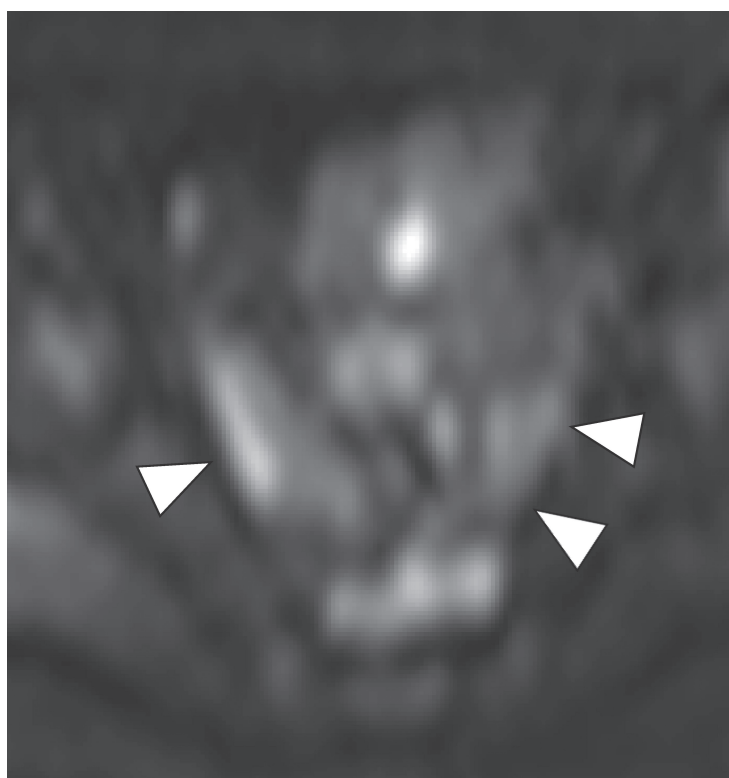


**Figure 3.** High b-value, diffusion-weighted magnetic resonance image of the inner portion of the ovarian masses, showing a high signal intensity, which was consistent with normal ovarian stroma (white arrow-heads).

-white (Fig. 4). A cystic lesion was also identified. The histopathological findings demonstrated proliferative, collagen-producing, spindle-shaped cells in incomplete clusters with a storiform pattern surrounding the expanded follicles (Fig. 5). Malignant findings were not present. On the basis of the pathological findings, a final diagnosis of bilateral ovarian fibromatosis was made.

The postoperative course was uneventful. The patient was discharged 6 days after the surgery, and her menstrual cycle normalized.



**Figure 4.** A sectioned specimen with mostly light gray and partly yellowish -white color.

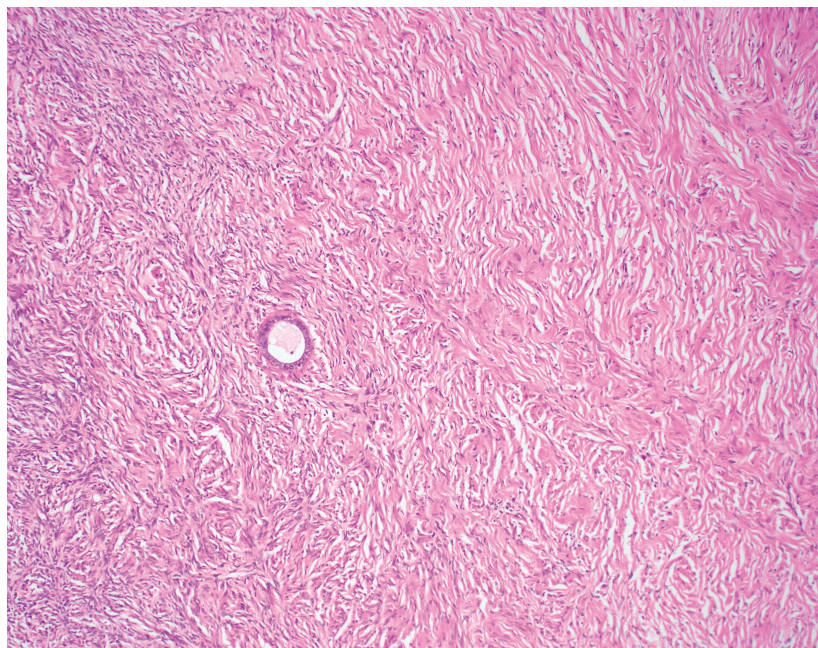


**Figure 5.** Histopathological finding demonstrating atypical, proliferative, collagen-producing, spindle-shaped cells in incomplete clusters, with a storiform pattern surrounding the expanded follicles in both ovaries (original magnification,  $\times 10$ ; Hematoxylin Eosin stain).

## **Discussion**

Ovarian fibromatosis is a rare clinicopathological entity, with only approximately 30 cases have been described in the literature<sup>1-8</sup>. In ovarian fibromatosis, one or both ovaries are enlarged owing to fibroblastic proliferation associated with collagen deposition within the ovarian stroma<sup>9</sup>. It is most commonly reported in women aged 13-39 years (mean, 25 years). Preservation of the preexisting ovarian structures is typical and unrelated to soft-tissue fibromatosis, which rarely involves the ovary. In approximately 20% of cases, ovarian fibromatosis involves both ovaries<sup>2</sup>. The predominant symptoms are menstrual abnormalities and abdominal pain, and sometimes, masculinization and hirsutism occur due to hormonal activities<sup>1,3-5</sup>. Tumor markers are within their normal ranges or slightly elevated<sup>3-7</sup>. The patient's slightly elevated tumor markers might be also caused by myoma uteri<sup>10,11</sup>. The pathogenesis of ovarian fibromatosis is unclear; however, local tissue disorders, surgery, and ovarian torsion are possible contributors<sup>1</sup>.

The pathogenesis of ovarian fibromatosis appears to be related to massive ovarian edema. Massive ovarian edema is characterized by ovarian enlargement and stromal edema. Russell and Farnsworth suggested that ovarian fibromatosis presented the “burned out” stage of reactive fibroblastic proliferation that result from massive edema at one end of the spectrum. Foci of stromal edema similar to those of massive ovarian edema have been reported in roughly 50% of cases of ovarian fibromatosis<sup>12</sup>. The presented patient had a history of ovarian hyperstimulation syndrome due to infertility treatment. This syndrome is characterized by cystic enlargement of the ovaries and a fluid shift from the intravascular to the third space due to increased capillary permeability and ovarian neoangiogenesis<sup>13</sup>. The syndrome may have caused massive ovarian edema<sup>13,14</sup>. The patient's history of ovarian hyperstimulation syndrome may be suggestive of the hypothesis that massive ovarian edema and ovarian fibromatosis are a series of pathological conditions.

The differential diagnoses of bilateral ovarian masses with very low signal intensity on T2-weighted image include ovarian stromal hyperplasia, metastatic ovarian tumors, and bilateral ovarian fibrothecomas<sup>15</sup>. Although ovarian stromal hyperplasia is generally associated with hyperandrogenism, obesity, hypertension, hyperinsulinemia, and glucose intolerance, without spared normal ovarian follicles<sup>16</sup>, these coexisting conditions were absent and normal ovarian follicles were observed in the present case. Metastatic ovarian tumors usually infiltrate and replace normal ovarian follicles, and fibrothecomas replace normal follicles. In the presented case, this phenomenon was not observed. Furthermore, most fibrothecomas are unilateral, but they may also be bilateral (8%)<sup>17</sup>, especially in patients with Gorlin or basal cell nervous syndrome (bilateral ovarian fibrothecomas, multiple basal cell carcinomas of the skin, odontogenic keratocysts, and other abnormalities)<sup>18</sup>. The fibrothecoma in Gorlin syndrome usually shows coarse calcification. In this case, no coarse calcification in both ovaries was observed.

Takeuchi et al described that the low intensity surrounding the ovary like a garland on T2-weighted MRI was a characteristic finding of ovarian fibromatosis and named it a “black garland-like” appearance<sup>5</sup>. In this case, a preexisting ovarian stroma with follicles was surrounded by thick fibrous tissue like a garland. This case can be added to cases with ovarian fibromatosis showing a “black garland-like” appearance.

On the basis of the characteristic MRI findings, a clinical diagnosis of ovarian fibromatosis was made. As MRI was useful in differentiating this disease from neoplastic diseases, ovarian function was preserved. Recognition of ovarian fibromatosis by surgeons and pathologists has important

therapeutic implications.

The magnetic resonance imaging finding, such as “black garland-like” appearance on T2 weighted image, may be a diagnostic clue to this rare disease. The patient’s history of ovarian hyperstimulation syndrome may be suggestive of the hypothesis that massive ovarian edema and ovarian fibromatosis are a series of pathological conditions.

### Acknowledgements

All authors have no COI to declare regarding the present study.

### References

1. Young RH, Scully RE. Fibromatosis and massive edema of the ovary, possibly related entities: a report of 14 cases of fibromatosis and 11 cases of massive edema. *Int J Gynecol Pathol* 1984;3:153-178.
2. Bakshi N, Kaushal V. Ovarian fibromatosis. *J Obstet Gynaecol India* 2014;64:368-369.
3. Bazot M, Salem C, Cortez A, et al. Imaging of ovarian fibromatosis. *AJR Am J Roentgenol* 2003;180:1288-1290.
4. Onderoglu LS, Gültekin M, Dursun P, et al. Bilateral ovarian fibromatosis presenting with ascites and hirsutism. *Gynecol Oncol* 2004;94:223-225.
5. Takeuchi M, Matsuzaki K, Sano N, et al. Ovarian fibromatosis: magnetic resonance imaging findings with pathologic correlation. *J Comput Assist Tomogr* 2008;32:776-777.
6. Fukunishi H, Murata K, Takeuchi S, et al. Ovarian fibromatosis with minor sex cord elements. *Arch Gynecol Obstet* 1996;258:207-211.
7. Beurdeley M, Sabourin JC, Drouin-Garraud V, et al. Ovarian fibromatosis and sotos syndrome with a new genetic mutation. *J Pediatr Adolesc Gynecol* 2013;26:e39-41.
8. Roche WR, du Boulay CE. A case of ovarian fibromatosis with disseminated intra-abdominal fibromatosis. *Histopathology* 1989;14:101-107.
9. Young RH, Harris NL, Scully RE. Lymphoma-like lesions of the lower female genital tract: a report of 16 cases. *Int J Gynecol Pathol* 1985;4:289-299.
10. Babacan A, Kizilaslan C, Gun I, et al. CA 125 and other tumor markers in uterine leiomyomas and their association with lesion characteristics. *Int J Clin Exp Med* 2014;7:1078-1083.
11. Tsao KC, Hong JH, Wu TL, et al. Elevation of CA 19-9 and chromogranin A, in addition to CA 125, are detectable in benign tumors in leiomyomas and endometriosis. *J Clin Lab Anal* 2007;21:193-196.
12. George V, Tammisetti VS, Surabhi VR, et al. Chronic fibrosing conditions in abdominal imaging. *Radiographics* 2013;33:1053-1080.
13. Lee TH, Liu CH, Huang CC, et al. Serum anti-Müllerian hormone and estradiol levels as predictors of ovarian hyperstimulation syndrome in assisted reproduction technology cycles. *Hum Reprod* 2008;23:160-167.
14. Daboubi MK, Khreisat B. Massive ovarian oedema: literature review and case presentation. *East Mediterr Health J* 2008;14:972-977.
15. Rosenkrantz AB, Popiolek D, Bennett GL, et al. Magnetic resonance imaging appearance of ovarian stromal hyperplasia and ovarian hyperthecosis. *J Comput Assist Tomogr* 2009;33:912-916.
16. Fujii S, Kiyokawa T, Tsukihara S, et al. Magnetic resonance imaging findings of ovarian stromal hyperthecosis. *Acta Radiol* 2009;50:954-957.
17. Dockerty MB, Masson JC. Ovarian fibromas: a clinical and pathologic study of 283 cases. *Am J Obstet Gynecol* 1944;47:741.
18. Johnson AD, Hebert AA, Esterly NB. Nevoid basal cell carcinoma syndrome: bilateral ovarian fibromas in a 3 1/2-year-old girl. *J Am Acad Dermatol* 1986;14:371-374.

# Instructions for Authors

*The Osaka City Medical Journal* will consider the publication of any original manuscript, review, case report, or short communication. Articles should be in English.

**Manuscript submission.** Manuscripts should be sent to the Editor, Osaka City Medical Journal, Osaka City Medical Association, Osaka City University Medical School, 1-4-3 Asahimachi, Abeno-ku, Osaka 545-8585, Japan; phone and fax 06-6645-3782; e-mail shiigakukai@med.osaka-cu.ac.jp

The Journal accepts only manuscripts that contain material that has not been and will not be published elsewhere. Duplicate publication of scientific data is not permitted. If closely related papers might be considered to be duplicate publications, the possible duplicate should be submitted with the manuscript and the authors should explain in their covering letter what is original in the submitted paper. Submit three copies of the manuscript (two of which may be photocopies) together with CD-R or DVD-R containing the body text, tables and figures. The manuscript should be prepared by Microsoft Word or its compatible software (doc or docx). Acceptable formats for figures are JPG or TIF. Use only 12-point font size and a standard serif font. Double-space throughout the manuscript and use standard-sized (ISO A4, 212×297 mm) white bond paper. Make margins at least 25 mm wide on all sides. Number pages consecutively starting with the title page and ending with the reference list. Begin each of these sections on a separate page: title page, abstract, text, acknowledgements, references, tables (each one separate), and figure legends. Do not use abbreviations in the title or abstract and limit their use in the text, defining each when it first appears. Manuscripts should meet the requirements outlined below to avoid delay in review and publication. Authors whose native language is not English must seek the assistance of a native English speaker who is familiar with medical sciences. Please attach the certificate from the person(s) who edit the manuscript. Some minor editorial revision of the manuscript will be made when the editorial committee considers it necessary.

**Title page.** All submissions must include a title page. The full title of the paper, should be concise, specific, and informative, and should contain the message of the paper without being in sentence form. Next, include the full names and academic affiliations of all authors, and indicate the corresponding author, address, phone, fax, and e-mail address. Give a running title (not to exceed 50 characters including spaces), and three to five key words. Last, give the word count for text only, exclusive of title, abstract, references, tables, and figure legends.

**Structured abstract.** The abstract of 250 words or less should consist of four paragraphs headed **Background, Methods, Results, and Conclusions.**

**Text.** Full papers about experiments or observations may be divided into sections headed **Introduction, Methods, Results, and Discussion.**

**Tables.** Each table should be typed on a separate sheet in characters of ordinary size, double-spaced (with at least 6 mm of white space between lines). Each table must have a title and should be assigned an Arabic numeral ('Table 3'). Vertical rules should not be used.

**Figures.** For black-and-white figures, submit three original glossy prints or laser-quality proofs and three photocopies of each. One transparency and three color prints should be submitted of each color figure. Label the front of figures with the figure number. Indicate on the back of each figure the first author, the first few words of the manuscript title, and the direction of the top of the figure (if needed). Photomicrographs should have scale markers that indicate the magnification. Provide figure legends on a separate page, double-spaced, immediately after the tables. All illustrations and graphs, to be referred to as figures, should be numbered in Arabic numerals ('Fig. 2' etc.). The approximate position of each figure in the text should be indicated in the right margin of the manuscript. Illustrations in full color are accepted for publication if the editors judge that color is necessary, with the cost paid by the author.

**References.** Reference must be double-spaced and numbered consecutively in the order cited in the text. When listing references, follow the style of the Uniform Requirements (<http://www.icmje.org/>) and abbreviate names of journals according to PubMed (<http://www.ncbi.nlm.nih.gov/sites/netrez>). List all authors up to three; when there are four or more, list the first three and use et al.

## Examples of reference style

1. Priori SG, Schwartz PJ, Napolitano C, et al. Risk stratification in the long-QT syndrome. *N Engl J Med* 2003;348:1866-1874.
2. Schwartz PJ, Priori SG, Napolitano C. The long-QT syndrome. In: Zipes DP, Jalife J, editors. *Cardiac electrophysiology: from cell to bedside*. 3rd ed. Philadelphia: W.B. Saunders; 2000. pp. 597-615.

**Proofs.** One set of proofs together with the original manuscript will be sent to the author, to be carefully checked for any essential changes or printer's errors. The author is requested to return the corrected proofs within 48 h of their receipt.

### ***Short communications and case reports.***

1. A short communication should have between 1500 and 2000 words, including the abstract. This word count is equivalent to about four double-spaced manuscript pages.
2. The original and two copies including three sets of figures and tables should be sent to the Editorial Office.

***Manuscript submission fee.*** A nonrefundable fee of 10,000 JPY is due on submission of original manuscripts, case reports, and short communications. A manuscript returned beyond six months of the date of the initial decision will be considered a new submission.

***Page charges and reprints.*** Authors are required to pay page charges of 10,000 JPY per printed page to share in the high costs of publication. Authors receive with the proofs a reprint order form that must be filled out and returned with the proofs to the Editorial Office. Later orders cannot be filled because reprints are made at the time the journal is printed.

***Studies of human subjects.*** It is the responsibility of the authors to ensure that any clinical investigation they did and report in manuscripts submitted to the Osaka City Medical Journal are in accordance with the Declaration of Helsinki (<http://www.wma.net>).

***Animal studies.*** It is the responsibility of the authors to ensure that their experimental procedures are in compliance with the “Guiding Principles in the Care and Use of Animals” ([http://www.the-aps.org/pub\\_affairs/humane/pa\\_aps\\_guiding.htm](http://www.the-aps.org/pub_affairs/humane/pa_aps_guiding.htm)) published each month in the information for authors of the American Journal of Physiology.

### ***Conflict of Interest (COI) Disclosure.***

1. It is the responsibility of the authors to disclose any COI by signing the form.
2. If the authors have no conflicts, please state “All authors have no COI to declare regarding the present study” in the Acknowledgements.

Authors are required to disclose any relationships with company or organization (such as funds, consultancy fee, grant, fee for speaking, stock or shares). At the time of initial submission, the corresponding author is responsible for obtaining conflict of interest information from all authors.

[Revised: April 2019]

## COPYRIGHT TRANSFER AND STATEMENT OF ORIGINALITY

We approve the submission of this paper to the Osaka City Medical Association for publication and have taken to ensure the integrity of this work. We confirm that the manuscript is original and does not in whole or part infringe any copyright, violate any right of privacy or other personal or priority right whatever, or falsely designate the source of authorship, and that it has not been published in whole or in part and is not being submitted or considered for publication in whole or in part elsewhere (abstracts excluded).

We agree to transfer copyright the manuscript entitled

\_\_\_\_\_

\_\_\_\_\_

to the Osaka City Medical Association upon its acceptance for publication.

Write clearly and signature

(Author: print or type)

(Signature)

(Date)

\_\_\_\_\_

\_\_\_\_\_

\_\_\_\_\_

(Author: print or type)

(Signature)

(Date)

\_\_\_\_\_

\_\_\_\_\_

\_\_\_\_\_

(Author: print or type)

(Signature)

(Date)

\_\_\_\_\_

\_\_\_\_\_

\_\_\_\_\_

(Author: print or type)

(Signature)

(Date)

\_\_\_\_\_

\_\_\_\_\_

\_\_\_\_\_

(Author: print or type)

(Signature)

(Date)

\_\_\_\_\_

\_\_\_\_\_

\_\_\_\_\_

(Author: print or type)

(Signature)

(Date)

\_\_\_\_\_

\_\_\_\_\_

\_\_\_\_\_

(Author: print or type)

(Signature)

(Date)

\_\_\_\_\_

\_\_\_\_\_

\_\_\_\_\_

(Author: print or type)

(Signature)

(Date)

\_\_\_\_\_

\_\_\_\_\_

\_\_\_\_\_

(Author: print or type)

(Signature)

(Date)

\_\_\_\_\_

\_\_\_\_\_

\_\_\_\_\_

(Author: print or type)

(Signature)

(Date)

\_\_\_\_\_

\_\_\_\_\_

\_\_\_\_\_

# OCMJ for Conflict of Interest (COI) Disclosure Statement

The purpose of this form is to provide readers of your manuscript with information about your other interests that could influence how they receive and understand your work. The form is designed to be completed and stored electronically. Each author should submit this form and is responsible for the accuracy and completeness of the submitted information.

1. 1) Have you accepted from a sponsor or any company or organization (More than 1,000,000 JPY per year from a specific organization) ? (Please circle below)

- (1) Funds ? .....Yes / No
- (2) Consultancy fee ? .....Yes / No
- (3) Any grant ? .....Yes / No
- (4) Fee for speaking ? .....Yes / No

2) Do you hold any stock or shares related to the manuscript ?

- (1) Directly ? .....Yes / No
- (2) Indirectly, via family members or relatives ? .....Yes / No

3) If any of above items are “yes”, please provide detailed information below.

2. If none of the above apply and there is no COI please clearly state “All authors have no COI to declare regarding the present study”.

**Manuscript Title:**

**Name / Signature** \_\_\_\_\_ **Date** \_\_\_\_\_

**Manuscript Identifying Number (if you know it):**

## Editorial Committee

Masaaki Inaba, MD (Chief Editor)

Yasuhiro Fujiwara, MD

Motoharu Imanaka, MD

Shoji Kubo, MD

Masahiko Ohsawa, MD

Daisuke Tsuruta, MD

Wakaba Fukushima, MD

Koki Inoue, MD

Yukio Miki, MD

Toshiyuki Sumi, MD

Kazuo Ikeda, MD

Norifumi Kawada, MD

Yukio Nishiguchi, MD

Masahiro Tanaka, MD

The volumes and issues published in 1954-2018 were as follows: Vol 1 (one issue), Vols 2-5 (2 issues, each), Vols 6-7 (one issue, each), Vols 8-9 (2 issues, each), Vol 10 (one issue), Vol 11 (2 issues), Vol 12 (one issue), Vol 13 (2 issues), Vols 14-20 (one issue, each), Vol 21 (2 issues), Vol 22 (one issue), Vols 23-65 (2 issues, each)

Publisher : Osaka City Medical Association,  
Osaka City University Medical School,  
1-4-3 Asahimachi, Abeno-ku, Osaka 545-8585, Japan